UNCLASSIFIED

CLASSIFICATION CANCELLED

DATE   FEB 27 1957   * DE*

For The Atomic Energy Commission

H.F. Cansee

Chief, Declassification Branch

SODIUM GRAPHITE REACTOR
QUARTERLY PROGRESS REPORT
MARCH—JUNE, 1954

EDITED BY:

Sidney Siegel
Guy M. Inman

Price $ 0.65

ATOMIC ENERGY RESEARCH DEPARTMENT
NORTH AMERICAN AVIATION, INC.

P. O. BOX 309   DOWNEY, CALIFORNIA

ISSUE DATE
SEPTEMBER 1, 1954

UNCLASSIFIED

CONTRACT AT 11-1-GEN-8

PREFACE

The Atomic Energy Commission has undertaken a development program to provide the technology needed for the evaluation and economic design of nuclear power plants.[1] This program is to be carried out during the next five years at several national laboratories and industrial organizations. The Sodium Graphite Reactor (the SGR) is one of those to be investigated and experimentally tested as part of this 5-year effort. The program on the SGR is intended to expand our area of information covering sodium-graphite technology, experimentally demonstrate the feasibility of this reactor complex and extend its performance limits, and apply the information developed to designs suitable for the full-scale nuclear power plant. As a principal part of this program, a Sodium Reactor Experiment (the SRE) is to be constructed and operated; it will be the major experimental facility in which the performance of this reactor will be studied and new technological advances tested.

This report continues an earlier series[2-7] in which previous work on the SGR and the SRE has been described. In this report, the progress on the program is described in two main sections. Section A is devoted to work relating to the general technology of Sodium Graphite Reactors, and to studies relating to the full-scale plant. Section B covers progress on the analytical, experimental, and design efforts devoted solely to the SRE, required for its design and construction.

This report is based upon studies conducted for the Atomic Energy Commission under Contract AT-11-1-GEN-8.

TABLE OF CONTENTS

SECTION A
TECHNOLOGY OF THE SODIUM GRAPHITE REACTOR

(Section Editor - Sidney Siegel)

SECTION B
SODIUM REACTOR EXPERIMENT

(Section Editor - Guy Inman)

TABLE OF CONTENTS (Continued)

TABLE OF CONTENTS (Continued)

LIST OF FIGURES

CONFIDENTIAL

LIST OF FIGURES (Continued)

LIST OF FIGURES (Continued)

SECTION A

TECHNOLOGY OF THE SODIUM GRAPHITE REACTOR

I. FULL-SCALE REACTOR STUDIES

A. Analysis of Nuclear Performance (C. Roderick)

1. Plutonium Feedback Fuel Studies - It would be highly desirable to use fuel in sodium graphite reactors which would not require enrichment in the gaseous diffusion plant. A mixture of plutonium and natural uranium apparently would be a suitable fuel under certain conditions. It is the purpose of the plutonium feedback study to define these conditions and to investigate the feasibility of operating reactors utilizing this type of fuel.

Plutonium feedback in a thermal power reactor has promise of producing substantial reductions in fuel feed costs by extending the reactivity lifetime of the fuel. There are two possible feed schemes: (1) remove the Pu from the irradiated fuel and return it to the reactor with fresh uranium feed, e.g., natural uranium; the depleted uranium, at a U^{235} concentration comparable to the waste from a diffusion plant, would be discarded; (2) separate only fission products from the irradiated fuel and add small amounts of quite highly enriched uranium, e.g., 20 per cent U^{235}, to replace the burned U^{235} and U^{238}. With either scheme the concentrations of the plutonium isotopes in the feed material are always the same in "steady state."

In order to assess the value of plutonium feedback, some "steady state" calculations have been made; the transient, between start-up with slightly enriched uranium and operation with constant plutonium concentrations in the feed fuel, will be investigated when the desirable "steady state" conditions are determined. The calculations are done for sodium graphite reactors but the trends determined are applicable to any thermal reactor using slightly enriched uranium fuels. The feed is assumed to be natural uranium, and the important variables are the initial amount of excess reactivity, lattice spacing and α, the ratio of Pu^{239} to U^{235} in the feed fuel. The system is called "steady state" in that the ratios

$$N_{40}/N_{49} = \sigma_{c(49)}/\sigma_{a(40)}$$

$$N_{41}/N_{49} = \sigma_{c(49)}/\sigma_{a(41)} \cdot$$

obtained from setting the build-up differential equations to zero, are used for the feed concentrations, and the feed material to the reactor is always the same; in the calculations these ratios change only slightly. During irradiation of a fuel element the U^{235} and U^{238} steadily decline, while the plutonium isotope concentrations initially increase then decline. In order to have enough plutonium for feed material it is necessary to remove the fuel from the reactor before the plutonium content drops below its initial value.

The fact that the plutonium concentration increases initially makes possible the fueling of additional reactors without resorting to a diffusion plant for enriched fuel; if desired, a part of the plutonium could be removed and used to fuel another reactor.

In the calculations a value of α is chosen fixing the amount of Pu^{239} added to the natural uranium feed material; the concentrations of Pu^{240} and Pu^{241} are then determined by the above ratios. The variations in reactivity and in the concentrations of the various isotopes are then computed as functions of exposure. Some of the results are given in Figs. 1-6. The constants used in these calculations pertain to 400° C neutrons and are as follows:

$$\nu(25) = 2.48 \qquad \nu_{49} = 2.91 \qquad \nu_{41} = 3.00$$

$$\sigma_a(25) = 400 \text{ b} \qquad \sigma_{a\,49} = 1015 \text{ b} \qquad \sigma_{a\,41} = 1480$$

$$\sigma_f(25) = 340 \qquad \sigma_{f\,49} = 675 \text{ b} \qquad \sigma_{f\,41} = 1080$$

$$\sigma_a(26) = 5.36 \qquad \sigma_{a\,40} = \text{variable}^8$$

$$\sigma_a(28) = 1.62$$

A report summarizing the results of these calculations is in preparation.
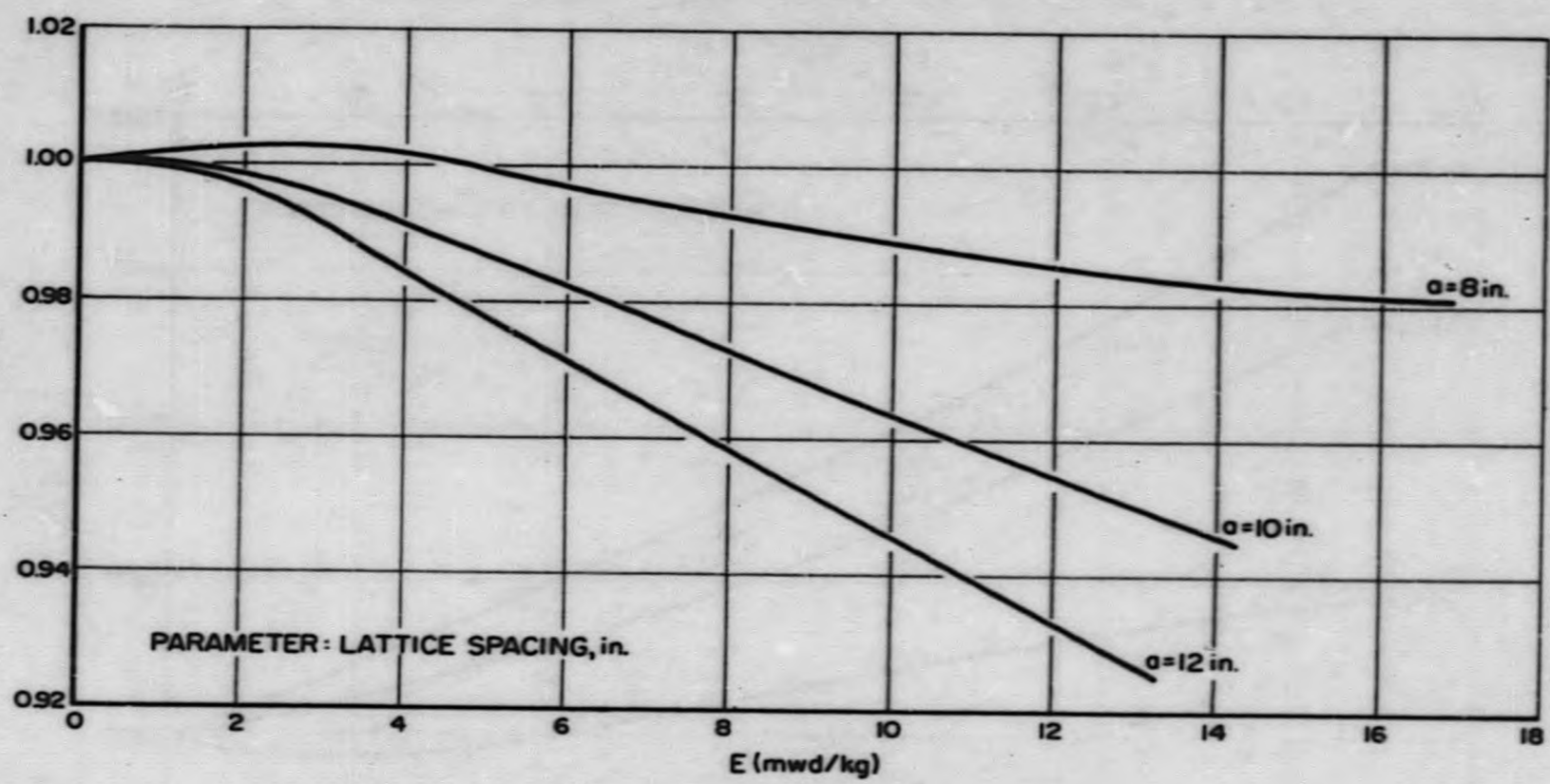
Fig. 1.   Reactivity Changes vs Specific Energy, $\alpha = 0.5$
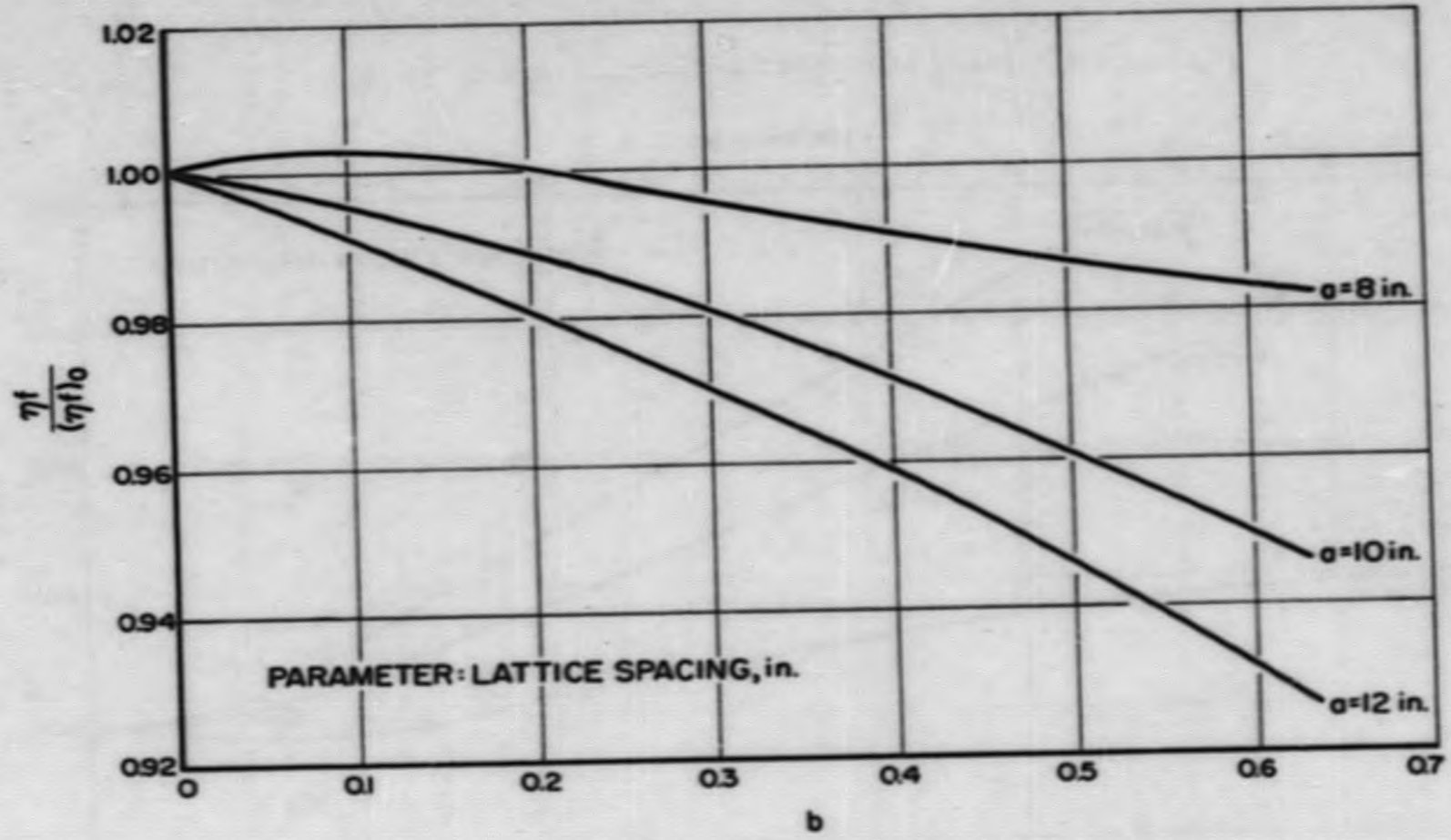
Fig. 2. Reactivity Changes vs Fractional Burnup of Uranium-235, $\alpha = 0.5$
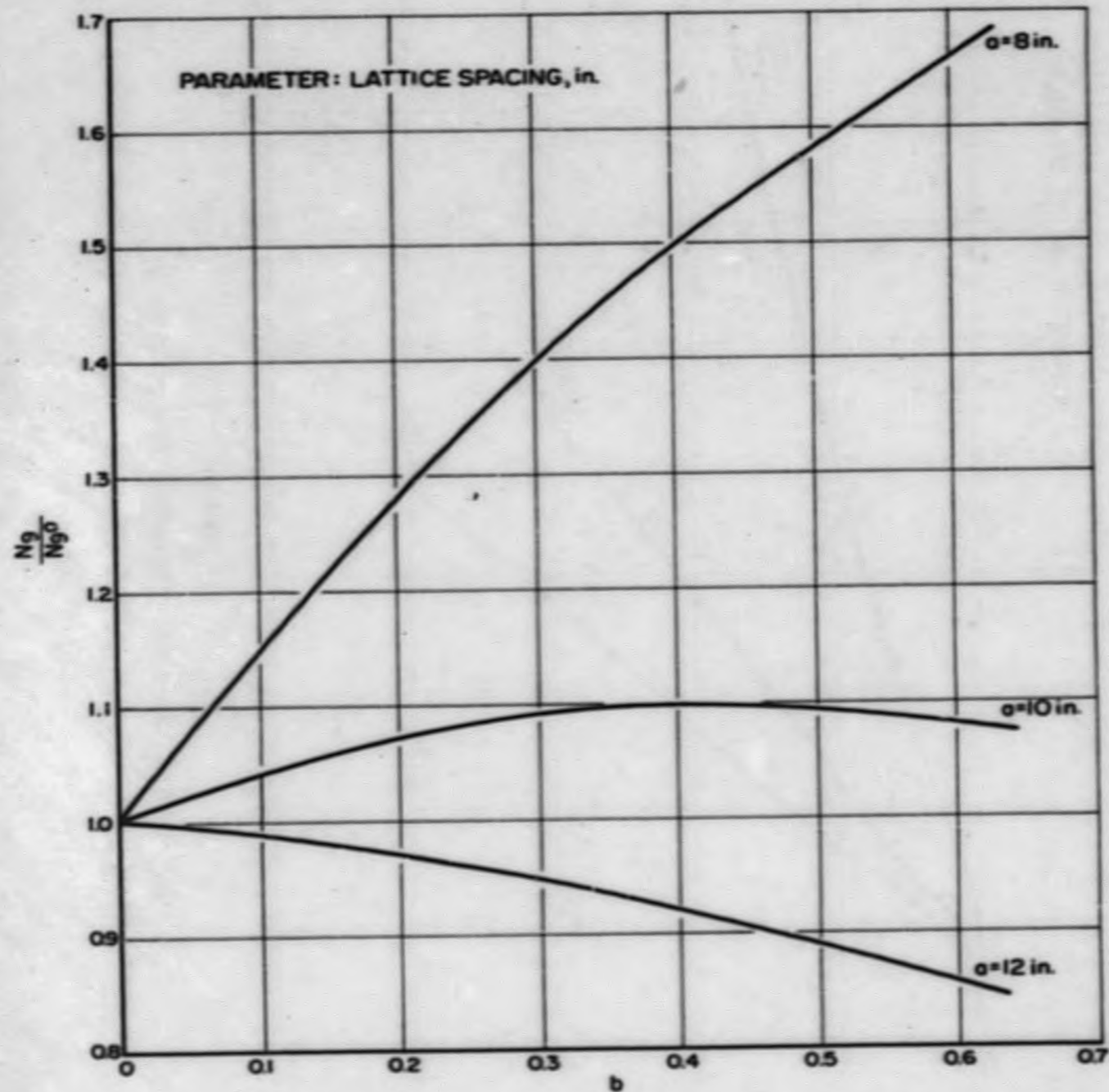
Fig. 3. Variation in Plutonium-239 Concentration vs Fractional
Burnup of Uranium-235, $\alpha = 0.5$
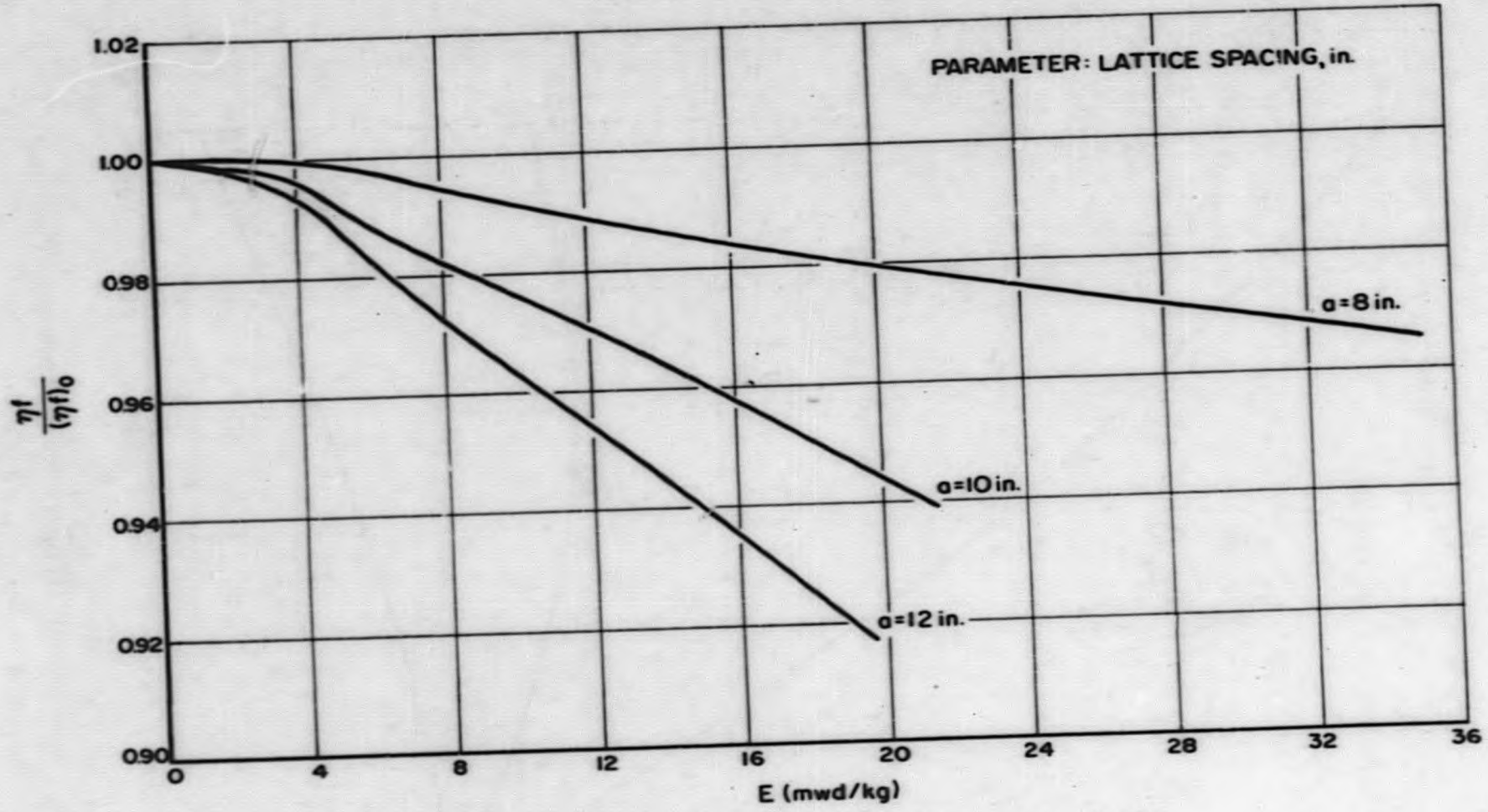
Fig. 4. Reactivity Changes vs Specific Energy, $\alpha = 1.00$
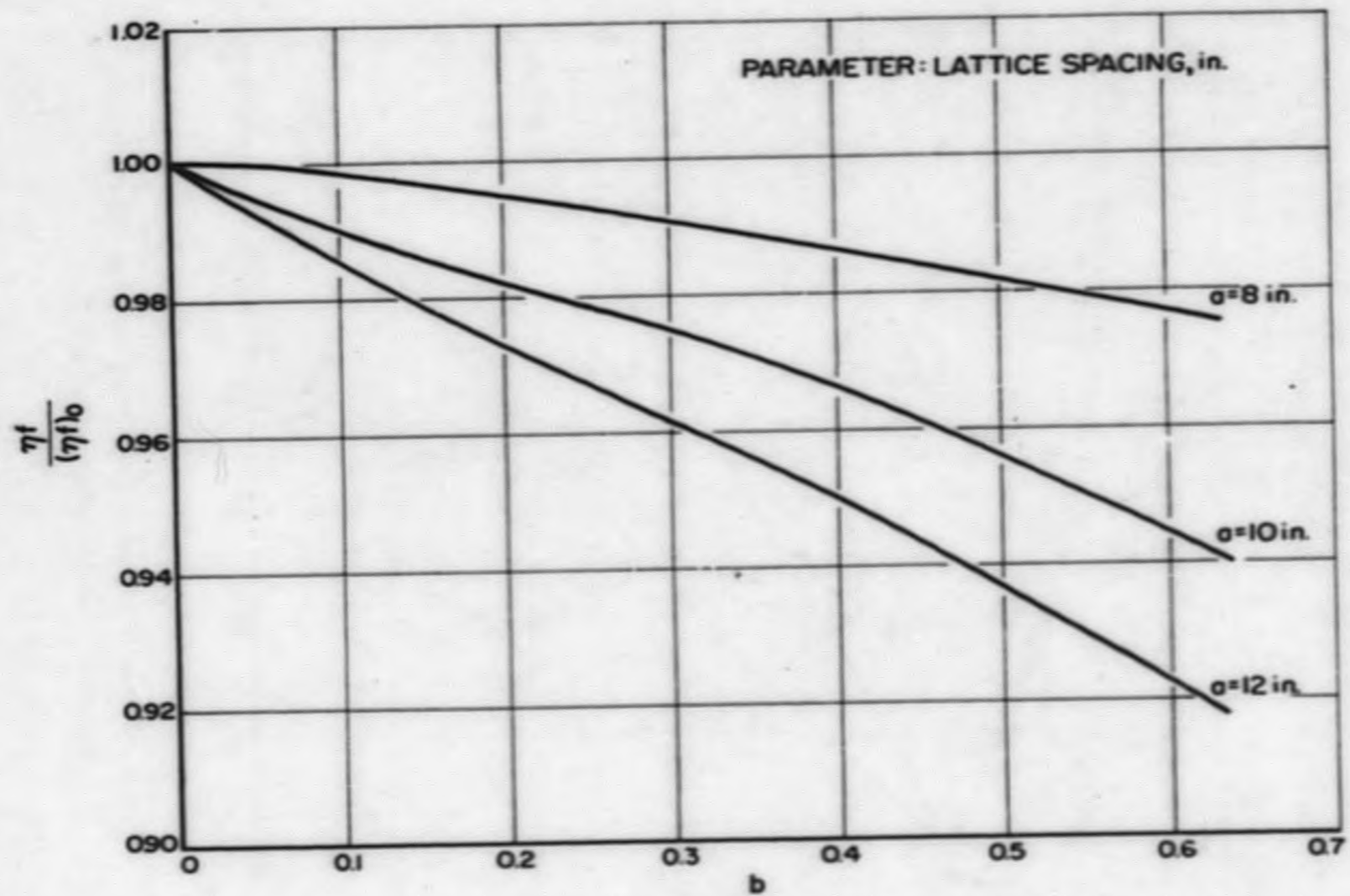
Fig. 5. Reactivity Changes vs Fractional Burnup of Uranium-235, $\alpha = 1.00$
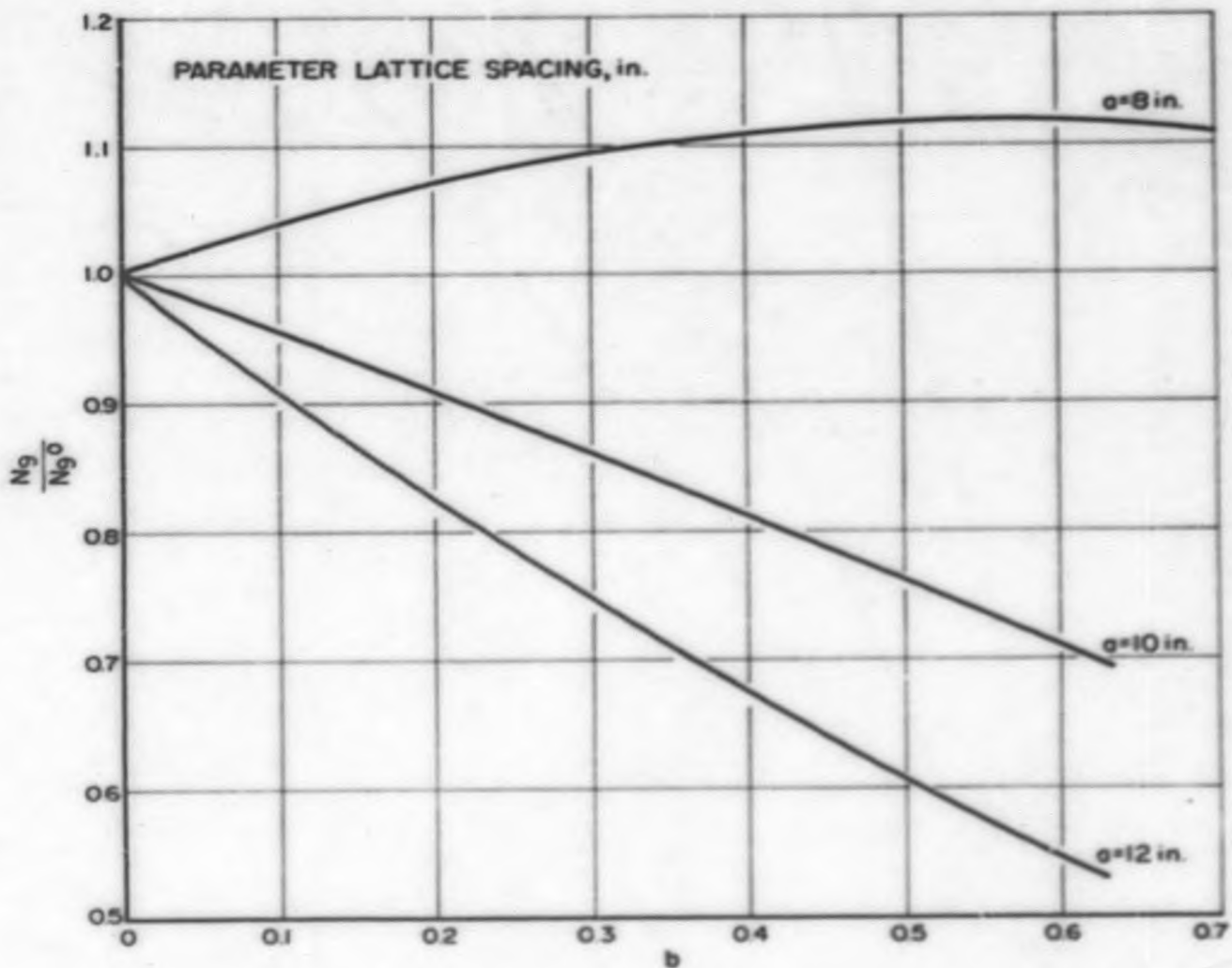
Fig. 6. Variation in Plutonium-239 Concentration vs Fractional
Burnup of Uranium-235, $\sigma = 1.00$

16

B. Study of Full-Scale Sodium-Graphite Reactor Designs (W. E. Abbott)

As part of the continuing study of the full-scale sodium graphite reactor, alternate types of fuel elements, permitting more economical operating conditions, are under consideration. A preliminary survey of various arrangements of fuel which might be adapted to a large, sodium-cooled, tank-type reactor utilizing the zirconium-canned-graphite moderator concept has been initiated. In one arrangement examined the fuel is contained in thimbles inserted in the coolant channels of the moderator cans. The thimbles are fixed semi-permanently to the reactor structure and serve the function of separating the fuel from the sodium coolant. The thimble configuration is adaptable to both unclad solid fuels and to liquid (fluid) fuels. The use of unclad solid or liquid fuels promises substantial savings in chemical processing and fabrication. Liquid fuels have the additional possible attractive features of essentially un-limited burn-up and high operating temperatures. A bismuth-uranium solution and a fused uranium salt mixture both appear to offer possibilities for use as a liquid fuel in such a system.

Attention has been directed to the advantages of separating the fissionable and fertile materials within the fuel assemblies. Such a separation appears to have attractive features for the $Th-U^{233}$ system and the U-Pu (Plutonium Feedback) system.

II. REACTOR PHYSICS

A. Determination of Power and Temperature Coefficients of Reactivity
(G. W. Rodeback)

The increase in the effective resonance absorption integrals of some of the reactor materials with temperature ordinarily results in a negative temperature coefficient of reactivity in a graphite-moderated reactor. The temperature effect of the neutron absorption in the fuel elements is usually predominant and is all the more significant when a fast "runaway" is being considered. It has, therefore, been deemed advisable to measure the temperature effect on the effective resonance integral of U^{238} up to as high a temperature as feasible and for the particular geometry of the SRE. It is also planned to make a similar

measurement for Th^{232} since its use as a breeding material is contemplated for the SGR.

Ideally, the greatest precision for measuring the temperature coefficient of the effective resonance integral could probably be obtained by using the "danger coefficient" method, or the pile oscillator method. However, the difficulties attendant on maintaining the uranium samples at elevated temperatures while doing the above experiments would be considerable in the particular research reactors which may be available for these measurements.

An experiment is being planned using an alternative method, measuring the activation of U^{238} through the β^- activity of U^{239} formed as a result of the $U^{238} (n,\gamma) U^{239}$ reaction. Instead of irradiating ordinary uranium and separating out the contaminants chemically before counting, as was done in 1943 by Mitchell, et al,[9] it is proposed to irradiate foils of U^{238} which are highly depleted in U^{235}. The methods to be used are based on those used by Risser, et al.[10] As was done in the above experiment, a sector-shaped thin foil of depleted uranium will be placed in the center diametral plane of a slug of the uranium fuel material and the entire slug will be surrounded by cadmium. The resulting foil activity will then be representative of the resonance activation of the U^{238} in the slug. The epithermal flux entering the slug is monitored by an indium foil and the temperature coefficient will be determined by measuring the ratios of U^{239} activity to indium activity at the various temperatures of exposure.

A simplified schematic drawing of the apparatus to be used appears in Fig. 7. The uranium slug essentially consists of two halves carefully fitted together. In the inner face of one is a carefully machined depression into which fits the sector-shaped depleted uranium foil. The slug rests on ceramic pieces which are fastened to stainless steel supporting members. The slug is centered in an evacuated aluminum cylinder which is water-cooled on the outside. This is sealed on both ends by removable covers with the right end opening into a pump-out tube.

The inner surface of the aluminum cylinder will be plated with a layer of cadmium, which in turn will be plated with a very thin layer of chromium. The former serves as a thermal neutron shield while the latter serves as a heat reflector. The reflector should permit the slug to be heated to near 1000° C with several hundred watts in an axial resistance heating element.

DEPLETED FOIL

INDIUM FOIL

CADMIUM LINER

ALUMINUM TUBES
FOR COOLING

THERMOCOUPLE WIRES

HEATER LEAD WIRE

GROUND WIRE
FOR HEATER

RELIEF
VALVE

VACUUM TUBE

LEAD GASKET

STAINLESS STEEL
SUPPORT

CHROME
PLATED

INSULATING
SUPPORT

GRAPHITE
STRINGER
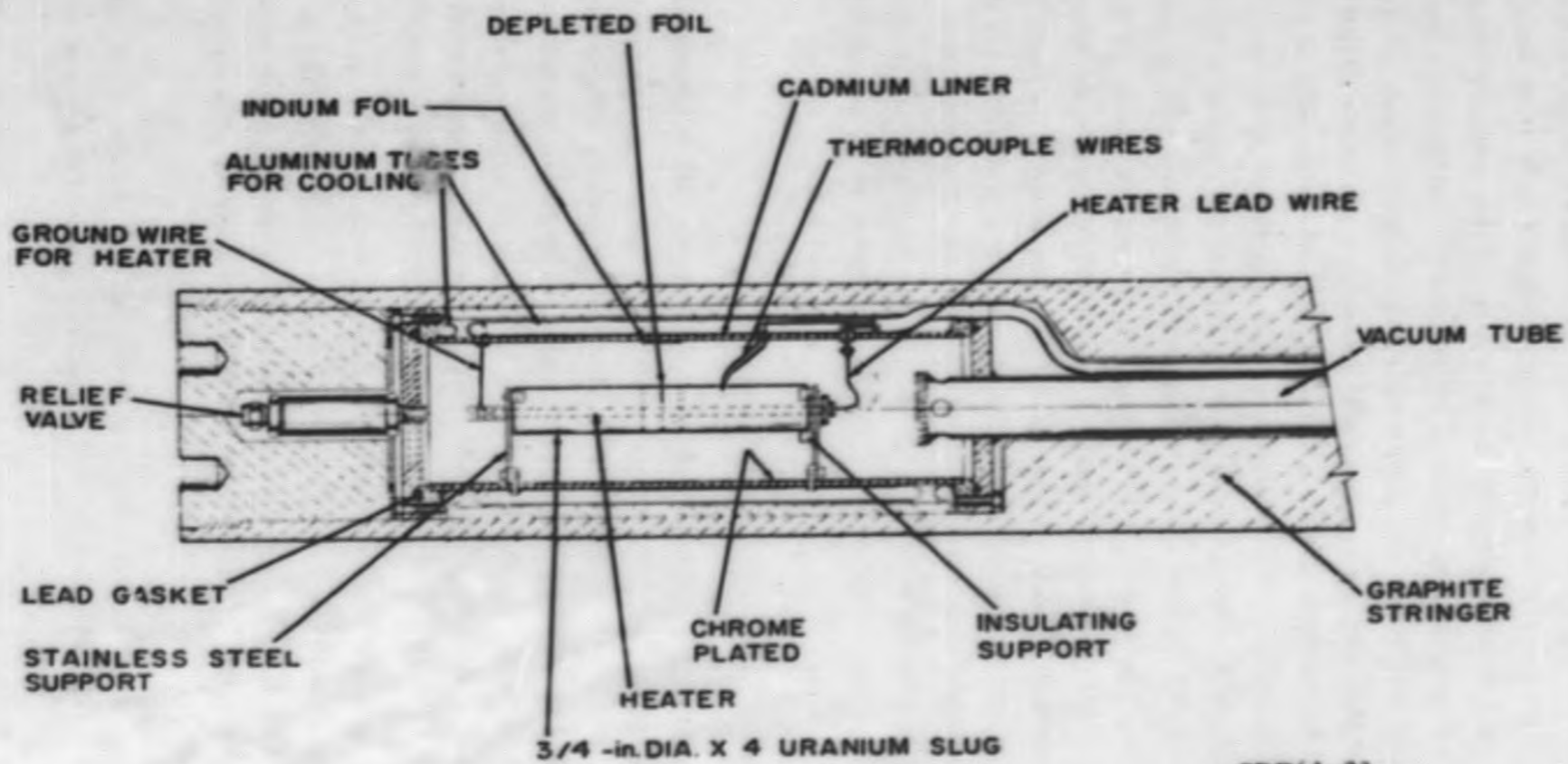
HEATER

3/4 -in. DIA. X 4 URANIUM SLUG

SRP61-23
CONFIDENTIAL

Fig. 7. Schematic Diagram of Resonance Absorption Capsule

19

The heater is to consist of molybdenum wire helically wound on an aluminum oxide core (over-all diameter approximately 1/8 inch) which will fit in a concentric hole in the length of the uranium slug. The neutron absorption resonances of molybdenum do not overlap those of U^{238} and therefore this metal should be well suited for a high temperature heating element. It appears that the slug with heater and core will have an effective resonance integral not appreciably different from that of a solid core, at least in the region of the depleted foil. However, neutron distribution measurements are to be made to check this conclusion. The heater lead on the left side is grounded to the aluminum cylinder and after irradiation will be removed together with the left half of the slug. The depleted foil can then be removed for counting. The indium monitor foil will also be removed from its position next to the water-cooled cylinder wall. The entire capsule together with pumping, electrical, and water lines will be embedded in a graphite stringer and irradiated in the reflector of a water boiler-type reactor of suitable flux. The irradiation, adequate to give counting rates from the foil of about 50,000 c/min, is not expected to activate the assembly to the level where remote manipulations are necessary.

B. Nuclear Parameters of Sodium-Graphite Lattices

1. Exponential Experiments (R. A. Laubenstein) - More information is needed on the nuclear characteristics of sodium-graphite reactors to enable accurate design calculations for full scale reactors for power production and accurate predictions of power cost. An exponential experiment has been selected as the most economical method of determining the validity of theoretical reactor physics calculations and of indicating the sources of possible discrepancies between the theoretical calculations and experimental lattice parameters.

An exponential assembly for investigation of sodium graphite type lattices has been designed and is now under construction with delivery expected by August 1. The assembly will be placed on top of the vertical graphite thermal column of the water boiler reactor which will provide a source of neutrons for the experiments.

A graphite assembly 5 feet high and 42 to 57 inches square will be used depending on the lattice spacing desired. The basic graphite pieces will be

columns 7 inches square and 5 feet high which will each have a hole for the fuel cluster lengthwise down the center. These basic pieces can be used to build up a square lattice with a 7-inch spacing. By the use of graphite spacer blocks, 9-1/2 inch and 12 inch lattices will also be constructed.

Two different types of fuel cluster assemblies have been designed for use in the exponential assembly. The first type will utilize a four-rod cluster (quatrefoil) of 1-inch diameter uranium rods. Since 1-inch diameter uranium slugs of 0.9 per cent U^{235} enrichment are now available at NAA, this first fuel cluster will enable some preliminary measurements to be made before fuel for the SRE is available. The second type of fuel cluster will have a seven-rod cluster of 3/4-inch diameter uranium rods. Pending the availability of the necessary quantity of SRE fuel, preliminary experiments with seven-rod clusters of 3/4-inch diameter rods will be accomplished using natural uranium now available at NAA.

Aluminum will be used in the fuel cluster of the exponential assembly to mock up the sodium coolant. The macroscopic absorption cross section of 2S aluminum is only 14 per cent larger than that for sodium at room temperature. A preliminary measurement of the intra-uranium flux distribution in a seven-rod fuel cluster has indicated that streaming of neutrons between the rods is important in determining the flux in the uranium. Therefore, it is desirable to use a material to mock up the sodium which has a similar macroscopic scattering cross section. 2S aluminum with a macroscopic scattering cross section of 0.098 cm^{-1} for low energy neutrons has the lowest cross section of any commercial alloy found, and compares favorably with the 0.073 cm^{-1} scattering cross section of sodium at room temperature. The fuel clusters will consist of solid aluminum cylinders with holes drilled in them for insertion of the uranium slugs.

Initial experiments with the exponential assembly will consist of buckling and intra-cell flux distribution measurements.

2. Intra-Uranium Flux Distributions in a Seven-Rod Cluster (E. Martin, S. W. Kash, F. E. Estabrook) - A preliminary investigation of the intra-uranium flux distribution in a seven-rod cluster has been completed in preparation for full-scale lattice measurements on septafoils in graphite moderator.

As a matter of expediency, the moderator for the preliminary measurements was D_2O and the uranium was the 0.90 weight per cent enriched material which was already available.

Each rod of the cluster consisted of five 4-inch long, 1-inch diameter uranium slugs in water-tight aluminum tubing. These seven aluminum tubes fitted into cavities in an aluminum cylinder, shown in cross section in Fig. 8. The cluster was suspended in the center of the D_2O tank and was buffered by a lattice of 1-inch diameter uranium rods, of the same enrichment, in a 6-inch square array. The central 12 rods had been removed from the buffer lattice.

Flux measurements within the central rod of the cluster and one outside rod were made by the standard intra-cell procedure.[11] Because of the symmetry of the cluster, it was sufficient to map out the flux in a 30° sector of the central rod. In an outside rod, the line of symmetry is the diameter connecting the centers of the outside and central rods. Flux distributions were investigated along this diameter, and along diameters 30° and 60° therefrom. Bare foil activities were corrected to thermal by subtracting 1.05 times the cadmium-covered activity. All flux values reported have been normalized to the thermal flux at the center of the cluster.

Measurements in the central rod did not indicate any angular flux variation. Figure 9 presents the thermal flux vs the square of the radius for this rod. An average flux for the central rod was obtained by mechanical integration and the disadvantage factor, F, was calculated. F is the ratio of the surface to the average flux, and is here equal to $\frac{1.37}{1.15} = 1.19 \pm 0.04$.

Figure 10 presents the thermal data across a diameter of an outside rod as a function of distance from the center of the rod and angle between the diameter and the line of symmetry. The flux is plotted vs r^2 to obtain an expanded scale. A combination of data from Figs. 9 and 10 gives the flux pattern from the center of the cluster directly through an outside rod (Fig. 11).

An average thermal flux over the outside rod was obtained in the following manner: The flux values at, say, the surface of the rod, were plotted against θ. This was mechanically integrated to give a flux, averaged from 0 to 2π, at r = 1.27 centimeters. Similar procedures resulted in average fluxes at r = 0.72 and r = 1.01 centimeters, the points of measurement. Then one more integration over these radial values sufficed to yield an average flux for the
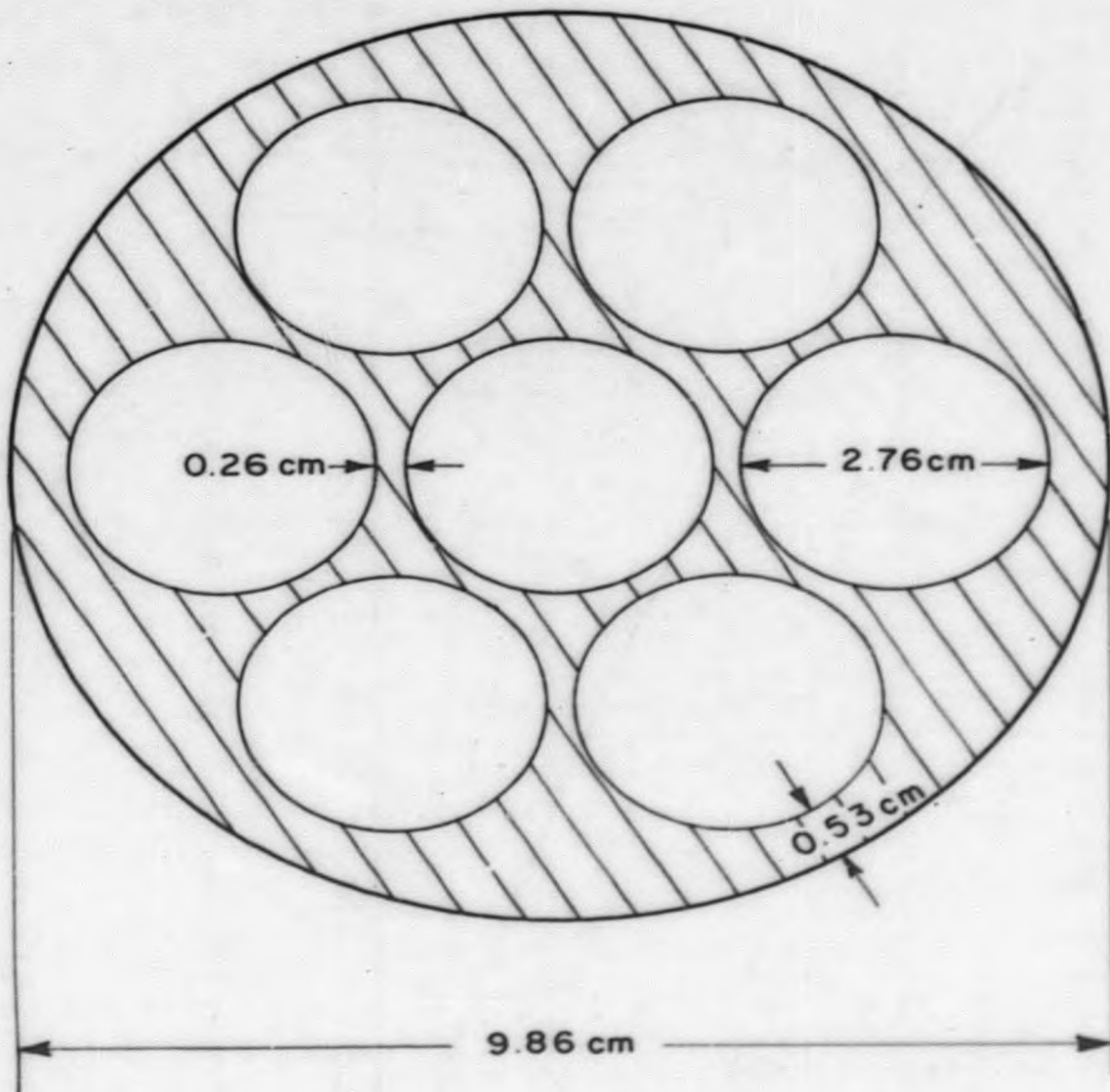
Fig. 8.   The Seven-Rod Cluster

DECLASSIFIED
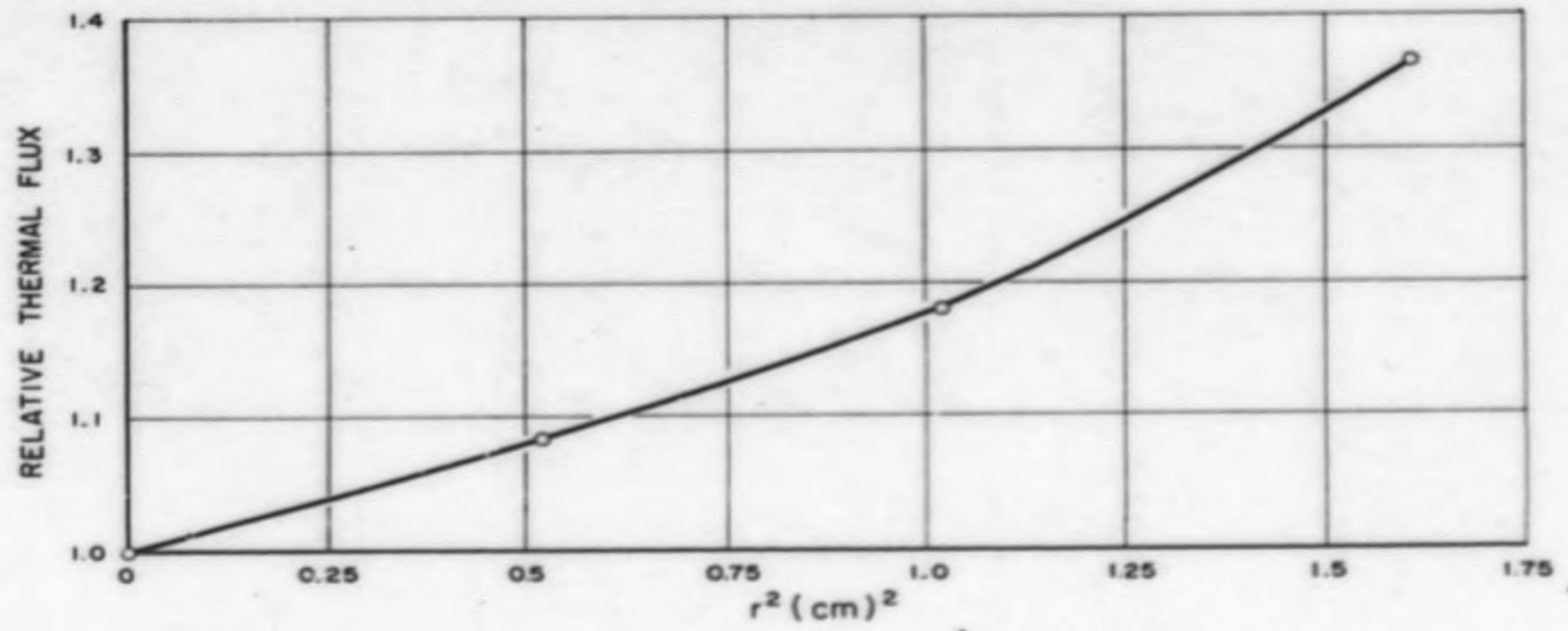
Fig. 9. Thermal Flux in the Central Rod of a Seven-Rod Cluster

7464-SR10419
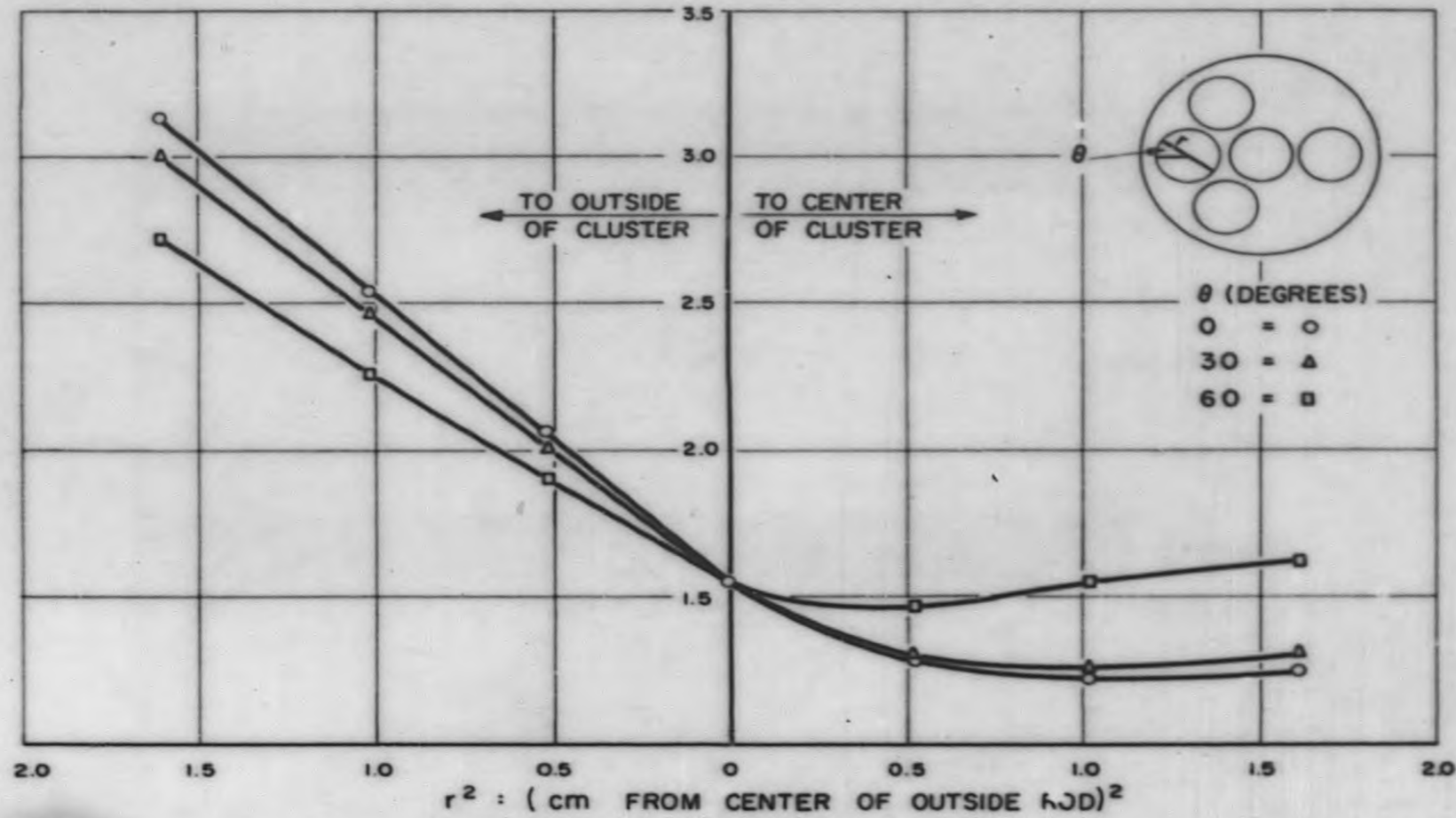
Fig. 10. Thermal Flux Across an Outside Rod of a Seven-Rod Cluster
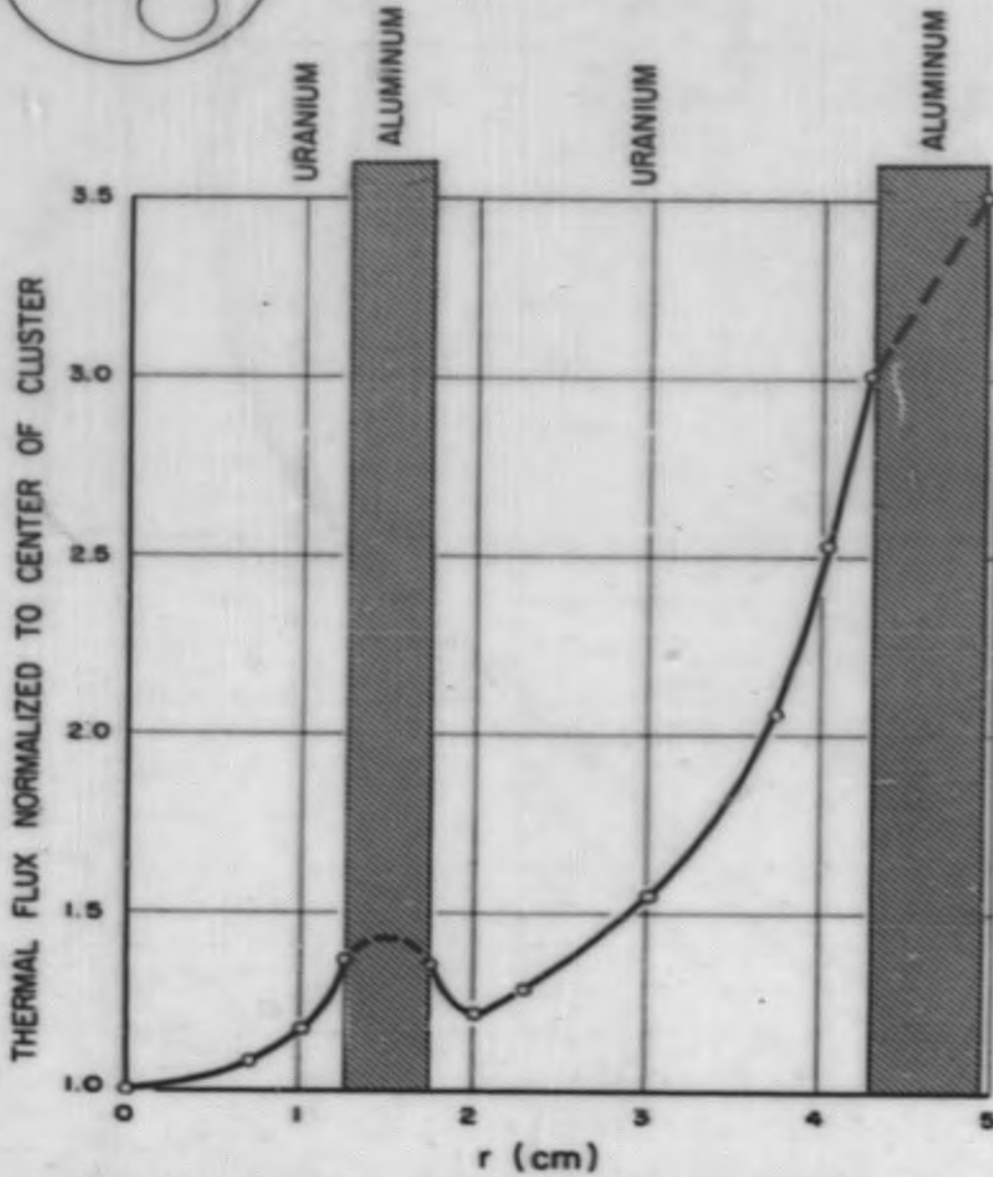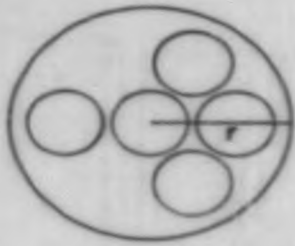
Fig. 11. Thermal Flux Through the Seven-Rod Cluster

outside rod = 1.82 ± 0.03. Figure 12 is a plot of ϕ vs r^2. If a synthetic disadvantage factor, F_s, is defined as the ratio of an average surface flux to the average over the rod, then $F_s = \frac{2.16}{1.82} = 1.19 \pm 0.04$.

The individual flux values reported are believed reproducible to ± 6 per cent, with an internal consistency of ± 3 per cent or better.

The arrangement of uranium rods in a cluster introduces two important effects: (1) relatively large streaming of neutrons through the aluminum between the rods, and (2) hardening of the neutron spectrum in each rod due to the influence of neighboring rods. The first effect explains the fact that the thermal neutron current is everywhere into the rods (see Figs. 10 and 11). It also accounts for the small but definite increase in the flux from the inner surface of the outside rod to the opposing surface of the central rod (Fig. 11), since the outside rod point is partially shadowed by uranium from the neutrons streaming in through the gaps. Also, due to this streaming, the angular distribution of the neutrons at the surface of the central rod is highly anisotropic, and is directed chiefly towards the center of the rod.

The hardening of the neutron spectrum results from the approximate $1/v$ absorption of uranium. The neutrons which reach the central rod after passing through the outside rods will have an average thermal energy higher than that of the neutrons in the D_2O.

Previous work in this laboratory has determined the disadvantage factor of a single enriched uranium rod to be 1.23. In the cluster, F of the central rod and F_s of the outside rod were equal to 1.19. The decrease for the central rod is explicable on the basis of the two previous arguments. The anisotropy of the neutron distribution at the surface of the rod means a relatively higher flux in the center of the rod and hence a smaller F. The hardening of the energy spectrum implies less absorption in the rod, and again, a smaller F.

The exact coincidence of F and F_s may be fortuitous. However, the same hardening undoubtedly affects the flux in the outside rods, and is most likely the major cause of the decrease of F in this case.

In this connection, some experimental work done at Argonne National Laboratory is of interest.[12] Argonne used 1-inch diameter natural uranium rods, and investigated the flux distribution in a single rod, and in a quatrefoil with
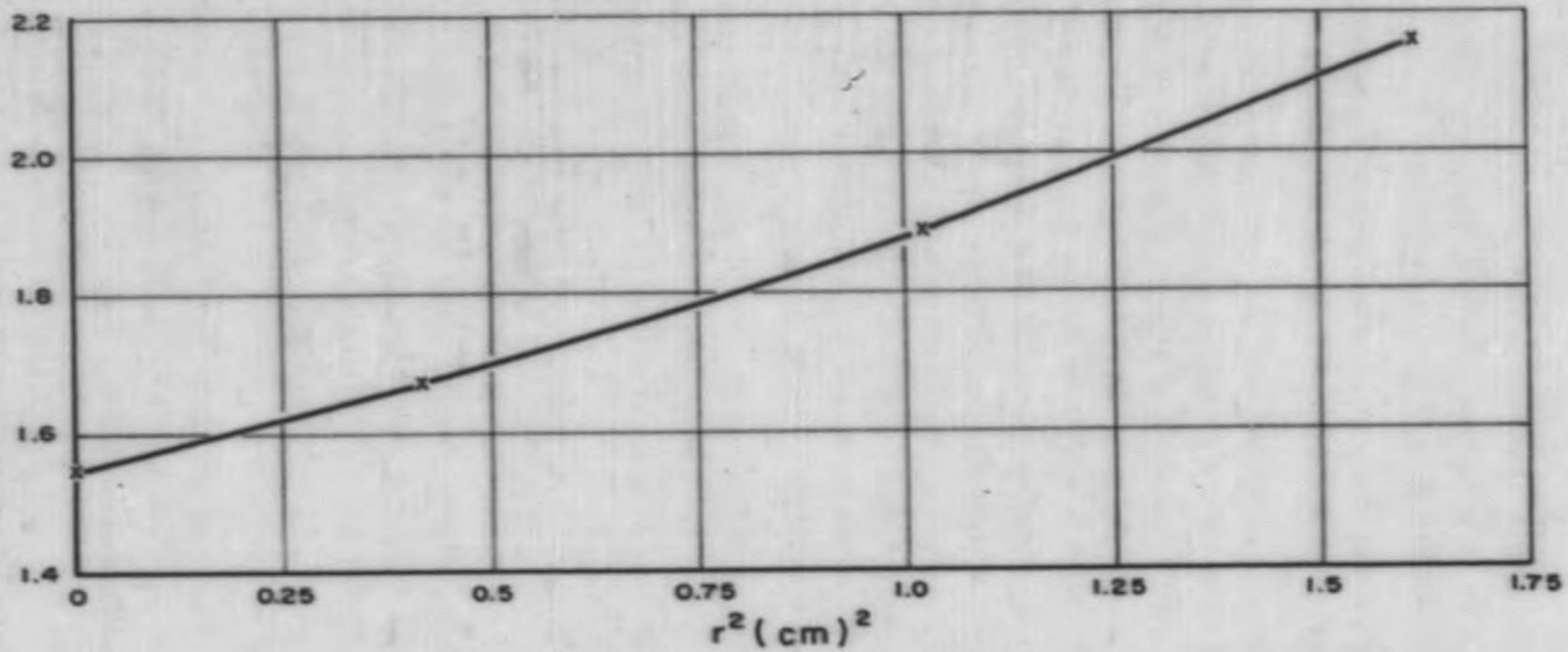
Fig. 12. Outside Rod Radial Distribution of Thermal Flux Averaged over All Angles

D_2O circulating between the rods. They measured the disadvantage factor of a single rod in the CP-2 and obtained $F = 1.19$. They presented the experimental data for the quatrefoil in complete detail, so that it was possible to evaluate an F_s for a quatrefoil rod by a method similar to the one used on the cluster. F_s was equal to 1.14, again lower than the single rod value.

This preliminary experiment has suggested certain experimental modifications for flux determinations within a cluster of uranium rods. It has also emphasized the inadequacy of diffusion theory and the necessity for an empirical approach in this case.

C. Neutron Leakage Through Shield (F. L. Fillmore)

Multi-group diffusion theory in slab geometry for non-multiplying regions can be formulated by matrix methods in such a manner that computations on a desk computing machine are within reason for several groups of fast neutrons. The reasons for this are that the eigenvalues and eigenfunctions of the problem are easily found for the case of non-multiplying regions; the eigenvalues are all distinct, and the computation can be arranged so that only diagonal and triangular matrices are involved. Moreover, certain reasonable simplifications can be made for the case of a reactor shield so that the required boundary conditions lead to formulas which are readily evaluated.

The multi-group diffusion equations for this case can be written in the matrix form

$$y' = My \quad , \qquad \qquad \ldots(1)$$

where

$$M = \begin{pmatrix}
0 & 0 & 0 \ldots \ldots \ldots 0 & D_1^{-1} & 0 \ldots \ldots \ldots 0 \\
0 \ldots \ldots \ldots \ldots \ldots 0 & 0 & D_2^{-1} & 0 \ldots \ldots 0 \\
\ldots \ldots \ldots \ldots \ldots \\
0 & 0 & 0 \ldots \ldots & 0 & 0 & \ldots \ldots 0 & D_n^{-1} \\
\Sigma_1 & 0 & 0 \ldots \ldots \ldots \ldots \ldots \ldots 0 \\
-p_1\Sigma_1 & \Sigma_2 & 0 \ldots \ldots \ldots \ldots \ldots \ldots 0 \\
0 & -p_2\Sigma_2 & \Sigma_3 & 0 \ldots \ldots \ldots \ldots \ldots 0 \\
\ldots \ldots \ldots \\
0 \ldots \ldots \ldots 0 & -p_{n-1}\Sigma_{n-1} & \Sigma_n & 0 \ldots \ldots \ldots 0
\end{pmatrix}$$

Here y_i is the flux, $-D_i y_{n+i}$ the current, Σ_i the removal cross section, and p_i the capture escape probability, in the i-th group. It can be shown that the eigenvalues of M are $\pm \varkappa_i$ where $\varkappa_i$ is the inverse diffusion length for the i-th group.

The solution of Eq. (1) can be written in the form

$$y(x) = SY(x)\, \bar{a}$$

$$Y = \begin{pmatrix} e^{\varkappa_1 x} & & & & & 0 \\ & \ddots & & & & \\ & & e^{\varkappa_n x} & & & \\ & & & e^{-\varkappa_1 x} & & \\ & & & & \ddots & \\ 0 & & & & & e^{-\varkappa_n x} \end{pmatrix}$$

and S is a matrix which diagonalizes M. Thus

$$S^{-1}MS = \begin{pmatrix} \varkappa_1 & & & 0 \\ & \varkappa_n & & \\ & & -\varkappa_1 & \\ 0 & & & -\varkappa_n \end{pmatrix}$$

$\bar{a}$ is an arbitrary vector which is determined by the boundary conditions of the problem.

These 2n-rowed matrices are partitioned into n-rowed matrices, thus separating the fluxes and currents, in order to facilitate the application of the boundary conditions. It is found that the submatrices into which S and S^{-1} are partitioned are triangular, and such matrices are easy to invert. The solution to the following two problems can then be readily derived:

Case I. (Two Regions)

Region I of thickness x_1

Region II of infinite thickness

Flux known at $x = 0$

Flux and current continuous at the interface

Flux vanishes at infinity

Case II. (One Region)

Region of thickness x_1, including the extrapolation in length

Current known at $x = 0$

Flux vanishes at $x = x_1$

The form of the flux and current equations in both cases is

$$\phi(x) = D^{-1} PD \left[Y_1(x) \bar{a}_1 + Y_2(x) \bar{a}_2 \right]$$

$$0 \le x \le x_1$$

$$J(x) = -P D \varkappa \left[Y_1(x) \bar{a}_1 - Y_2(x) \bar{a}_2 \right]$$

where

$$D = \begin{pmatrix} D_1 & & 0 \\ & \ddots & \\ 0 & & D_n \end{pmatrix} \qquad\qquad \varkappa = \begin{pmatrix} \varkappa_1 & & 0 \\ & \ddots & \\ 0 & & \varkappa_n \end{pmatrix}$$

$$Y_1(x) = \begin{pmatrix} e^{\varkappa_1 x} & & 0 \\ & \ddots & \\ 0 & & e^{\varkappa_n x} \end{pmatrix} \qquad\qquad Y_2(x) = \begin{pmatrix} e^{-\varkappa_1 x} & & 0 \\ & \ddots & \\ 0 & & e^{-\varkappa_n x} \end{pmatrix}$$

$$P = \begin{pmatrix} 1 & 0 & 0 \dots 0 \\ A_{21}^1 & 1 & 0 \dots 0 \\ A_{21}^1 A_{31}^2 & A_{32}^2 & 1 \dots 0 \\ \text{-----------------------------------} \\ A_{21}^1 \dots A_{n1}^{n-1} & A_{32}^2 \dots A_{n2}^{n-1} & \dots \dots 1 \end{pmatrix}$$

$$A_{\beta\alpha}^\alpha = \frac{P_\alpha \varkappa_\alpha^2}{\varkappa_\beta^2 - \varkappa_\gamma^2}$$

The vectors $\bar{a}_1$ and $\bar{a}_2$ are determined by the boundary conditions, and $\bar{a}_1 = 0$ if x_1 is infinite.

The application of these results to the calculation of the flux in the thermal shield of a reactor consists of the following steps:

1. The two-group core-reflector criticality problem is first solved and the thermal and fast flux at the core-reflector boundary is determined. It is then assumed that the energy distribution of the fast flux is $1/E$ and the multi-group fast fluxes are calculated subject to the condition that their sum equals the fast flux previously obtained.

2. These fluxes are used as the boundary condition in a Case I problem which consists of the reflector of thickness x_1 and an infinite thermal shield. The currents are evaluated at the reflector-shield boundary.

3. These currents are used as the boundary condition in a Case II problem which consists of a thermal shield of thickness x_1 less the extrapolated boundary. The fluxes in the shield and the leakage at the outer boundary can then be calculated.

4. For a cylindrical reactor a simple correction is made to the above results by multiplying $\phi(x)$ and $J(x)$ by $\sqrt{x/R}$, where R is the core radius and x is the distance measured from the core boundary.

Six-group calculations have been carried out for a 76-centimeter graphite reflector and a 15.8-centimeter iron shield. The group constants were calculated from cross sections given in AECD-2040 and are listed in Table I.

The data for graphite have been adjusted to be consistent with the experimental values for the age.

TABLE I

Group	E(ev)	Graphite			Iron		
		$x^2 (cm^{-2})$	D(cm)	p	$x^2 (cm^{-2})$	D(cm)	p
1	$2x10^6 - 3x10^4$	0.00645	1.18	1.0	0.00205	1.17	0.992
2	$3x10^4 - 10^4$	0.0588	1.06	1.0	0.00429	1.61	0.991
3	$10^4 - 142$	0.0150	1.06	1.0	0.0159	0.449	0.947
4	142 - 1	0.0128	1.06	1.0	0.0397	0.372	0.640
5	1 - 0.074	0.0250	1.106	1.0	0.191	0.367	0.257
6	thermal	0.000395	0.906	1.0	0.324	0.364	-

Figure 13 shows the fluxes in an infinite iron shield as obtained from Case I. Figure 14 shows the fluxes in the 15.8-centimeter iron shield as obtained from Case II.

This method can be extended to multi-region shield calculations without incurring an unreasonable amount of computational labor by doing two regions at a time, the second region in each case except the last being taken as infinite. The boundary condition for the problem for each pair of regions is obtained from the preceding two-region problem by evaluating the current at the interface between the two regions. The same number of groups must be used in each problem, and a sufficient number should be used so that a reasonable representation of the cross section vs energy curves in each region can be made by taking constant values for $\sigma(E)$ over each group. For a graphite-sodium-iron-concrete system it was decided that six groups was a reasonable number to choose. Six-group computations for the radial and axial SRE fluxes are in progress.

An experiment has been planned in which iron slabs will be placed on top of the WBNS reflector and the thermal flux measured as a function of position through the iron. These measurements will be compared with the thermal flux for this geometry as calculated by the above method. The results of this comparison will indicate the reliability of this type of calculation and will also be useful in predicting better values of the neutron leakage to be expected in SRE.

34
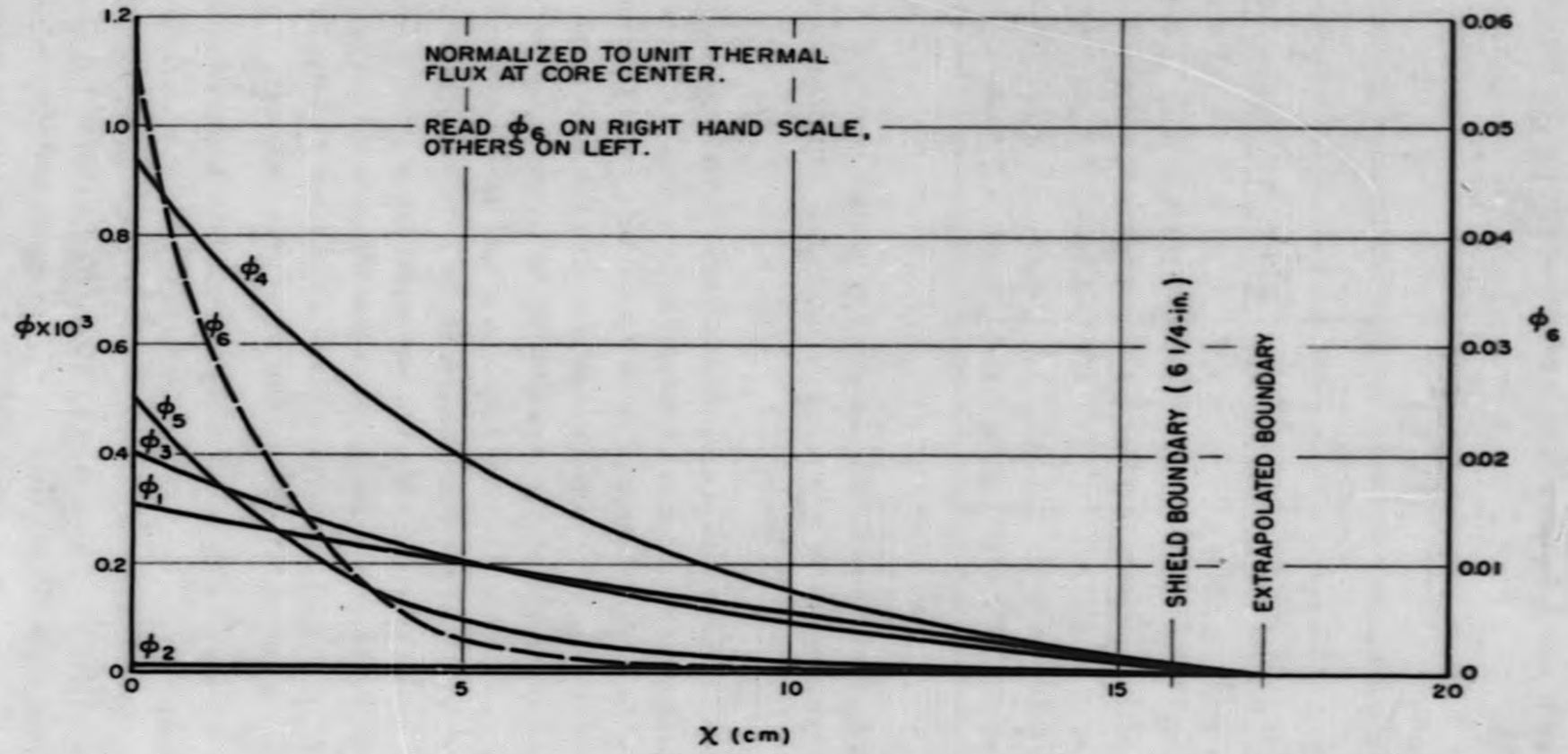
Fig. 13. Six-Group Flux in Infinite Iron Shield
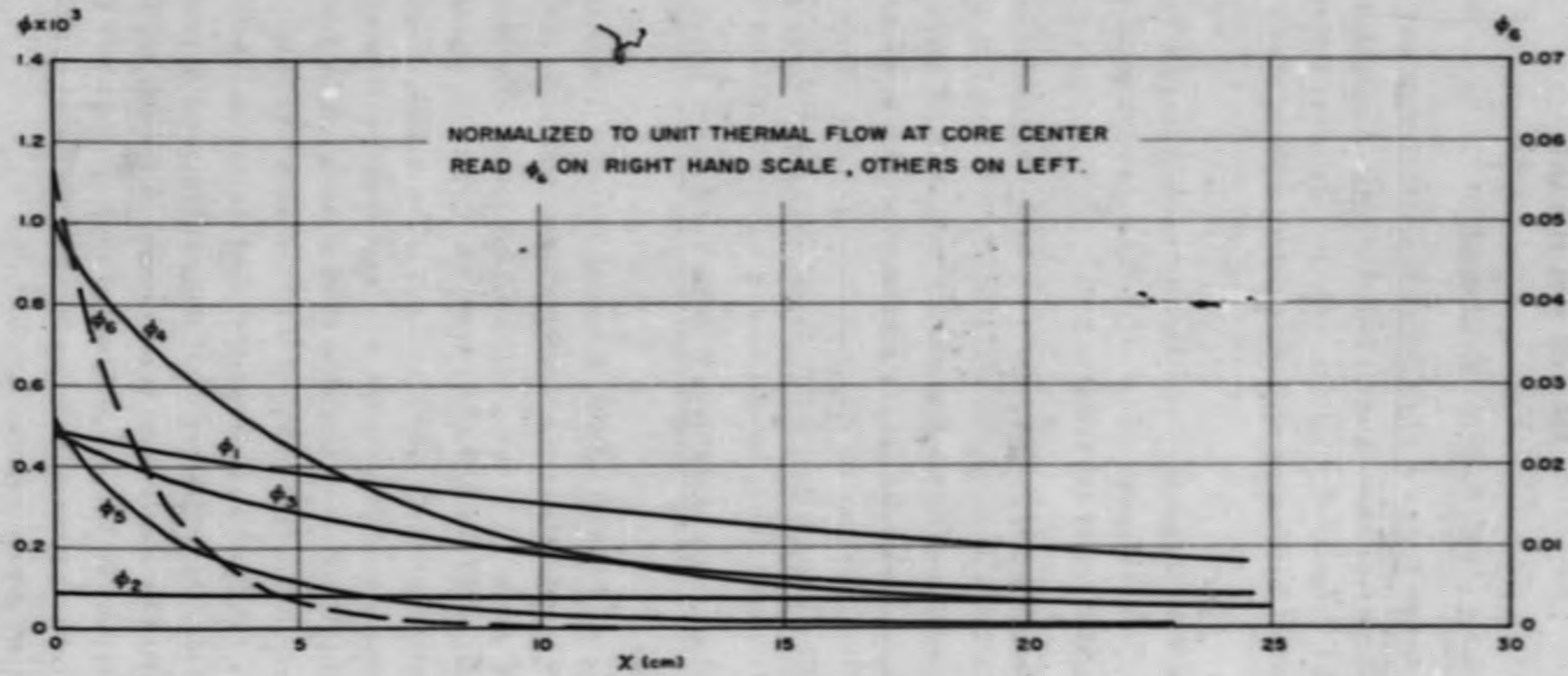
Fig. 14. Six-Group Flux in 6 1/4-Inch Iron Shield

III. REACTOR FUEL ELEMENTS

A. Metallurgy of SGR Fuel (B. R. Hayward)

1. **Hollow Slugs** - A single hollow tube fuel element may have significant advantages over a cluster of small diameter rods. Among these are nuclear parameters, fabrication simplicity, reduction in number of pieces to be handled. A test batch of large hollow cylinders has been made by powder metallurgy at Sylvania.

One of the ten powder-compacted hot-pressed uranium hollow slugs has been completely sectioned and is currently being examined for uniformity through metallography and hardness tests.

A large thermal cycling furnace has been designed and built for cycling the large hollow cylinders (2.42 inches OD by 1.38 inches ID by 4 inches). The hollow cylinder is vertically mounted in a vacuum sealed pyrex tube which is raised and lowered in and out of a stationary furnace, by means of a cam operated program controller and a series of limit switches. Tests with dummy slugs indicate the slug heats quite uniformly and will require an approximate cycle of 35 minutes heating and 85 minutes cooling for cycling between 100° C and 500° C.

2. **Dimensional Stability of Uranium and Uranium Alloys at High Temperatures**

a. **Uranium Alloys** - A number of powder-compacted uranium specimens have been thermal cycled from the lower alpha phase (200° C) to the beta phase (700° C) for a test of approximately 500 cycles. The specimens were powder-compacted uranium alloys of Bi, Nb, Cr, Al, Si, and Mo. All of the alloys were hot pressed. The results are shown in Figs. 15 and 16. As illustrated, some of the alloys showed very large dimensional changes and others were relatively stable. A tabulation of all of the results to date indicates that the hot-pressed alloys of U-Nb and U-Cr are much less stable in this cycling test than uranium alloys of comparable compositions which were cold-pressed and sintered. The cold-pressed and sintered specimens however have lower densities than the similar hot-pressed alloys. A possible explanation for the greater stability for the cold-pressed and sintered alloys may be that the more complete alloying takes place during the sintering operation (~1000° C) than during the hot-pressing operation (~600° C).

Uncycled specimen. All specimens (Figs. 15 and 16)
are to scale and all specimens were approximately
the same size as this specimen.

U-Bi, 1.0 w/o Bi
Change in diameter   = +20%
Change in length   = +16%
Surface   = Severely cracked and bumpy
Internal porosity   = Many small and large holes

U-Nb, 1.6 w/o Nb
Change in diameter   = +27%
Change in length   = +65%
Surface   = Bumpy and porous
Internal porosity   = Very porous

U-Cr, 1.0 w/o Cr
Change in diameter   = +8%
Change in length   = -9%
Surface   = Slightly rough
Internal porosity   = None

Fig. 15.   Results of 500 Thermal Cycles (200 - 700° C) on
Powder Compacted Uranium Alloys

DECLASSIFIED

U-Al, 1.0 w/o Al
Change in diameter = +23%
Change in length = -13%
Surface = Rough and badly cracked
Internal porosity = One medium size hole

U-Si, 0.49 w/o Si
Change in diameter = +5%
Change in length = +3%
Surface = Slightly rough
Internal porosity = None

U-Mo, 0.35 w/o Mo
Change in diameter = +9%
Change in length = +7%
Surface = Slightly rough
Internal porosity = Some porosity throughout

Fig. 16.   Results of 500 Thermal Cycles (200 - 700° C) on
Powder Compacted Uranium Alloys

The metallographic analyses of this series of alloys after the 200° C to 700° C cycle test revealed the following facts:

(1) The 1.0 w/o Bi-U hot-pressed alloy changed from fine grained to very large grained with the alloying constituent completely reacted and dispersed. The hardness decreased on an average from 273 to 257 DPHN.

(2) The 1.6 w/o Nb-U hot-pressed alloy was fine grained and the Nb was present as globules in the original condition. As a result of the test, the grains grew in a range of medium to large and the Nb appeared completely reacted. The average hardness decreased from 278 to 238 DPHN.

(3) The cycling of the 1 w/o Cr-U hot-pressed alloy resulted in only partial alloying of the Cr and the grain size increased moderately. The average hardness increased from 283 to 365 DPHN.

(4) In the as-received condition the 1.0 w/o Al-U hot-pressed alloy had fine irregular grains with incomplete alloying of the Al. A second phase was present in large agglomerates. The matrix grain size increased and the Al-U compound was more homogeneous and completely reacted as a result of the cycling. The average hardness decreased from 288 to 249 DPHN.

(5) In the 0.49 w/o Si-U hot-pressed alloy the grain size increased from small to medium and the unreacted second phase (perhaps Si compound) remained in large agglomerates. The average hardness increased from 297 to 347 DPHN.

(6) As a result of the test, the 0.35 w/o Mo-U hot-pressed alloy became somewhat porous throughout; the alloying constituent was still incompletely reacted and the irregular shaped grains varied from small to very large. The average hardness changed very little, from 272 to 278 DPHN.

b. Unalloyed Uranium - To evaluate further the large dimensional changes, as previously reported, resulting from alpha-beta thermal cycling between 630° C and 680° C, an alpha-rolled rod specimen was cut perpendicular to the axis of rolling from a 2-inch diameter rod. After 200 alpha-beta cycles the rod length increased only slightly but the rod became severely oval shaped

along its entire length. The short axis of the oval was the original axis of roll-ing. This dimensional change agrees in direction to the decrease in length found in the other specimens. In addition to the dimensional changes, there were sur-face cracks but with no particular pattern.

B. Metallurgy of Breeder Fuel (F. E. Bowman, B. R. Hayward)

A program has been started to establish the performance of thorium-base-uranium alloys as fuel materials for a sodium graphite reactor. Present data indicate that thorium base fuel elements may be operated at higher temperatures and may be carried to greater burn-up than uranium fuel elements. Further-more, the use of thorium-base fuel may result in a reactor with a breeding ratio of one or higher, which would replace the fuel it burns.

In conferences at ANL it was indicated that little is known of the physical metallurgy of the Th-U system in the region of interest. Some alloys have been prepared and are now undergoing irradiation in the MTR. Preliminary work has been started at NAA toward studying the solubility of uranium in thorium. An experiment is underway to establish the feasibility of obtaining quantitative solubility data through the use of diffusion couples. A thorium specimen has been prepared by melting iodide material in a Kaufman type arc-melting furnace in order to retain the highest possible purity. Powder-compacted uranium will be used for the other member of the couple. It is hoped that from the initial couple a relationship between uranium content and thorium alloy lattice param-eter can be established. If this can be established, then X-ray diffraction will provide a convenient means for analyzing subsequent specimens.

In conferences at SEP and at FMPC both concerns have indicated a willing-ness to undertake the production of pilot quantities of such Th-U alloys as might prove to be of interest for the SGR.

C. Determination of Maximum Operating Temperature Limits of SGR Fuel

1. Restrained Slugs (B. R. Hayward) - In uranium metal fuel elements operating above 1200° F (alpha-beta phase transformation), without greatly in-creasing the sodium coolant temperature, there will be a temperature gradient within the fuel element in which the lower density beta phase region at the fuel element core is entirely surrounded by a higher density alpha phase region. The change in volume, due to the change in density, results in a large stress

which may either (1) rupture the alpha shell, (2) exceed the yield strength of the alpha shell resulting in a permanent over-all dimensional increase, or (3) cause a temporary increase in dimensions which would return to normal upon a decrease in temperature. The relative cross section of beta material to alpha material and the geometry and temperature level are important factors.

Laboratory tests were made to simulate the above conditions without the large temperature gradients in which duplicate samples of stainless steel-jacketed alpha-rolled uranium slugs were cycled 400 times between 630° and 680° C. The wall thickness of the stainless steel jacket varied between 0.020 inch and 0.060 inch. The ends were unrestrained. The 0.020 inch wall specimens became progressively more out of round as the number of cycles increased, with severe distortion after 400 cycles. The jacket remained intact. The 0.040 inch wall specimens had a minor increase in diameter (0.005 inch maximum) between zero and 100 cycles and only a slight increase (0.001 inch maximum) between 100 and 400 cycles. After 100 cycles with the 0.060 inch wall specimens, the maximum increase in diameter was 0.003 inch. This diameter increased insignificantly after 300 additional cycles. There were no jacket failures in either the 0.040 inch or 0.060 inch jacket specimens. A previously reported jacket rupture in a 0.060 inch wall jacket was not duplicated in these tests. All of the unjacketed control specimens with the above tests were similar in the direction and amount of distortion. The following table indicates the typical change in dimensions vs the number of cycles of the unjacketed control specimens.

TABLE II

Number of Cycles	Max. $\Delta l \%$	Max. $\Delta d \%$
100	-7.0	+6.1
200	-10.8	+9.8 (slightly out of round)
400	-12.4	+21.6 (out of round)

2. Resistance Heating Experiment (B. R. Hayward) - The 500 kva thermal cycling unit at California Research and Development Company was partially tested for use with a full scale SRE fuel slug. In this apparatus, the dimensional

SECRET

behavior of a slug would be studied under temperature conditions simulating a
beta phase core and an alpha phase surface. This equipment had not been pre-
viously checked out for leaks and operating procedures. Limited results indi-
cated the equipment is more than adequate for heating; however, the high surface
temperatures desired were not achieved. The surface temperature can be in-
creased by using either (1) a high temperature coolant such as Dowtherm, or
(2) a thermal barrier on the slug which would permit the use of a water coolant.
There are about 150 large and small threaded joints in the present cooling sys-
tem which makes the use of Dowtherm doubtful. Under present consideration is
the use of similar equipment at the reactor site.

3. Thermal Conductivity of Uranium (J. J. Droher) - Data on the ther-
mal conductivity of unalloyed uranium are very meager in the temperature
range above 400° C. Further measurements of the radial thermal conductivity
of alpha-rolled beta-treated uranium have been made. Data confirming results
previously reported in NAA-SR-1027 were obtained for temperatures up to the
gamma range at 770° C. Attempts to extend the measurement up into the high
gamma range have been unsuccessful due to failure of either the main or an end
heater. The most successful main heater for the particular geometry has been
found to be 0.010 inch diameter molybdenum wire wound on a lavite core. An
insert of 0.125 inch diameter molybdenum rod prevented the lavite core from
warping when the heater was brought up near the softening temperature of the
lavite. It also aided in maintaining the heater at a more uniform temperature
along the length. The end heaters have been made of Kanthal embedded in
alundum cement in grooves in a lavite disc. This heater design will have to be
modified because failures caused termination of the last two runs.

The apparatus to measure the conductivity of uranium in a longitudinal
direction is based upon the Forbes bar method.[13] This apparatus has been
modified for measurements with uranium specimens and is shown in Fig. 17.
A stainless steel tube encloses the specimen and the heavy wall copper tube.
An inert atmosphere of argon or helium is maintained in this tube to prevent
oxidation of the specimen at elevated temperatures. The specimen length has
been extended from 12 inches to 40 inches so that electrical contacts are made
out beyond the furnace zone. This allows a steel to uranium screw contact to
be made without the formation of the iron-uranium eutectic when the center

42

SECRET

POSITION OF THERMOCOUPLES INDICATED BY V.
COUPLES ARE 0.8 IN. APART ALONG SPECIMEN
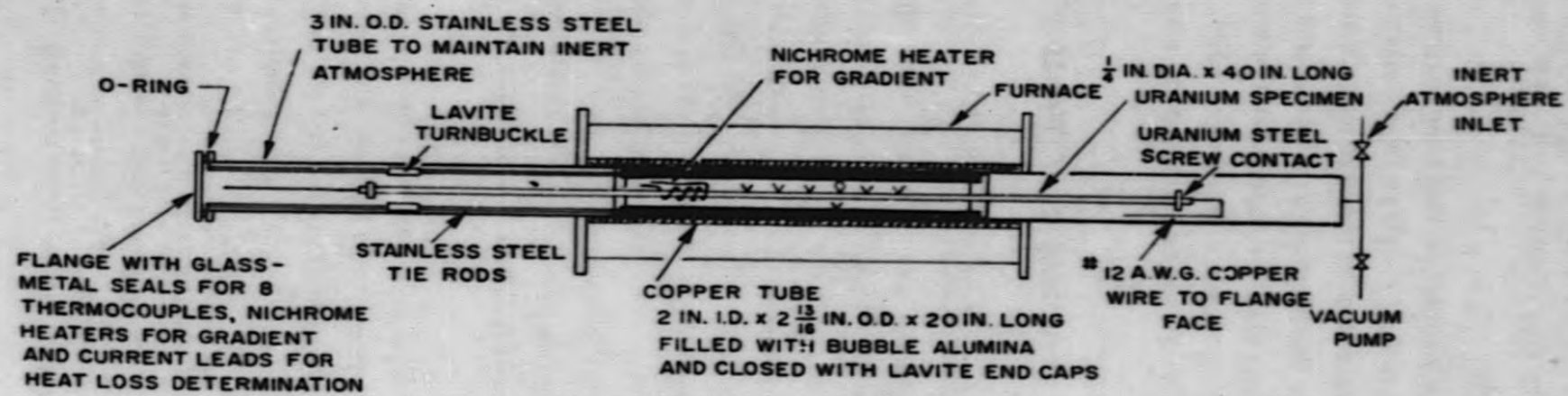
Fig. 17. Schematic of Apparatus for Longitudinal Thermal
Conductivity Measurement (Modified for Uranium)

portion of the specimen is heated up to 1000° C. It is also hoped that discrepancies due to end heating effects caused by contact resistances will be decreased with the longer specimen.

The end plate was modified so that it was rigidly connected to the heavy wall copper tube by tie rods of stainless steel connected with a lavite turnbuckle. The entire assembly could then be inserted into the stainless steel tube with minimum damage to the thermocouples. It was found that a number of 0.005 inch diameter platinum vs platinum-rhodium thermocouples were broken during assembly even with the increased structural stability. Thermocouples of 0.010 inch diameter chromel vs alumel will be used for greater strength.

IV. REACTOR MATERIALS

A. Engineering Evaluation of Graphite (R. E. Durand, D. J. Klein)

An experiment is under way to determine the effect of reactor irradiation on the thermal conductivity of type AGOT-CSF graphite in the range of temperatures 300° to 700° C, covering the design temperatures of the SGR. One set of three samples has been irradiated for four weeks in the L-42 position tangent to the surface of the MTR core, where the thermal flux is 4×10^{14} neutrons/cm^2 sec. Success in the measurements on these first samples was hampered by (1) failure and subsequent repair of a gas seal, which had the effect of changing the gas pressure surrounding the samples, hence their temperatures, during the run, and (2) fluctuation of the thermocouple readings of unknown origin. An attempt is made to minimize the effect of these fluctuations by an averaging process in taking the data.

The data have not yet been corrected for certain geometrical factors (e.g., finite length of cylindrical samples), which are expected to be of the order of 1? per cent. The results of the run show saturation of the thermal conductivity at 0.6 watts cm^{-1} (C°)$^{-1}$ for a sample irradiated at 425° C, and 0.4 watts cm^{-1} (C°)$^{-1}$, for samples irradiated at 635° and 660° C. These samples showed an unirradiated value (in the same apparatus) of 1.2 watts cm^{-1} (C°)$^{-1}$ at 350° C, which agrees with extrapolated values of other measurements made in this laboratory. The exposure were carried out to 1.3, 2.9, and 2.9 kwh/gm, respectively, for the three samples. The larger of these exposures

corresponds to approximately one year in SRE. It was impossible to follow the build-up of damage, since saturation seemed to occur before 0.2 kwh/gm, the first point of measurement in the case of the 425° C sample.

The second set of samples is ready for irradiation, and is expected to be irradiated during the next quarter. The thermocouples in this assembly have been more securely cemented in place in an effort to reduce the fluctuations in their readings. Sulphur monitors have been included to permit a direct determination of the fast flux.

B. Corrosion and Transfer of Radioactivity by Sodium

1. Transfer of Radioactivity from Zirconium (S. Nakazato, A. M. Saul) - Experiments to study the transfer of Zr^{95} by liquid sodium have been initiated. The experiments will be used to compare the order of magnitude of the Zr^{95} activity transferred with that transferred from Type 347 stainless steel. The effect of oxygen concentration in the liquid sodium on the transfer will be studied. Further, the "gettering" action of the Zr will be determined.

The experiments will be identical with the capsule experiments used to study the transfer of Type 347 stainless steel, as reported in NAA-SR-284. In the present experiments, Zr foils 2 inches by 0.5 inch by 0.005 inch will be used as a source. These foils were prepared by irradiation in the MTR to a total nvt of 10^{19} neutrons/cm^2. The capsules will be 1 inch outside diameter by 12 inches long, of Type 304 stainless steel. A temperature gradient of 700° to 400° C will be maintained from the bottom to the top of the capsule.

The foils have been returned from the MTR, have been loaded into the capsules, and the capsules should be filled with sodium and the soaking period started within the next week or two.

C. Organic Coolant Investigations (E. L. Colichman)

Certain organic compounds show promise of being useful as special purpose coolants in reactors as well as perhaps auxiliary coolants in sodium graphite type reactors. Of the more stable components, the terphenyls seem to have

the most desirable physical properties and, therefore, are being investigated here as being possible organic coolants. Advantages, disadvantages, and possible reactor applications for such materials are listed below.

1. Advantages

    a. Greater safety. Do not react chemically with water, liquid metals, or uranium.

    b. Low corrosion. Do not scale heat transfer surfaces, permit use of lower cost materials of construction.

    c. Good moderating properties. Permit smaller reactor size than Be or graphite.

    d. Low vapor pressure. Permit use of low pressure coolant system.

2. Disadvantages

    a. Poor heat transfer characteristics compared with Na.

    b. Subject to decomposition by heat and radiation. Will sludge and form infusible mass if decomposition is allowed to proceed uncontrolled.

3. Applications

    a. Primary coolant and moderator at temperatures up to 750 - 850° F.

    b. Secondary coolant up to about 900° F.

    c. Shield coolant.

Recent progress in the determination of the practical limits of application of these coolants at various temperatures, under the influence of different kinds of radiation, are reported in NAA-SR-1026; details of procedures and experimental methods are given in that document.

The pump loop described in NAA-SR-1026 has been operated with m-terphenyl up to about 750° F. Due to operational difficulties encountered in using the various components at high temperature, no significant heat transfer data have yet been obtained. These difficulties are gradually being surmounted.

The greatest difficulty was experienced with the Viking pump. The pump packing did not hold the fluid, the bearing cracked, and the head gasket burned. The electrical insulation in the Waugh flowmeter could not withstand the high operating temperature and failed in service.

SECTION B
SODIUM REACTOR EXPERIMENT

V. REACTOR DESIGN AND EVALUATION

A.   General Engineering and Physics Evaluation   (W. E. Abbott)

The fuel enrichment for the SRE is being determined by two independent analytical approaches.   The "hot, poisoned" enrichment is being calculated on the basis of a criticality loading with 31 fuel elements.   The required enrichment so calculated is then increased to provide the necessary excess reactivity for control and compensation for the poisoning effects of experimental equipment in the reactor.   A survey is also being made of all available data regarding reactor critical experiments.   The correlation between the theoretical predictions and the experimental data is being determined.   Experimental data from critical and exponential experiments are being used to check the calculations for the SRE core.   Calculations to date indicate the required enrichment will be between 2.0 and 2.5 per cent.

An independent machine calculation will be made to check the hand-computed enrichment mentioned above, which is required to obtain criticality in the SRE.   This calculation will be a two-region, eight-group representation. An IBM 701 machine has been chosen in preference to a UNIVAC because checking of the coding of a problem for the UNIVAC would require an unwarranted amount of time and effort for the single SRE criticality problem.

B.   Reports, Specifications, Drawings

Quarterly reports describing the progress on the SRE program will be issued to cover engineering analysis, development, design, and construction. A topical report is now in process which will emphasize the design and operational features of the SRE.   Special emphasis will be given to the over-all safety of this sodium-graphite reactor.

Specifications required for equipment, materials, and processing procedures are being prepared as required.   They are being written according to North American Aviation, Inc. (NAA) Standards and are being issued through normal company channels.

A preliminary group of 39 scope drawings for the reactor has been completed. The majority of design emphasis is now being devoted to component assembly and detail drawings.

C. Land, Buildings, Services (J. F. Stolz)

The proposed construction area for the SRE is at the Santa Susana NAA Field Laboratory which is located in the Santa Susana Mountains, 20 miles northwest of the center of Los Angeles. The present work has been concerned with the layout of the site and the arrangement of the Reactor Building and the Engineering Test Building. Progress to date is reported under the following headings:

1. Site - Three site areas at the Field Laboratory have been compared with regard to cost, future expansion area, and over-all desirability. Survey work has included both ground and aerial topographic mapping, drainage studies, and the location and testing of wells. The site now tentatively selected is indicated in Fig. 18. It meets the requirements that the reactor shall not be closer than 2,000 feet to the southerly NAA property line, ample security control area is available, and surface water drainage may be controlled. The arrangement of the buildings and facilities at the site are shown in Fig. 19. Space is available for future expansion of both Reactor and Engineering Test Buildings. Space is also available for the future construction of a "water boiler" reactor. The arrangement of the buildings permits the maximum economy of services and utilities such as roads, drainage, water supply, fire protection, electrical power distribution, and security (Fig. 19).

2. Reactor Building - The Reactor Building (Fig. 20) consists of the following areas:

    a. High Bay Area (46 feet high, 5,850 square feet).
       This area houses the reactor primary cooling system, traveling bridge crane, a service and storage area for the fuel handling coffin, and a dry underground storage area for radioactive materials. This building area is windowless and is constructed to minimize air infiltration.

    b. Low Bay Area (4960 square feet).
       This area will contain the Reactor Control Room, various experimental facilities, and the service equipment required for the building and reactor.

Fig. 18. Santa Susana Facility and Surrounding Area

SRP29-24
Official Use Only

c. Secondary Cooling System Housing (320 square feet).

This area will enclose those units of the secondary cooling system which are above ground and which are serviceable because they are not radioactive.

d. Sodium Service Area (480 square feet).

The sodium melt tanks and other units of the sodium service system will be located in this area.

e. Radioactive Laboratory Area (2280 square feet).

This area will contain a hot cell for dismantling irradiated fuel elements and other items for inspection and testing. All contaminated work will be performed in this area, and access will be through change rooms which contain the necessary monitoring and decontamination equipment.

f. Irradiated Fuel Handling Area (1120 square feet).

This area contains a pond in which irradiated fuel elements will be cleaned and stored. Other components, such as control rods and safety elements will be stored here following removal from the reactor.

g. Administrative Area (1320 square feet).

This area contains the administrative offices and the rooms required by Health Physics.

h. Outside Area.

This area is outside of the reactor building and will contain the secondary cooling system piping and fin-fan heat exchangers. A low wall surrounding this area will confine any sodium which may leak from the system.

A traveling bridge crane is located in the High Bay Area to transport the fuel handling coffin, the top shielding plugs, and auxiliary equipment. The fuel handling coffin, when not in use, will be stored in a side bay area adjacent to the main bridge runway. The coffin is self-propelled and may be transferred from the storage runway area onto the bridge. The coffin will service the reactor room area from the reactor to the irradiated fuel storage pond. A 75-ton auxiliary trolley to handle other loads remains on the bridge at all times; it can be placed so it will not interfere with normal operation of the coffin. The over-all length of the bridge runway is approximately 101 feet, the main bridge span
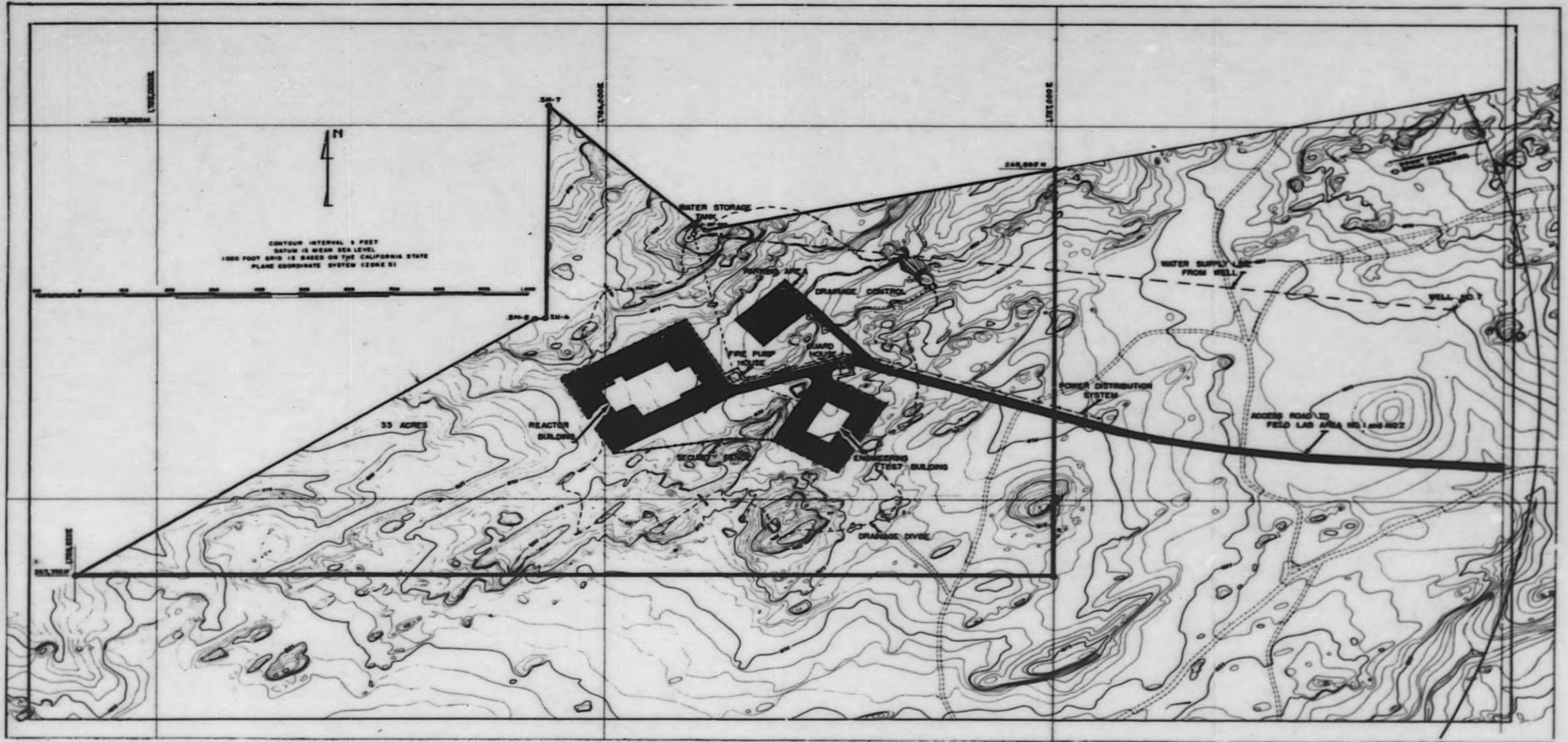
Fig. 19. SRE General Site Layout
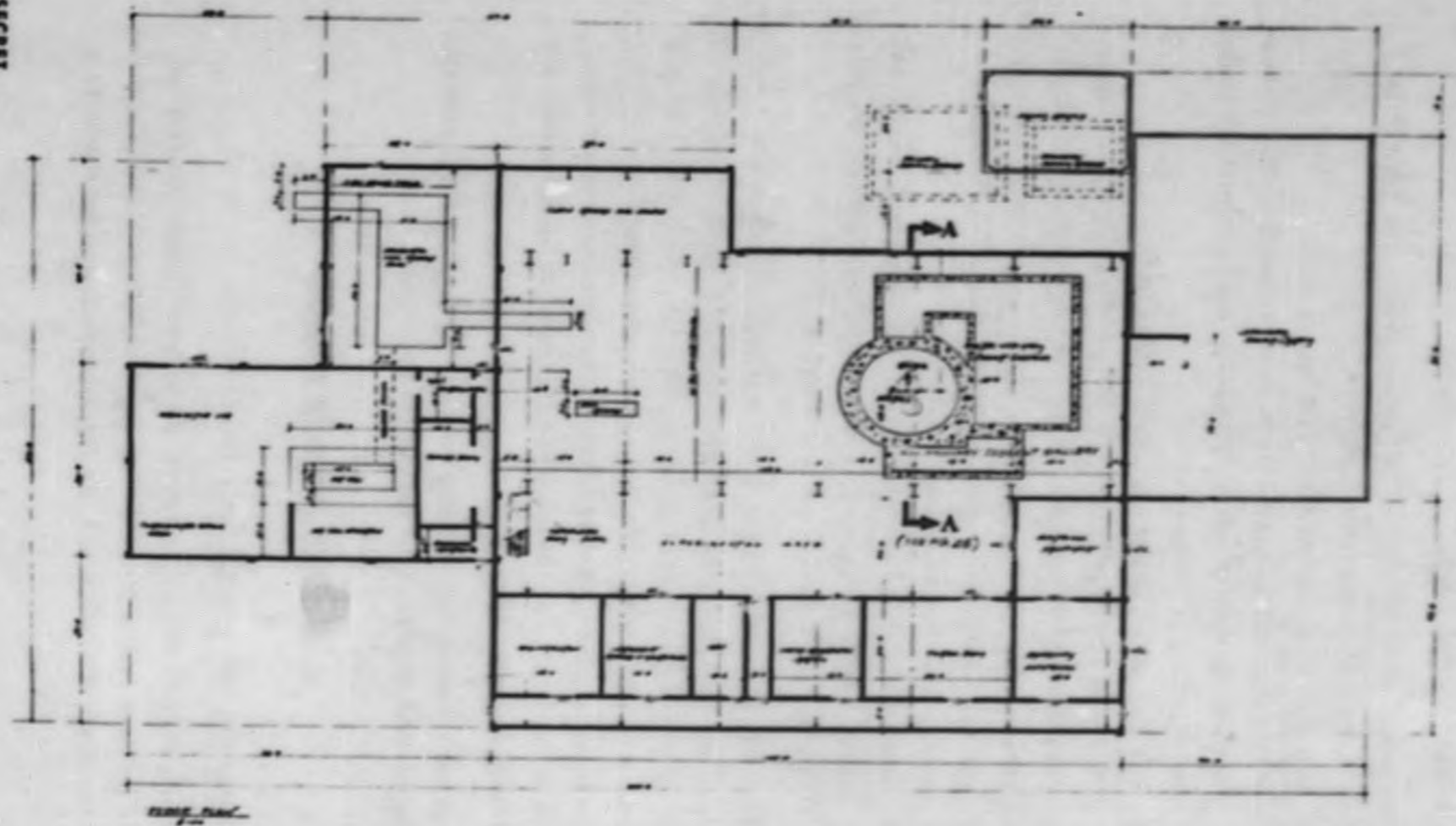
Fig. 20.   Reactor Building Arrangement

is approximately 42 feet, and the distance from the finished floor to the under-side of the bridge is 32 feet clear.

 3. Engineering Test Building - (7200 square feet). The Engineering Test Building is divided into the following areas:

 a. High Bay Area (26 feet high, 2400 square feet).
In this area will be located the facilities required for fuel element fabrication, moderator cell fabrication, and equipment for testing and annealing operations.

 b. Low Bay Area (12 feet high, 2500 square feet).
This is an experimental area required for fabricating and testing components to be inserted into the reactor. Engineering data regarding control rods, corrosion, dimensional stability, and thermal characteristics will be obtained here. This area will contain a storage vault for SF materials.

 c. Administrative and Laboratory Area (10 feet-6 inches high, 2300 square feet). This area will contain offices, electronic laboratory, counting room, lavatories, and showers.

All building construction will be of the noncombustible type with reinforced concrete floors and corrugated metal superstructure. A masonry wall will enclose the SF material vault and fuel fabrication area. A masonry wall will also separate the shops and laboratories from the administrative area. All areas of the building will be provided with thermostatically controlled industrial forced air heaters. The electrical requirements are approximately 400 kva, 4160 volts, 3-phase, 60 cycle.

All general construction including finishes, hardware, doors, painting, etc. will follow NAA specifications and standard practice.

VI. FUEL AND PRODUCER ELEMENTS

A. Development of SRE Fuel Elements (W. J. Hallett)

The original fuel element design for the Sodium Graphite Reactor contained a 12 foot long section of uranium slugs. This design has been modified to reduce the length of uranium to 6 feet for the Sodium Reactor Experiment,

as shown in Fig. 21. The guide fins above and below the fuel rod section assist in guiding the fuel element into position when charging into the reactor core. The design of the weld joint between the fuel loading jacket and the end plug has been modified to improve the strength. Tensile tests indicate the joint is now stronger than the jacket tubing.

Recently acquired information indicates a lack of heat-treating data for the originally desired U-Zr (2 w/o Zr) wrought alloy. Difficulty was also encountered in producing large homogeneous ingots of this U-Zr alloy. The fuel material specification has therefore been changed to beta-treated unalloyed uranium.

Metallographic examinations of three or four stainless steel jacket tube specimens indicate a large number of nonmetallic inclusions. The fuel jacket tube must have a minimum number of inclusions or flaws which might reduce the life of the element or result in a rupture of a jacket. It may be necessary, in order to obtain tubing of the required quality, to use vacuum melted ingots and select the bloom as is done for bearing grade steel.

B. Nondestructive Testing of Fuel Element Components (J. Droher)

It is important that no voids exist in the liquid metal bond between the uranium slugs and the stainless steel jacket. Such voids would interfere with the heat flow from the slugs to the sodium coolant and might cause the slugs to over-heat. Several nondestructive bond testing methods have been previously described.[5,6] To date the most promising production test for voids in the bond appears to be the Cyclograph. The Cyclograph was used for extensive tests on seven, 12 foot long SGR fuel rods. Four of the seven rods were filled with the NaK eutectic and three were filled with sodium as a bond. Cyclograph traces were then made of each rod after welding in the end cap and before any heat treatment. Using a coil frequency of 4 kilocycles per second, it was possible to determine that the liquid metal bond filled the annulus between the uranium slugs and the jacket. The best traces were obtained from the NaK bond; the sodium bond gave rather poor traces. These tests were carried out at room temperature and the sodium was solid, while the NaK was liquid. This may account for the indicated superiority of NaK over sodium.

Fig. 21.   SRE Seven-Rod Fuel Element
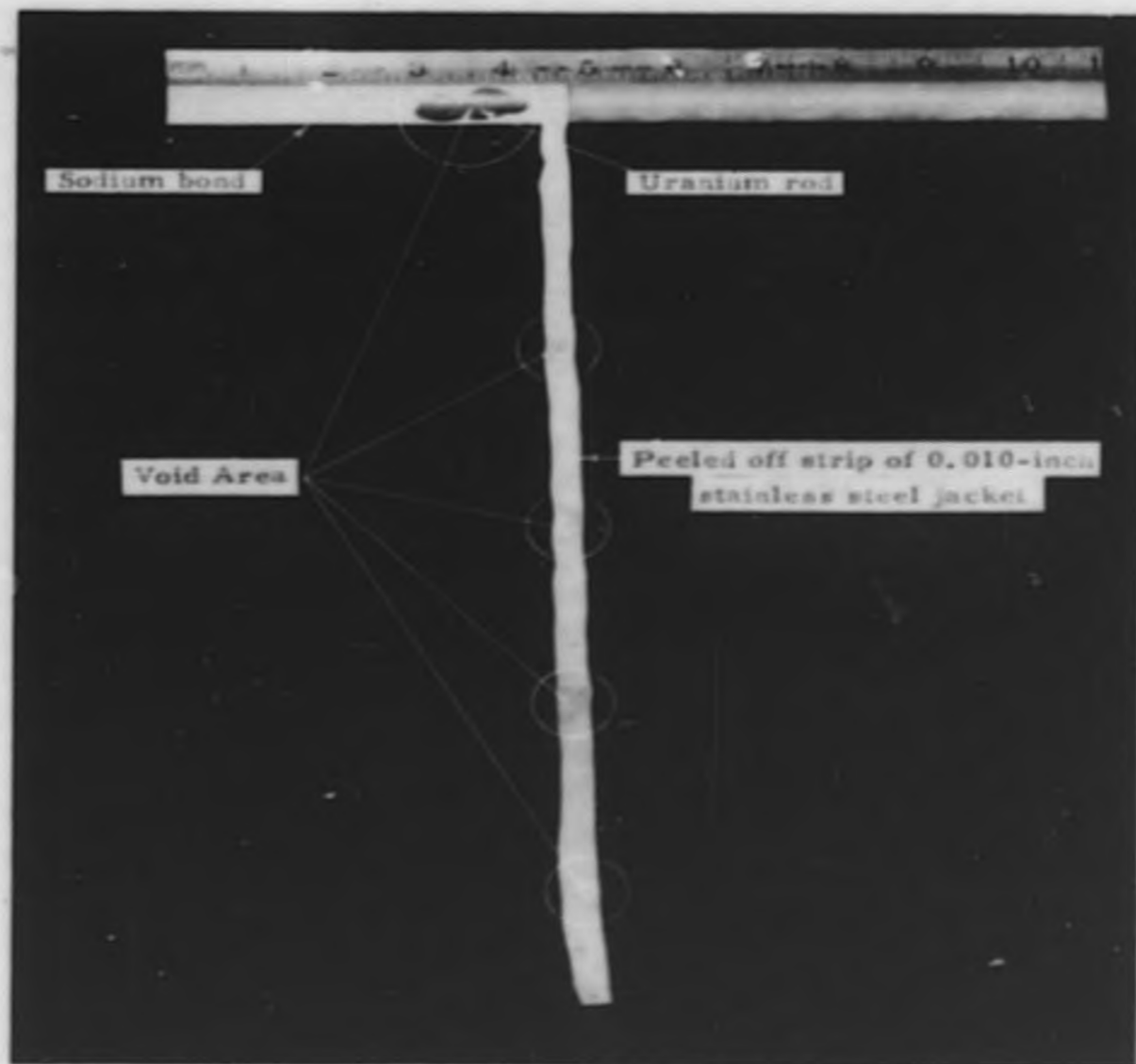
Confidential   SRP 47-87E

Fig. 22.   Large Void in Sodium Bond of Fuel Rod

In order to further evaluate the sensitivity of the Cyclograph the uranium slugs had been prepared with three different surface conditions: (1) slightly oxidized as received, (2) pickled in nitric acid, (3) polished slugs. The Cyclograph indicated no superiority of the pickled or polished surfaces over the light oxidized surface when the fuel rod contained either NaK or sodium.

Seven of the fuel rods were then assembled into a fuel element and heat-treated by soaking in sodium for 100 hours at 800° F. The fuel element was then withdrawn from the sodium, water sprayed and soaked to remove the external sodium, and disassembled. Each of the seven rods was then tested with the Cyclograph. The traces indicate less deviation from a straight line for the NaK bonded rods than for the sodium bonded rods. This seems to indicate the NaK bonding had been somewhat improved, while the heat treatment had not removed many voids from the sodium bond. In order to examine the bond the stainless steel jacket was removed from one of the rods by peeling back along a helical spiral. The sodium bonded region and a typical large void is shown in Fig. 22. A layer of oxide forms on both the sodium and the stainless steel jacket upon exposure to air. The void area on the uranium slug and the regions on the jacket which were adjacent to the void show a complete absence of sodium. The photograph also shows that the sodium adhered tenaciously to both the uranium and stainless steel, and that its adhesive strength to these materials was greater than its cohesive strength to itself.

In order to freeze the NaK in a NaK bonded fuel rod, the rod was placed in a kerosene dry-ice bath. The jacket was then cut along its entire length in a milling machine and pulled back to permit inspection of the solidified NaK. The NaK was well bonded, and only a line void was observed. This is believed due to the liquid NaK flowing away from the top surface of the slugs when the rod was placed in a horizontal position before freezing in the kerosene dry-ice bath. The bond was tenacious and wet both the stainless steel jacket and the uranium slugs.

The tests to date with the Cyclograph indicate it is not sufficiently sensitive to clearly distinguish between pin holes and the minor surface variations which exist in all tubing. Point probes have also been unsuccessfully used. Other methods of increasing the Cyclograph coil sensitivity are now being

investigated. Preliminary tests using a Reflectoscope, an ultrasonic instrument, were made on tubing, using a 5-megacycle searching unit. This instrument indicated some promise and tests are continuing.

C. Fuel Element Drop Tests (W. J. Hallett)

During the operation of changing a fuel element in the reactor, a failure of the handling equipment could result in dropping the fuel element into the core. Under the worst conditions a fuel element could fall approximately 24 feet before being abruptly stopped when the shield plug reaches its normal position in the reactor top shield. If the uranium slugs have sufficient kinetic energy to rupture the fuel jacket, the slugs would fall into the plenum chamber below the core. This would contaminate the sodium coolant with fission products and present a very difficult recovery problem. It was impossible to calculate whether or not the fuel rod jackets would rupture under these conditions, and a series of tests were made.

The failure of the stainless steel jacket will depend upon many factors, such as, the quality of the end cap welds, the metallurgical treatment of the jacket, and the temperature of the cladding at the time of fall. Because the impact strength of the jacket will vary significantly with temperature, it was decided to conduct the tests at a temperature simulating that of an accident in the reactor. The amount of energy which the stainless steel jacket can absorb was estimated by integrating stress-strain curves. Calculations indicate that if the jacket were fully annealed and the kinetic energy of the fuel were uniformly distributed, a 12 foot drop at room temperature would rupture the jacket.

Four fuel rods were selected for testing. Each one was securely fixed to a 12-foot long hanger rod of 3/8-inch diameter steel pipe with a flange welded at the top end. The rods were suspended over a fuel storage cell by a cord. They were dropped into the cell by cutting the cord. Since the flange at the upper end of the hanger rod was much larger than the storage cell opening, the rods were abruptly stopped while in free fall. Before dropping, the rods were heated by a clam shell heater to a temperature simulating that expected in actual reactor operation. The four preliminary tests indicate the following:

(1) A fuel element may be dropped 12 feet without rupturing the jacket.

(2) If the jacket ruptures, it tends to shrink around the slugs and prevents most of them from falling out.

This should require the recovery of fewer slugs than originally anticipated and should simplify the recovery problem. Further fuel element drop tests are being planned.

VII. MODERATOR, REFLECTOR, STRUCTURE

A. Reactor Core Tank and Supporting Structure (W. Sanders)

A layout drawing of the reactor core assembly has been completed and detail drawings of the components are now being made. As shown in Fig. 25, the core assembly consists of a 304L stainless steel core tank which contains hexagonal graphite moderator cells individually canned in zirconium. The fuel elements hang vertically in coaxial holes in the moderator cells. Sodium enters through a pipe which discharges into a sodium plenum chamber below a grid plate which supports the moderator cells. The sodium flows upward through the coaxial coolant tubes into a sodium pond above the reactor core. The sodium is drawn from the pond through the coolant circuit and heat exchangers. Surrounding the core tank is a cast iron thermal shield, a quarter inch steel intermediate tank, thermal insulation (fire brick or stainless steel wool), a quarter inch steel plate cavity liner, and a concrete biological shield. Welded on the outside of the core cavity liner and imbedded in the concrete are shield coolant pipes through which toluene will flow. The core tank, as indicated in Fig. 23, is supported on steel support pedestals. All necessary calculations regarding thermal stresses and earthquake loads have been made and are now being checked.

B. Reactor Foundation (J. F. Stolz)

The biological shield serves also as the reactor foundation (Fig. 24) and is made of reinforced concrete. This structure distributes the bearing load to a supporting strata and retains all lateral earth, building column, and other surcharge pressures. The total reactor assembly weighs approximately 400,000 pounds and when combined with the shield itself and other surcharges, produces a foundation soil pressure of approximately 6200 psf. The biological

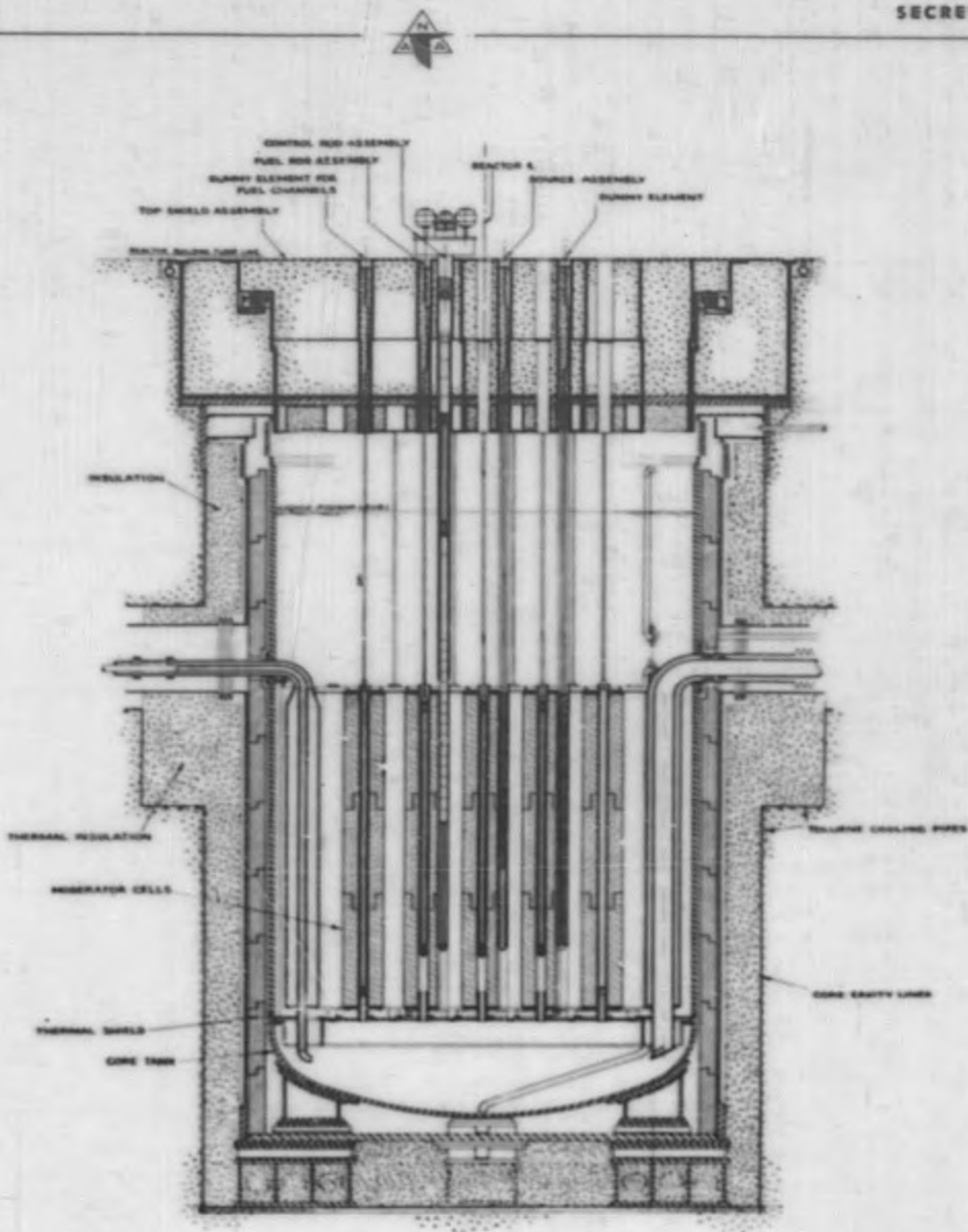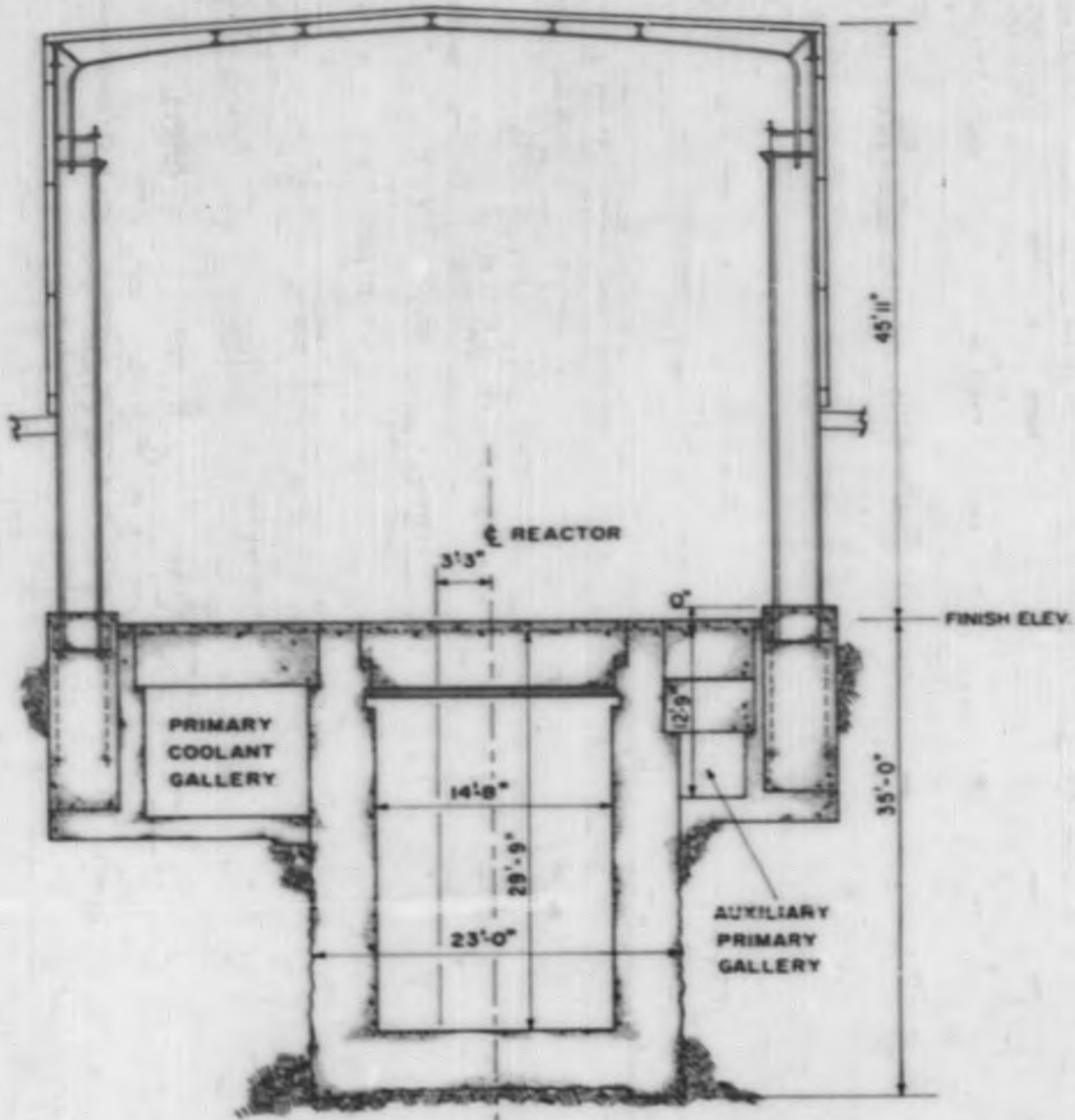Fig. 23. Reactor Core Arrangement

DECLASSIFIED

PRIMARY
COOLANT
GALLERY

REACTOR

3'3"

45'11"

FINISH ELEV.

0"

6'2"

14'8"

28'9"

23'0"

35'0"

AUXILIARY
PRIMARY
GALLERY

SECTION AA SEE FIG. 20

Fig. 24. Reactor Foundation and Biological Shield

shield (reactor foundation) is approximately 4 feet thick based upon a preliminary analysis of the structural and shielding requirements.

Previous soil report data from adjacent areas on NAA Field Laboratory Site were used in making the structural calculations. Final soil surveys will be made as required. Calculations indicate earthquake stability will be safe. Shale seams which promote slippage when permeated with ground water will be grouted and keyed if encountered.

C. Arrangement of Moderator and Reflector Cell Units (J. Facha)

As previously reported[5,6,] the moderator and reflector graphite is encased in hexagonal zirconium cans. The fuel elements are supported vertically in coaxial holes. Control rods, ball safety devices, and experimental channels are located at the corners of the cans as indicated on Fig. 25. A horizontal cross section through one of the moderator units is also shown in Fig. 27.

D. Development of Zirconium Moderator Cell Cans (R. C. Brumfield, W. Cockrell)

The zirconium moderator cell cans are approximately 120 inches long, as shown in Fig. 26. The zirconium for both the side wall and the coolant tube is 0.035 inch thick. Experiments are being conducted to develop the end closures (can ends). Three types are being studied: (1) corrugated, (2) a thick flat plate, (3) a rigid plate with a bellows attached to the lower end of the coolant tube. A design must be selected which will best withstand both hydrostatic pressure and the thermal strain introduced by longitudinal differential expansion between the coaxial coolant tube and the hexagonal side wall.

Several methods for adjusting and controlling the internal pressure in the cans have been considered in order to balance the hydrostatic loads and mitigate the build-up of internal pressures:

(1) Vacuum pack.
(2) Vacuum pack with "getter" to capture gases released by graphite during operation.
(3) Partial filling with helium with "getter".
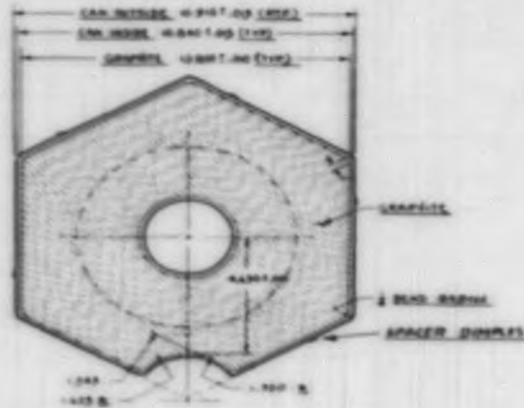
HORIZONTAL CROSS SECTION THROUGH MODERATOR CELL
WITH SCALLOPED CORNER WHICH FORMS A PART
OF WALL FOR CONTROL AND SAFETY ROD CHANNELS
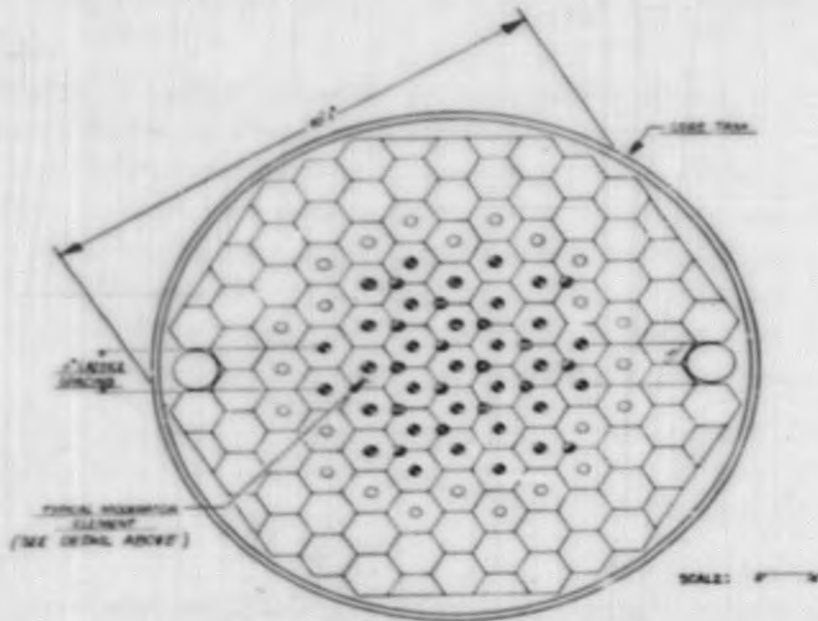
PLAN OF CORE AND REFLECTOR ARRANGEMENT

Fig. 25.   Arrangement and Detail of Moderator Cells

Fig. 26. Zirconium Canned Moderator Cell

(4) Manifolding to control internal pressure from external source.

(5) Use of snorkel connecting can to helium plenum chamber above the sodium.

Experimental work is now proceeding to evaluate the above methods. In any event the graphite will be out-gassed in vacuum at 1500° F before the final seal-off of the cans. A search for suitable "getter" material is underway.

Stainless steel end fixtures attached to the can will provide a handling attachment, a guide for fuel elements during loading, sodium flow control, and mechanical alignment.
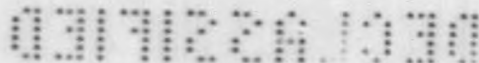
A maximum surface hardness of 170 Brinell has been specified for the zirconium sheet to be used in fabricating the cans. Fifteen zirconium ingots have been produced to date which satisfy this requirement; chemical analyses have also been made. Calculations of the zirconium cross section based on these analyses give a value which is the same as that used for the nuclear calculations for the SRE, namely 0.22 barn. A specification covering the conversion of the zirconium ingot to sheet, strip, and plate has been written, and discussions are under way with several potential vendors. Discussions are also under way with potential fabricators who can form the plate into tubing and zirconium cans. A pilot run of approximately 1000 pounds of zirconium is now being made to supply sheet for experimental work and the fabrication of six moderator cells.

An order has been placed for enough machined hexagonal graphite sections to permit the assembly of six moderator cells. AGOT or equivalent graphite has been specified and upon receipt in July, will be examined for chemical impurities, physical properties, nuclear properties, and out-gassing characteristics.

Experimental development work has continued on the welding of zirconium sheet and plate. Successful joints have been made between 2-7/8 inches OD by 0.045-inch wall tubing to end flanges of 0.035 inch and 3/16 inch thickness, as shown in Figs. 27 and 28. X-ray examination of a 10 foot long longitudinal can weld indicates gas holes along one side of the weld, as shown in Fig. 28. A study is now under way to determine the cause of these holes. A 14-foot welding stake at NAA is being modified to produce the six moderator cells previously
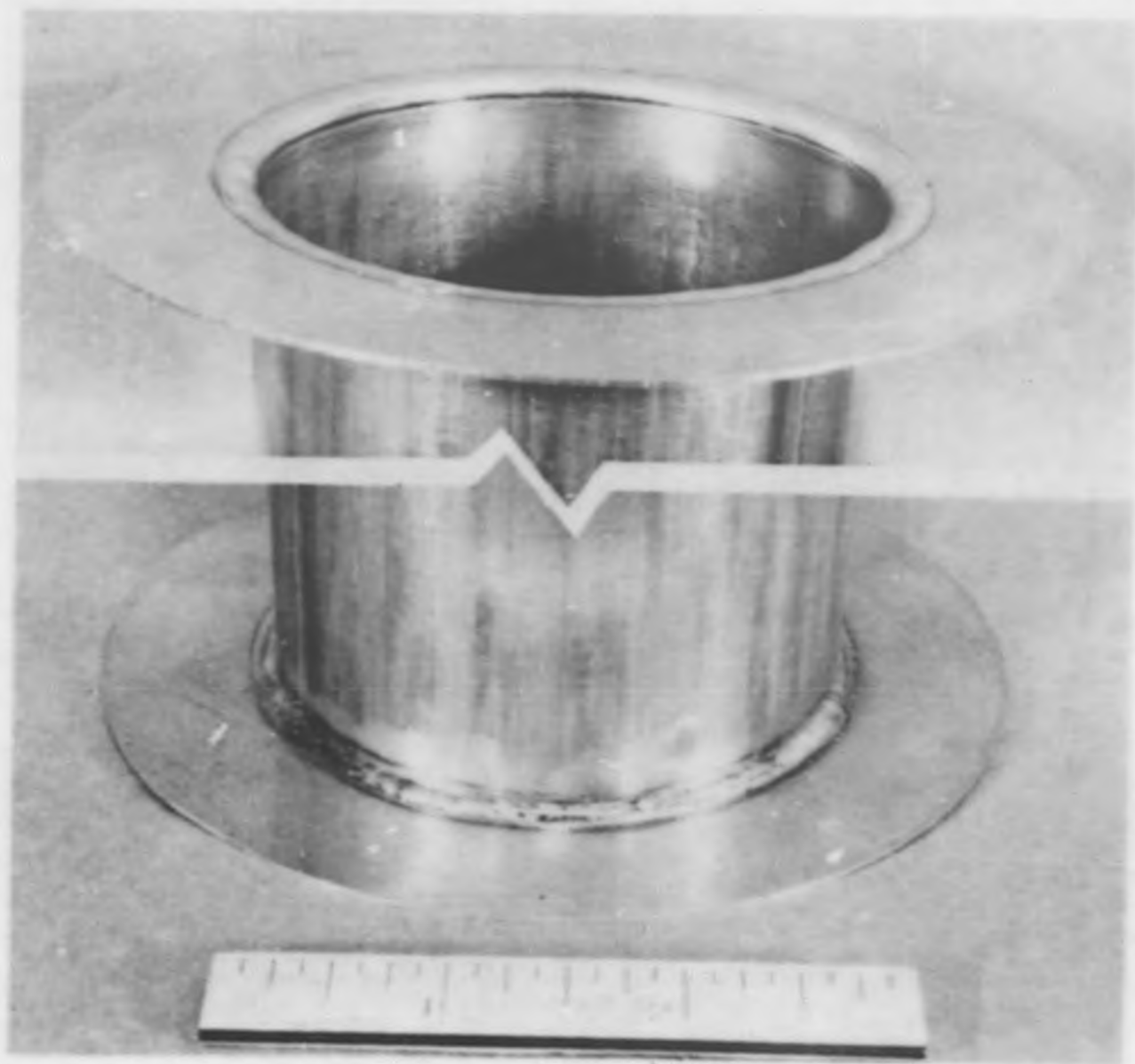
SRP 47-89 A

Fig. 27. Test Welds on Zirconium Tube and End Flanges

Unclassified   SRP 47-89 B

Weld of 0. 045 inch wall Zirconium tubing to 0. 1875 inch thick flange

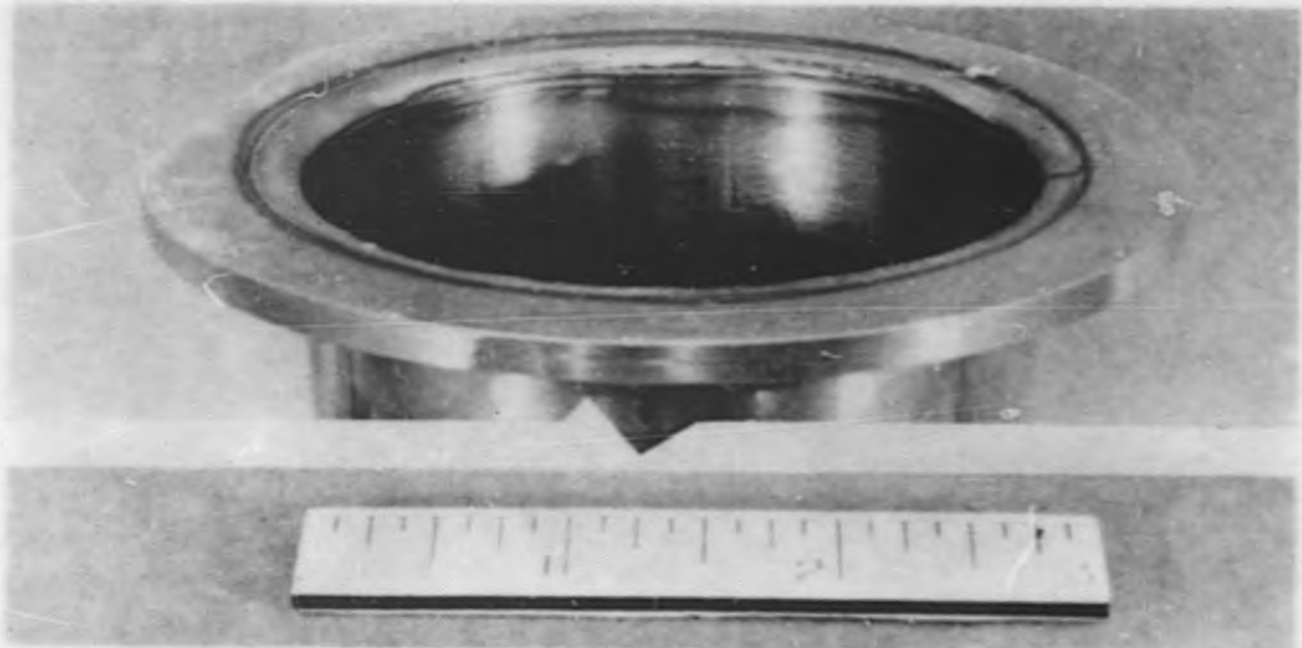X-ray (positive) of Shielded Arc Weld in 0. 050 inch Zirconium Sheet
(Note Bubbles)

Fig. 28.   Test Welds on Zirconium Flange and Sheet

mentioned. If the modified welding stake is satisfactory, it will be used for manufacturing all of the cans required for the SRE. A 150kw electric furnace is being installed for heat treating and out-gassing full scale moderator cells. A high temperature vacuum chamber and vacuum system auxiliaries for use with this furnace have been designed. The moderator units will be out-gassed under high vacuum at 1500° F in this equipment.

VIII. REACTOR COOLING AND HEAT TRANSFER

A.   Reactor Cooling Systems   (A. M. Stelle, G. R. Cogswell)

The reactor cooling system is used to conduct heat away from the core by means of liquid sodium. The system is divided into four separate loops (Fig. 29). The Main Primary and Auxiliary Primary loops are radioactive and have communication through the reactor core. The Main Secondary and Auxiliary Secondary loops are nonradioactive and transfer heat from the intermediate heat exchangers to air blast coolers (Fig. 29). The primary circuit is fabricated of 6-inch stainless steel pipe, while the secondary system is made of 2-inch pipe. The radioactive primary loops are located in two gas tight galleries adjacent to the reactor and below the floor level. Each gallery contains one loop and they do not communicate with each other. The nonradioactive secondary system is located outside of the reactor building and is weatherproofed and protected from water.

All operational valves in the primary loops are equipped with extension handles for manual operation. The nonradioactive secondary system has valves and instruments located for direct manual operation. The concrete shields of the galleries are so arranged that maintenance on the loops is impossible until the sodium has drained from them. Flush lines are provided for the loops. Since the two galleries are shielded from each other, one loop may be drained for maintenance work without affecting the other loop.

1.   Purging and Filling the System - The four coolant system loops will be purged by sweeping with helium. Sodium will then be charged to the loops from the sodium service system which will be described later.

2.   System Operation - Both the main and auxiliary circuits operate at all times. The main circuit is designed to remove 20 megawatts of heat and

the auxiliary circuit will remove 1 megawatt. The heat is rejected from the secondary loops to the air blast coolers which are manually controlled; automatic control may be added later. The temperature difference between the heat exchangers and the cold legs of the loops will be held at 460° F through the range of 10 to 100 per cent of maximum power. This control is provided by variable speed direct current motors on the two main pumps.

The temperature drive in the intermediate heat exchangers is limited to 60° F to simulate reactor operation. The exchangers are located as high as possible in the galleries in order to provide the high direct drive required for thermal convection circulation of the sodium in case of power failure. The air blast heat exchangers are also located high enough to provide a high pressure head driving force.

The main primary loop draws suction from the sodium pool in the core tank. The suction nozzle and pump are located below the free surface to provide positive pressure in the pump. The sodium flows through the pump, the intermediate heat exchangers, and back to the sodium coolant plenum in the core tank. The sodium loops will contain cold traps and plugging meters. The auxiliary primary loop draws suction from the sodium pool at a level below that of the main circuit. This arrangement prevents the loss of suction in the event of an accident which would discharge sodium into the main pipe galleries. The core tank serves as an expansion tank for both primary loops. The sodium pressure at the eye of the primary pumps will be regulated by helium pressure over the free sodium surface. The fill tank is also in communication with the core tank in order to provide a large gas volume which will prevent large or sudden pressure changes. The sodium pool volume in the core tank will accommodate a sodium temperature change of 400° F.

The arrangement of the two secondary loops is identical. The sodium flow in the auxiliary loop is constant, while the flow in the main loop may be varied. The secondary loops are independent closed loops between the intermediate and the air blast heat exchangers.

3. Draining Sodium from the System - Sodium may be drained from each of the four loops independently. Either primary loop may be drained by stopping the pump and introducing helium at the intermediate heat exchanger.
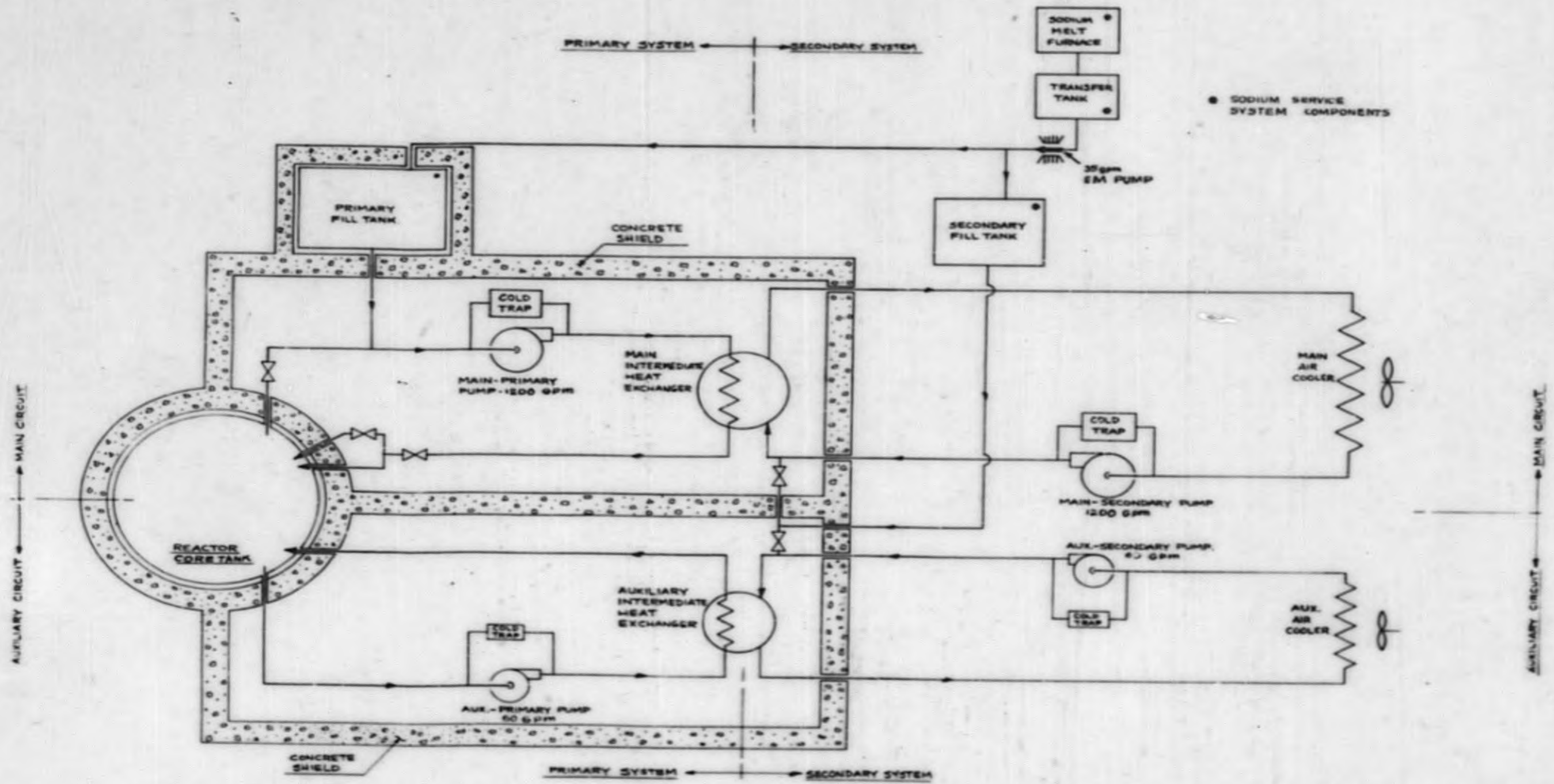
Fig. 29. Coolant System and Service System Flow Diagram

This will displace the sodium in the loop to the core tank. Valves may then be closed and the piping isolated from the tank. An alternate method of draining the system is to lower the sodium level in the core tank by means of a drain pump. The sodium will then drain from the loop to the core tank by gravity. Using this method, the fuel elements need not be removed from the reactor. If the fuel is removed from the reactor, the sodium will be completely drained from both primary loops and the core tank by means of a drain pump.

Either secondary loop may be drained by stopping the pump, opening the drain valves, and introducing helium at the air blast heat exchangers and expansion tanks. The sodium will then be forced into the fill tank.

4. Sodium Service System - All of the equipment required for melting, filtering, and transferring sodium to the fuel tanks comprises the sodium service system (Fig. 29). This system will be used intermittently, and all lines and vessels will be empty when not in use. All vessels and sodium bearing lines are electrically heated so they may be pre-heated to 300° F before the introduction of sodium. The system is designed to perform the following functions:

    a. Purge air from the system and maintain an inert atmosphere in the pipes and vessels.

    b. Melt and transfer virgin liquid sodium to either the main or auxiliary fill tanks.

    c. Recirculate and filter used sodium from either fill tank.

    d. Circulate sodium to the cold traps in the main and auxiliary cooling circuits to flush out precipitated contaminates.

    e. Drain sodium from the pipes and vessels for stand-by condition.

The system is purged by helium at the same time the coolant system is being purged. The helium from the coolant system will flow from the fill tanks to the transfer tank and out to the atmosphere. Sodium, which will be purchased in 55-gallon drums, will be charged to the system through a melting furnace and a filter. The sodium is then pumped by a 35-gpm pump to both the primary and secondary fill tanks. A check valve will prevent radioactive sodium from being accidentally forced from the primary fill tank back to the transfer tank. The sodium service system will also be used to recirculate sodium for filtering and cold trapping. Contaminated sodium will be drawn off to portable containers for disposal. Each cold trap in the reactor coolant system may be

isolated from its loop and flushed with sodium from the sodium service system. The cold traps are located at the low points in the system. Gas purging lines attached to each trap will allow the sodium to be blown out of the lines.

5. System Components -

    a. Pumps - The pumps being specified for sodium service are modified variations of hot process centrifugal pumps. The rating of the pumps are as follows:

	MAIN PUMPS	AUXILIARY PUMPS
Size	6 in. by 8 in. by 15 in.	1. 25 in. by 2 in. by 8 in.
Capacity	1200 gpm	60 gpm
Pressure	50 psi	30 psi
Speed	850 rpm	1000 rpm

Sodium freeze seals are used at the pump and for the shaft seal. Toluene coolant lines freeze the sodium to form the seals as shown in Fig. 30, which shows the arrangement of the auxiliary secondary pump. The primary pump is of the same design but has a 10-foot shaft connecting the pump coupling to the motor. This 10-foot section of the shaft is contained in a 12 inch diameter pipe housing which also contains lead for shielding purposes. An inert gas atmosphere is maintained in all pump access tubes at a pressure approximately equal to the sodium pressure on the shaft freeze seal. This will prevent the extrusion of solid sodium from the seal, and prevent contamination of the sodium. All pumps are mounted vertically and are designed for easy repair and maintenance of the rotary parts. The pump case joint is bolted to the outside of the gamma shield. After draining the sodium from the pump, the entire unit may be unbolted and all rotating parts withdrawn by lifting the floor plate. No remote cutting or disassembly operations are required.

    b. Valves - The number of valves in the main and auxiliary coolant circuits have been kept to a minimum. Most of the valves are in the sodium service system. The valves for the primary circuits are modified gear operated plug valves. The modifications include freeze seals for the stems. The other valves in the system are single bellows globe valves with the bellows located away from the sodium or high pressure side.

DETAIL Ⓐ

SODIUM FREEZE
SEAL AREA
SEE DETAIL Ⓐ

THOMAS FLEXIBLE COUPLING

DRAIN CONNECTION

TOLUENE COOLING COILS
FOR FREEZE SEAL

INSTRUMENT LEAD WIRE PORTS

FROZEN SODIUM SHAFT SEAL

NOTE:
PUMP IS ANNUNCIATED TO
OPERATE WITH SHAFT VERTICAL
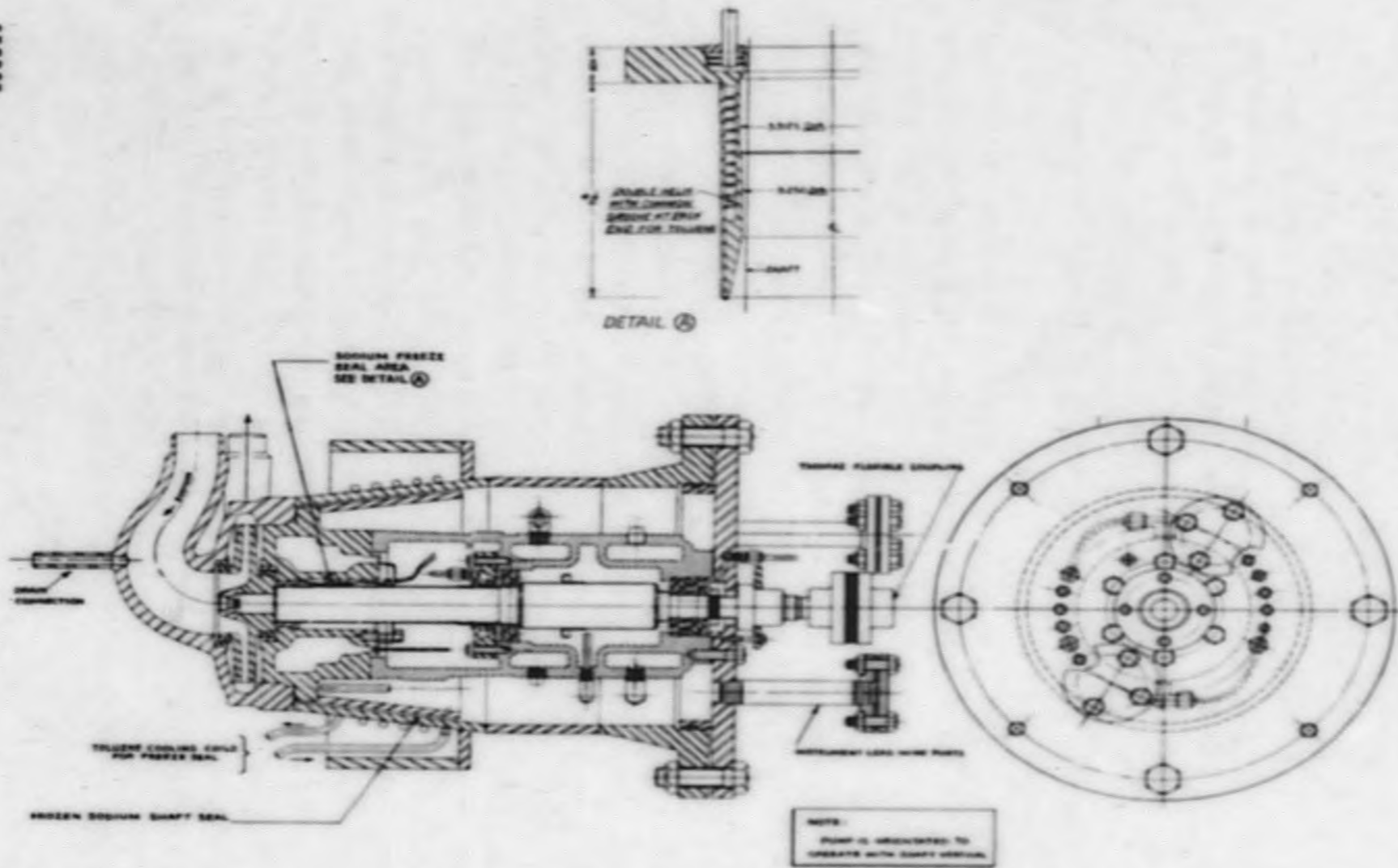
Fig. 30.   Auxiliary Secondary Pump Assembly

c. Heat Exchangers - Specifications have been issued for the purchase
of the intermediate heat exchangers for both the main and auxil-
iary circuits. These exchangers are horizontal, shell and tube
counterflow units with provision for complete gravity drainage
(Fig. 31). The heat exchangers are of all welded construction and
will be fabricated from 304L stainless steel. The air blast heat
exchangers are horizontal, finned tube, forced air units. Heat re-
jection control is achieved by shutter manipulation.

B. Engineering and Tests on SRE Components (D. Eggen, F. Bowman, R.
Cygan, K. Johnson)

1. Insulation - Two materials are being considered for the thermal in-
sulation which will surround the reactor core tank; (1) steel wool in a nitrogen
atmosphere; (2) insulating brick or mineral wool bats. The thermal insulation
will operate in temperature ranges around 1200° F, and nitrogen is being con-
sidered as the inert gas which forms the surrounding atmosphere. It is neces-
sary to know that steel wool and the 304L stainless steel, which forms the core
tank, will be stable under these conditions. Preliminary experiments have been
completed in which specimens of coarse, medium, and fine grades of stainless
steel wool were exposed in sealed capsules in a nitrogen atmosphere at 1200° F
for one month. Except for turning black, the steel wool specimens were not
affected. A second series of experiments using the same grades of steel wool
were conducted at both 1200 and 1500° F with a slow stream of nitrogen passing
over the samples. The specimens were examined weekly for four weeks. The
fine grade steel wool gave evidence of serious embrittlement after a four week
exposure at 1200° F. After one week at 1500° F, the three specimens had
become extremely brittle and were easily reduced to powder. This suggests that
the reaction is progressive and that the coarser grades of wool would probably
become embrittled over a period of time. Diffraction studies of the powder which
results from the treatment of the steel wool at 1500° F indicate the presence of
only iron and chromium oxide. The function of the nitrogen remains unknown.
A piece of 304L Stainless Steel plate given the same treatment indicated severe
scaling. The non-adherent character of the scale would indicate a relatively short
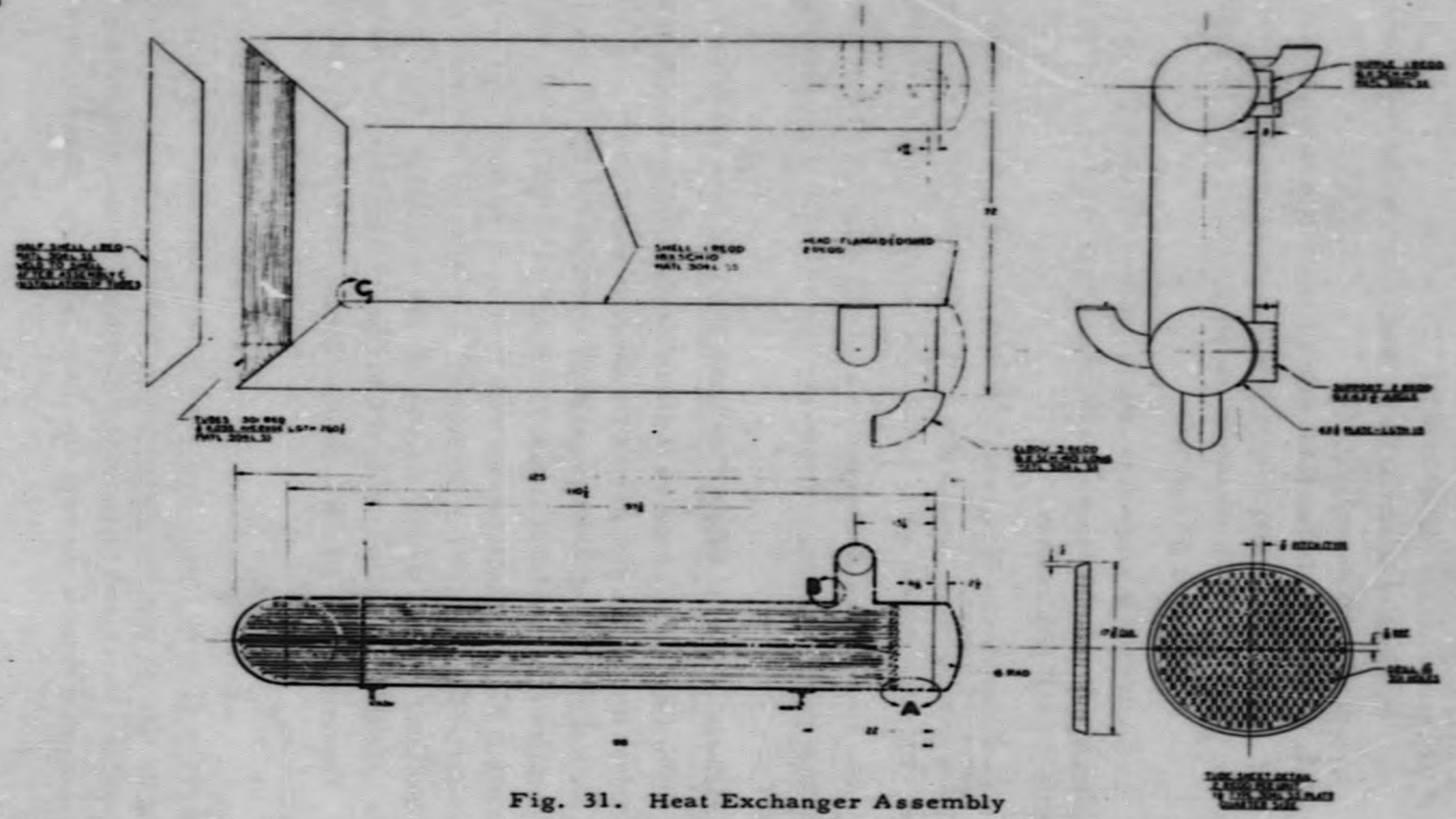life for a 304L Stainless Steel tank in a nitrogen atmosphere at 1500° F.

Fig. 31. Heat Exchanger Assembly

2. **Inert Gas Studies** - It is planned to use three inert gas systems in and around the reactor and the coolant systems. These are:

a. Oxygen-free helium inside all vessels and auxiliary equipment containing sodium coolant.

b. Commercial helium in the control, safety, and miscellaneous thimbles extending into the core tank and in the ball safety device.

c. Nitrogen (relatively oxygen-free) in the coolant galleries and the cavity around the core tank.

Studies are now in progress to develop a method of removing oxygen from commercial helium. The objective of the studies is to optimize a NaK bubbler train for the SRE requirements.

3. **Sodium System Components** - Various designs of sodium freeze seals are being investigated for use in a plug valve in place of a standard packing gland. The valve and seal will be tested under simulated operating conditions.

Five electro-magnetic flow meters are being calibrated prior to installation in a sodium pump loop. They will be used on the pump loop plugging indicator.

C. **Engineering Tests of Sodium Flow Under SRE Conditions** (R. Cygan)

Experimental measurements to determine the vibration characteristics and sodium flow pattern past a seven-rod fuel element were made. Vibration was checked by means of strain gauges and a recording Cyclograph. The strain gage bridges were mounted at various points along the length of a fuel rod as indicated in Fig. 32. Measurements were made using water and varying the flow velocity from 12 to 20 feet per second. No regular nor deleterious vibration was found at any of the flow rates tested, and aperiodical vibration was found to have a maximum amplitude of 0.015 inch at the mid-point of the fuel rod. The tests indicate there should be no vibration problem with the seven-rod fuel element.

Flow pattern observations were made to determine if stagnant fluid areas existed around the fuel rods. Variations in fluid flow velocity at various points along the element were also observed. The element was painted flat black and mounted in a transparent coolant tube. Aluminum particles of approximately 140 mesh were added to the water circulating in the loop. Examination of both
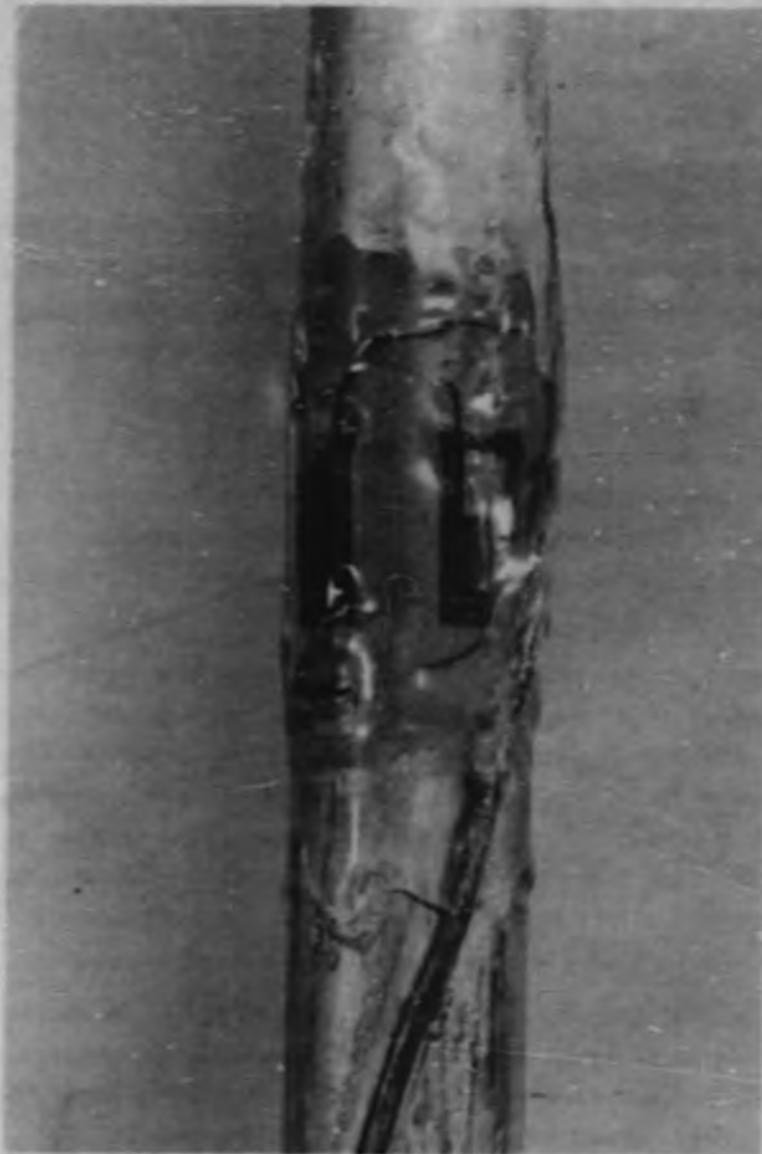
Unclassified   SRP 23-103A

Fig. 32. Strain Gage Bridge Mounted on Fuel Rod

still and motion pictures indicates no stagnant fluid areas. The spacer wire which is wrapped helically around the individual fuel rods does not cause a marked spiralling of the fluid around and between the rods. This is illustrated in Fig. 33, where a spacer wire is located in the center of the photograph.

D. Sodium Pump Development and Test

The sodium pump loop previously reported[5] has been assembled and delivered to the Santa Susana site. The loop is made of 304L stainless steel using the welding and cleaning specifications which have been prepared for the SRE coolant loops. The electric power supply to the pump is now being installed.

E. Stainless Steel Metallurgy for the SRE (F. Bowman)

A survey of all stainless steels which might have possible application for the SRE core tank and coolant circuits was made to compare the weldability, elevated temperature properties, and costs. It has been established that weld cracking is a problem in the case of 347 stainless steel; 316 stainless steel behaves in a similar manner.

On the basis of 3,000 hour heat tests, it has been established that sigma phase (an iron chromium compound) forms to a significant extent in both 347 and 316 stainless steels at temperatures as low as 1100° F. No sigma phase materials were found in 304 stainless steel tested in the same manner. Since the sigma phase is preferentially formed at grain boundaries and is essentially brittle material, its effect on elevated temperature ductility could become serious after long exposures at high temperature. Tests indicate that the sigma phase formation causes a serious decrease in creep strength.

In view of the difficulties which may be expected in the welding and high temperature operation of 347, 316, and 316L stainless steels, it is felt desirable to specify 304L stainless steel for use in the SRE. Material and welding specifications for 304L stainless steel have been issued.

F. Inert Gas Systems (W. D. Alderson)

Helium is used in the core tank and all components which come in direct contact with the sodium. It is also used in all fuel handling facilities, such as the fuel handling coffin, the cleaning cells and the fuel storage cells. Sodium pumps, valve freeze seals, control rods, and the ball safety device are also supplied with a helium atmosphere.
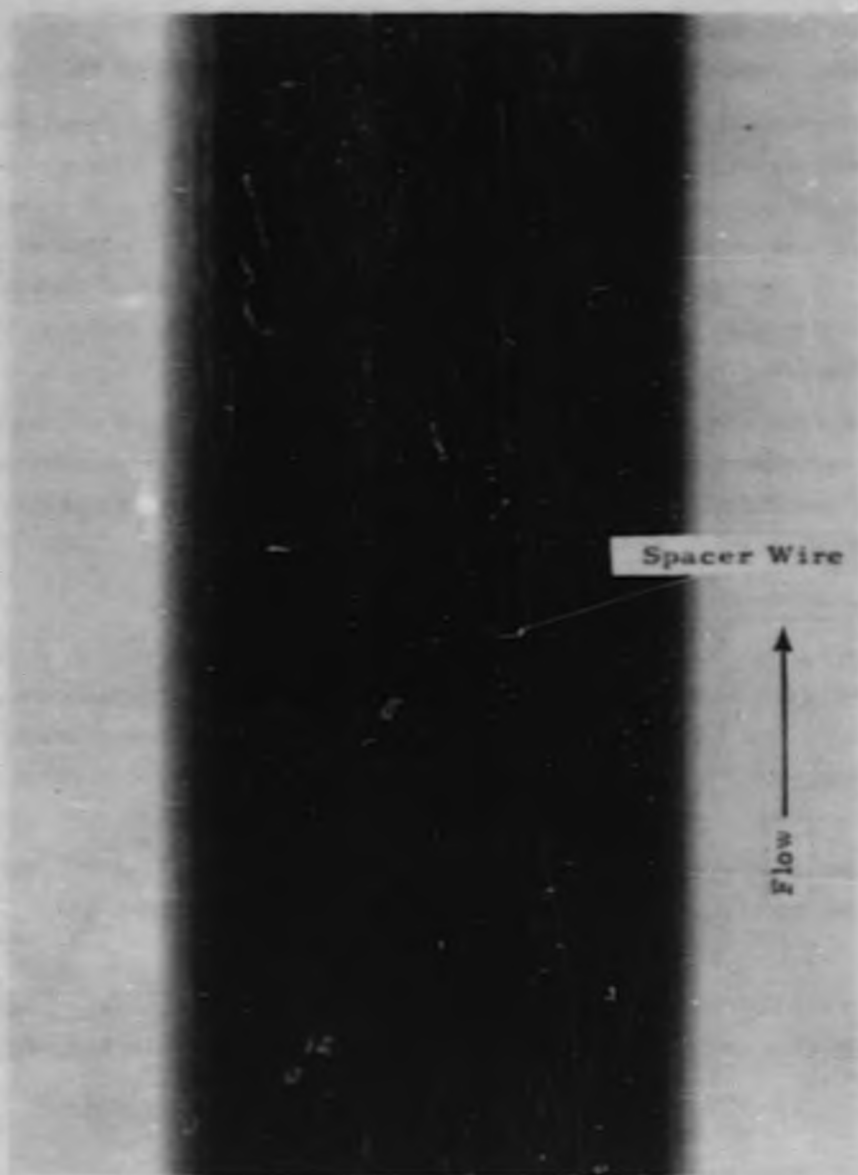
Spacer Wire

Flow

Fig. 33.   Liquid Flow Pattern Around Seven-Rod Fuel Element

DECLASSIFIED

Nitrogen will be used as the inert atmosphere in all other components. These include the sodium piping galleries, the cavity surrounding the core tank, the thermal insulation, and the double wall sodium inlet pipes to the core tank.

Both the helium and the nitrogen will be stored at 2400 psi and reduced to 50 psi for distribution to the various reactor components. The pressure will be further reduced as required by each component. Each gas system is noncirculating and is essentially stagnant except for the small volume of make-up gas required by the loops. All vent lines are normally closed and any gas containing radioactivity will be compressed into hold-up tanks before being released to the atmosphere.

Preliminary scope and layout drawings for the helium and nitrogen gas systems have been completed. Calculations are being made to determine the amount of shielding required by the activity in the gases. The capacities of the various components of the gas handling systems are also being calculated.

G. Toluene Cooling System

A toluene cooling system is used to transfer heat from various components and areas associated with the reactor (see Section X-B-2). Approximately 40 kw of heat are transferred to the toluene in air to liquid heat exchangers mounted on the walls of the pipe trenches. The nitrogen gas in the trenches is drawn through the heat exchangers and gives up its heat to the toluene.

A total of 32 kw are removed from the freeze seals on the sodium pumps and plug valves. The bearing housings of the sodium pumps are also toluene cooled (Fig. 30).

Approximately 66 kw of heat is removed by the toluene from other components, such as ion chambers, fission chambers, sodium cold traps, and vapor traps.

IX. INSTRUMENTATION AND CONTROL

A. Control Rod Systems (C. J. Thompson)

1. Arrangement and Design - The arrangement of the thimble type control rod arrangement being prepared for the SRE has been previously reported[6]. The 304L stainless steel thimble extends from the top of the reactor shield down

through the sodium pool to the bottom of the reactor core (Fig. 34). The neutron absorption material is 3 per cent boron steel in the form of centrifugally cast sleeves. The boron sleeves are 2.487 OD by 2.180 ID by 4 inches long. Eighteen sleeves are mounted on a pull tube which moves vertically in and out of the core. The sleeves fit loosely on the pull tube (Fig. 35-C), and will adjust to any warpage in the thimble. The boron sleeves may be moved entirely out of the core on the pull tube which has a total travel of 7 feet.

The pull tube is attached to a ball nut assembly of a ball screw (Fig. 35-B). The nut assembly rides up the screw as it is turned. The screw shaft is rotated by a two-tooth clutch (Fig. 35-A), which in turn is driven by an electric motor mounted outside the reactor shield. This clutch arrangement permits the removal of the motor and gear box by lifting out vertically. This permits clearing the top face of the reactor when the fuel handling coffin is in operation.

There will be four control rods located as indicated in Fig. 25. The rods are not located in the center tube of the moderator cells, but are in a tube-like space formed by the scalloped corners of three moderator cells. The four rods will be used as shim rods, and one will be arranged to have an override on the shim movement so it might function as a regulating rod. The shim movement will be manually operated, while the regulating rod will be instrument controlled.

The entire control rod assembly is designed so that helium will be used as the heat transfer medium between the boron steel sleeves and the coolant sodium flowing outside of the thimble. The entire internal mechanism of the control rod may be removed from the reactor by using the fuel element handling coffin. If required, the thimble may also be removed by the same method and equipment.

The position of the control rod will be indicated on the control console by Selsyn motors. A rotational counter mounted on the two-tooth clutch will indicate rod location within 0.1 inch. It may be necessary to know the rod position during the replacement of a drive motor assembly.

2. <u>Engineering Tests</u> (H. Strahl) - A technique for producing boron steel control rod sleeves by spraying a high boron content material on to a stainless steel mandrel has been previously reported[6]. Four inch long specimen sleeves

DECLASSIFIED

Fig. 34.   Control Rod Arrangement

BORON CYLINDER

FILL TUBE

VIEW C

CLUTCH (TWO TOOTH)

UPPER SHIELD TUBE

COUNTER

THIMBLE

BEARING SUPPORT TUBE

UPPER BALL BEARING

HELIUM ATMOSPHERE

VIEW A

GRAPHITE

304 L

HELIUM FLOW TUBE

2R

3 5/8" DIA.

VIEW D

(SEE FIG. 34)

BALL NUT

GUIDE BLOCK

BALL SCREW

BORON CYLINDER FILL TUBE

VIEW B
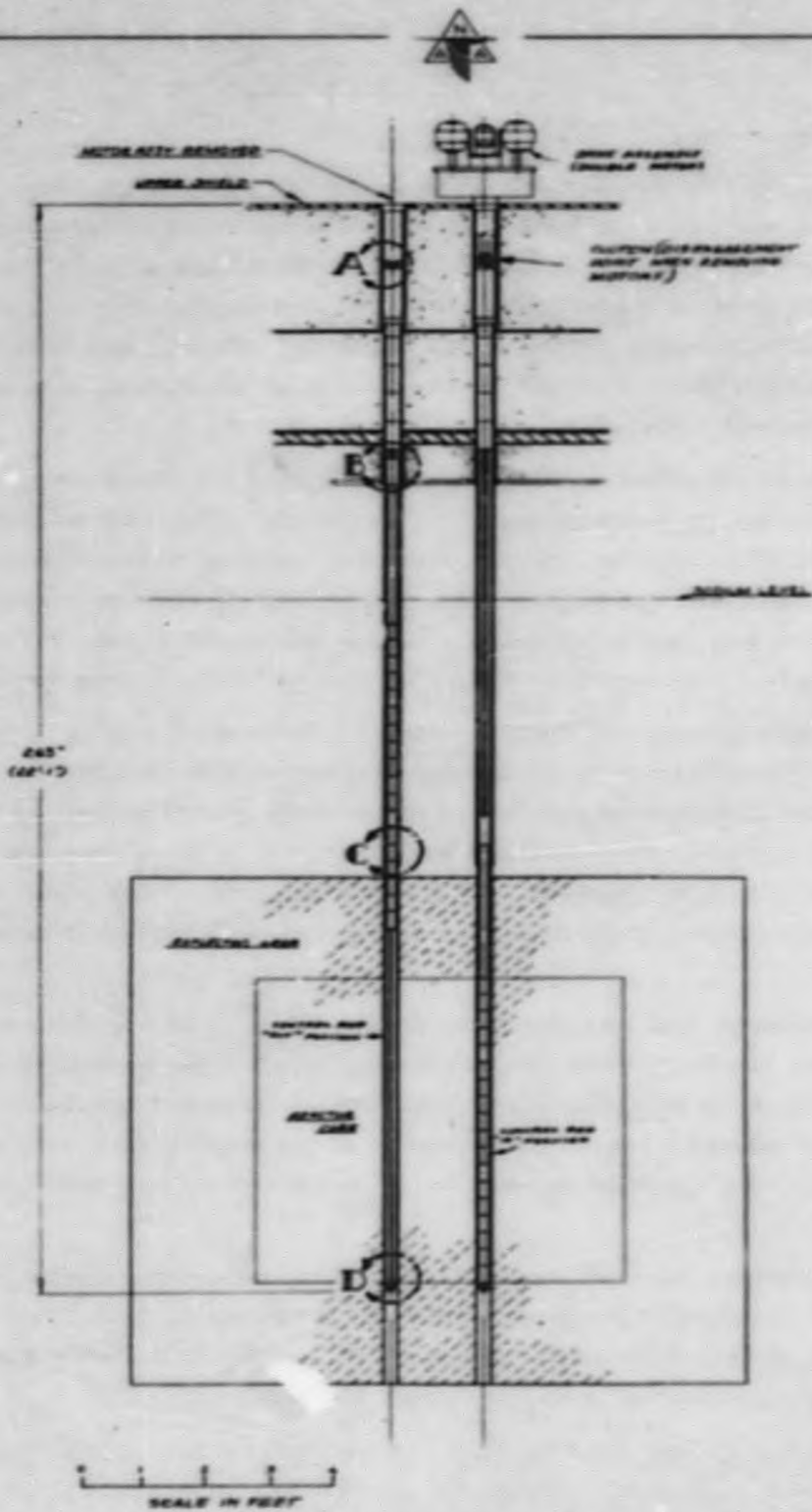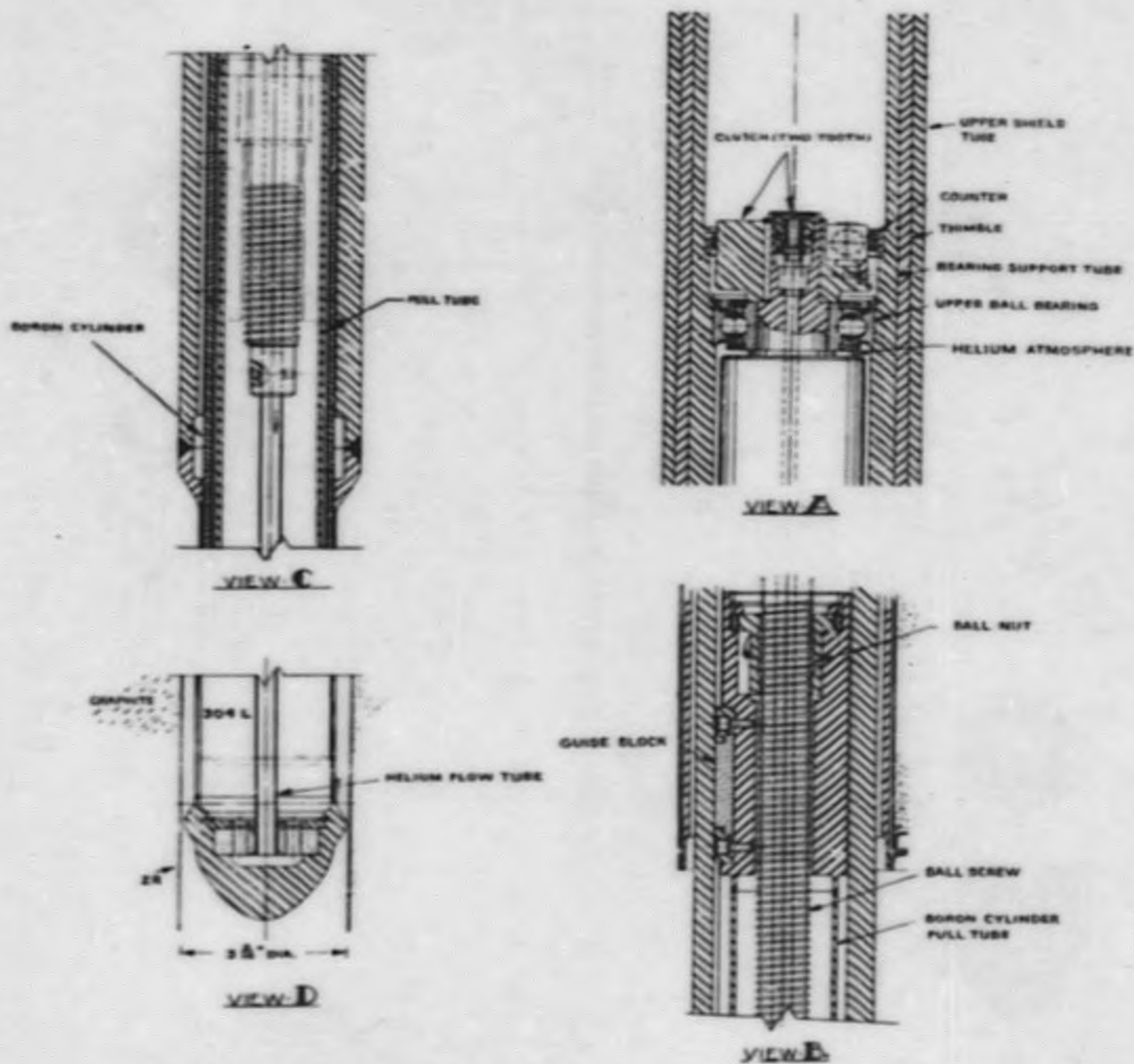
Fig. 35. Control Rod Details
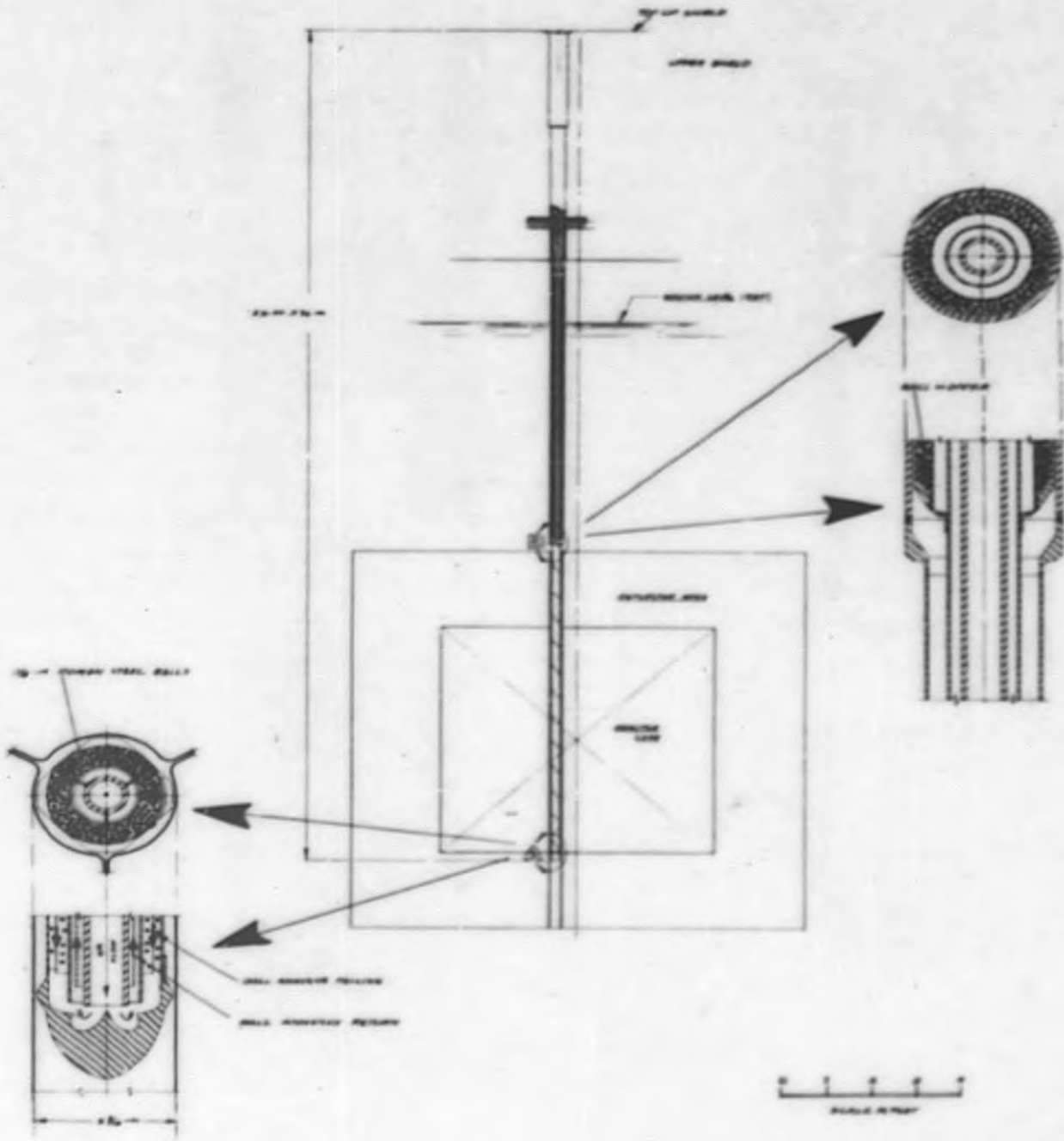
Fig. 36. Ball Safety Device Arrangement

were thermally cycled between 800 and 1300° F on a 1-hour cycle. Very fine cracks appeared on the surface. It is believed that these cracks may be reduced by flame spraying the metal onto a graphite mandrel and then removing the mandrel after the final machining and grinding operation.

Sleeve specimens which have been centrifugally cast of a boron nickel alloy have been prepared by local vendors. These specimens have a lower hardness than the flame sprayed specimens. It is also possible to machine this material and eliminate the grinding operation. It appears that these sleeves will be less expensive to fabricate than the flame sprayed ones. Physical tests are now being conducted.

B. Safety Device System (C. J. Thompson)

1. Arrangement and Design - A ball safety device is being designed for the SRE. Boron steel balls (1/8 inch diameter) are stored in a hopper located in the area of the sodium pool above the core (Fig. 38). Upon the deenergization of a solenoid, the balls are released and allowed to fall into a thimble which extends vertically through the reactor core. The 304L stainless steel thimble extends from the upper shield of the reactor through the sodium pool to the bottom of the core. Concentric tubes located within the thimble form two annuli and a center tube. The balls fall into the outer annulus and remain there until helium is forced down the center tube. This deflects the balls into the inner annulus and pushes them back into the storage hopper.

The ball gate which retains the balls in the storage hopper is supported by three rods which pass through the shielding portion of the thimble; this coincides with the lower portion of the upper shield. The rods are attached to a spider which in turn is attached to a triggering device. This design places the weight of the balls in the hopper upon a pair of fingers rather than directly on the solenoid. When the solenoid is energized the fingers are refrained from moving and permitting the ball gate to drop. When the solenoid is deenergized, it triggers the finger mechanism, which allows the gate to drop, and thus permits the balls to fall into the annulus which penetrates the reactor core.

The triggering mechanism is so designed that it will be recocked by the helium which blows the balls back into the storage hopper. This design makes the safety device as tamper-proof as possible. In the event of any mishandling

or mechanical failure, the mechanism will be triggered and the boron balls will drop into the core and shut down the reactor.

2. Engineering Tests (E. Phillips)

a. Ball Recovery Tests - Ball pick up tests previously reported have now been completed. The tests were performed using a transparent plastic mock-up of the lower end of the ball safety thimble as shown in Fig. 37. A stream of gas moving down the center tube is deflected by a cup into the annulus between the center tube and the outer annulus. As the air is deflected it picks up balls from the deflector cup and carries them up the annulus. The satisfactory mechanical configurations have been designed and tested and the optimum flow rates and gas pressures have been determined.

b. Sintering Experiments - Because of the high temperature in the reactor core and the pressure resulting from the weight of the boron steel balls pressing upon each other, it was thought possible that the balls might fuse together. In order to experimentally check this point, 1/8 inch diameter chrome steel balls were maintained at 1320° F for 23 days in an atmosphere of dry nitrogen. A pressure was maintained on the balls equivalent to a 36 inch long column of balls, as indicated in Fig. 38. The balls would stick together but could easily be separated. Two different tests were made under the same conditions using Type 440 stainless steel balls. They were heated to 1320° F for 20 days under a pressure equivalent to a 7-foot column of balls. These balls were pressure welded together. Parts of the sinter retort were also pressure welded together and could be separated only with great difficulty. These experiments are continuing.

c. Releasing Mechanism Studies (E. Hecker, M. Mueller) - A prototype of the upper section of the ball safety device has been assembled in order to determine the time and manner in which the boron steel balls are released from the storage hopper. The device has been modified to permit visual observation of the operating parts. The response time of the mechanical parts will be determined and the time lag between the deenergizing of the solenoid and the
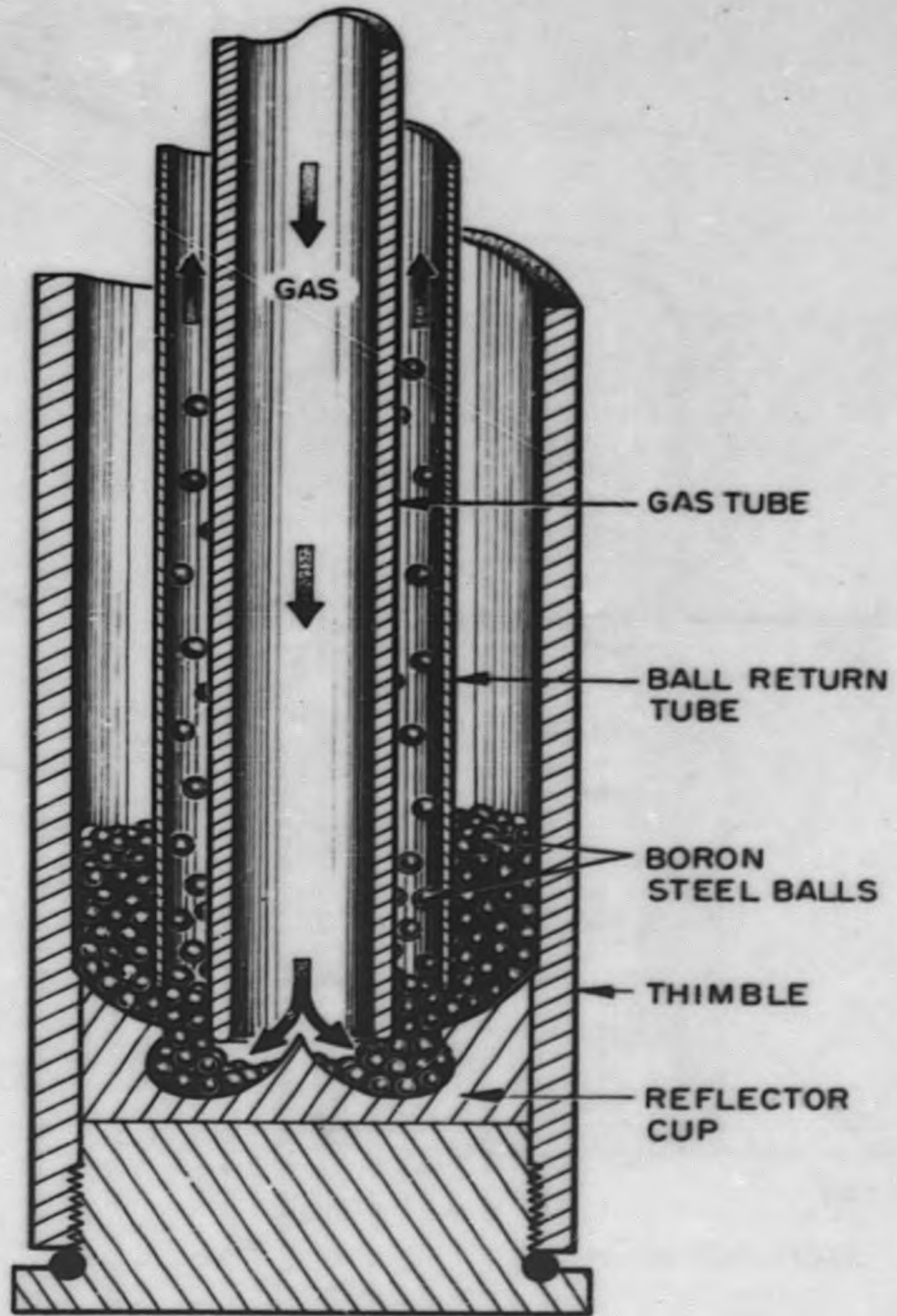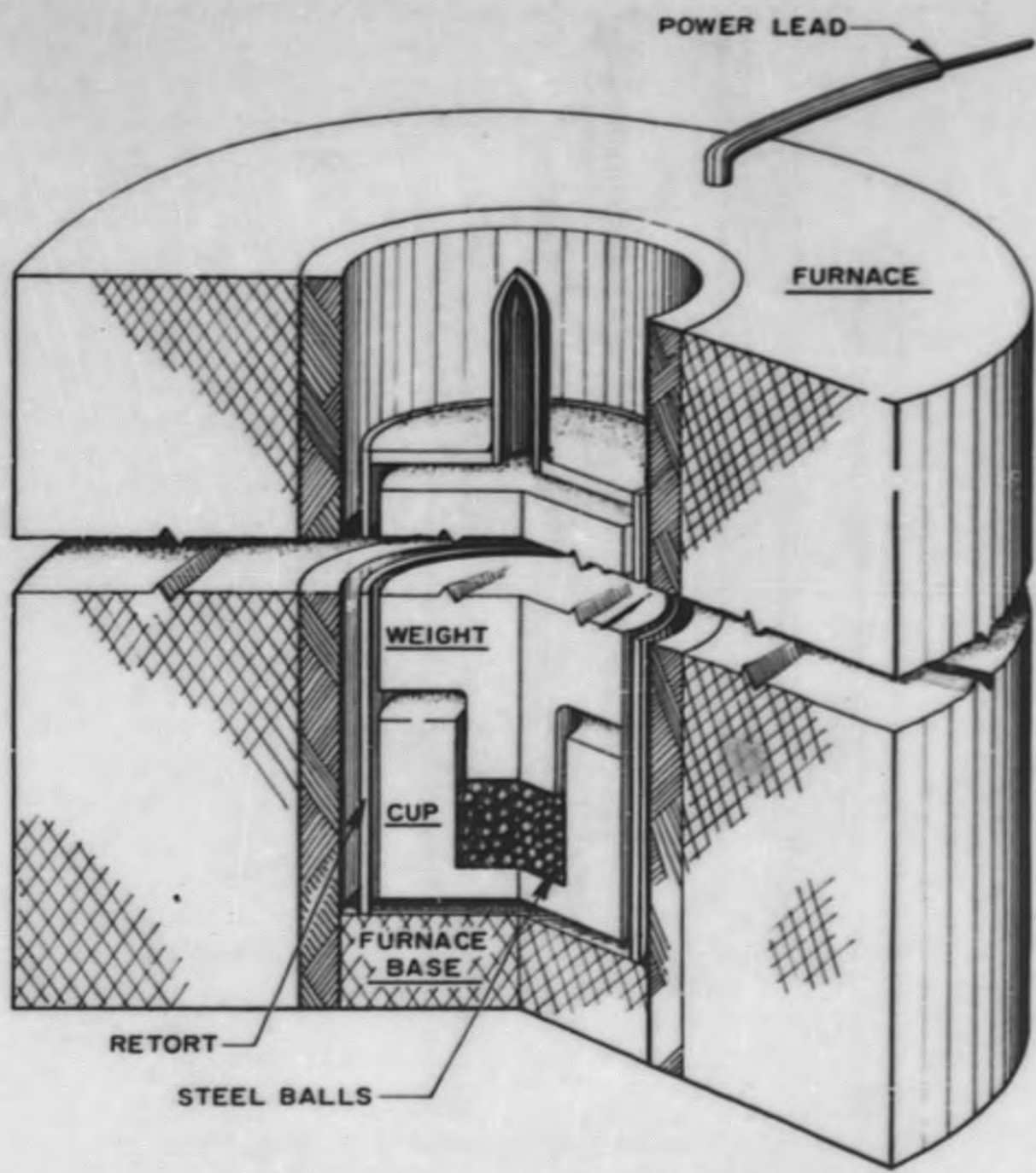
Fig. 37.   Ball Safety Device - Ball Return Section

GAS

GAS TUBE

BALL RETURN TUBE

BORON STEEL BALLS

THIMBLE

REFLECTOR CUP

Fig. 38. Ball Safety Device - Ball Sintering Apparatus

falling of the first balls from the storage hopper will be determined. Other studies will be made to determine the ball density in the various sections of the core thimble. Various electromagnets and solenoids for use in this equipment are being tested. The load capacity which the solenoid will hold and the release time are being measured. The optimum time is being determined using an electronic latching system. Magnetic amplifiers are being investigated as possible replacements for the electronic secondary circuit. Magnetic units are being tested which have a time lag of 16 to 50 milliseconds.

C. Instrumentation and Control System Arrangement (E. Matlin)

A layout drawing has been completed which indicates the location of the ionization chambers, the fission chambers, and the thermocouples which surround the reactor core tank (Fig. 39). As shown on the drawing, there will be two fission chambers and six ionization chambers. The ionization chambers will be located in thimbles on the horizontal center line of the core and in the region of the thermal insulation. Calculations indicate the neutron flux at this location will be sufficient to operate the chambers (approximately 10^9 nv at full power) if the section of the thermal shield adjacent to the chambers is reduced to a thickness of 3 inches. The two fission chambers are similarly located. Calculations indicate that if the thermal shield adjacent to the chambers is removed, a satisfactory counting rate will be obtained at start-up with a source of 5×10^7 neutrons/sec in the center of the core. After the reactor power level has risen to five decades above the source level, the fission chamber will be motorized out of the high flux area.

A design has been completed (Fig. 40) of an antimony-beryllium source for use during reactor start-up. The source will be initially activated in some other reactor. The antimony-beryllium will be contained in a graphite cylinder which is enclosed in a stainless steel case. The use of a large neutron source such as this allows the positioning of the fission chambers outside of the core tank. This is desirable because it allows the operation of the chambers in a low temperature region.

A preliminary layout has been made of the reactor control room, recorder and instrument panels, and other major control units.
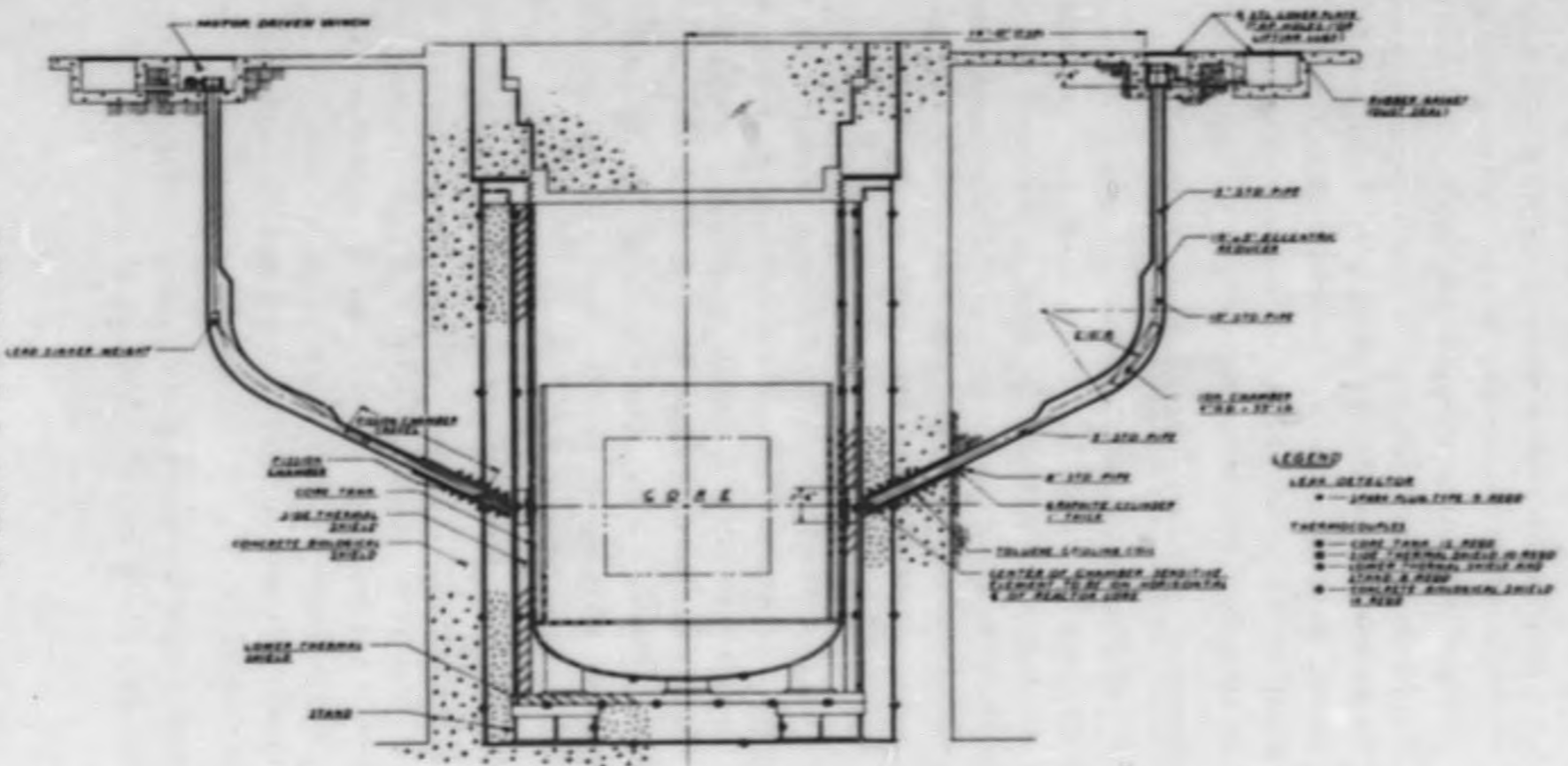
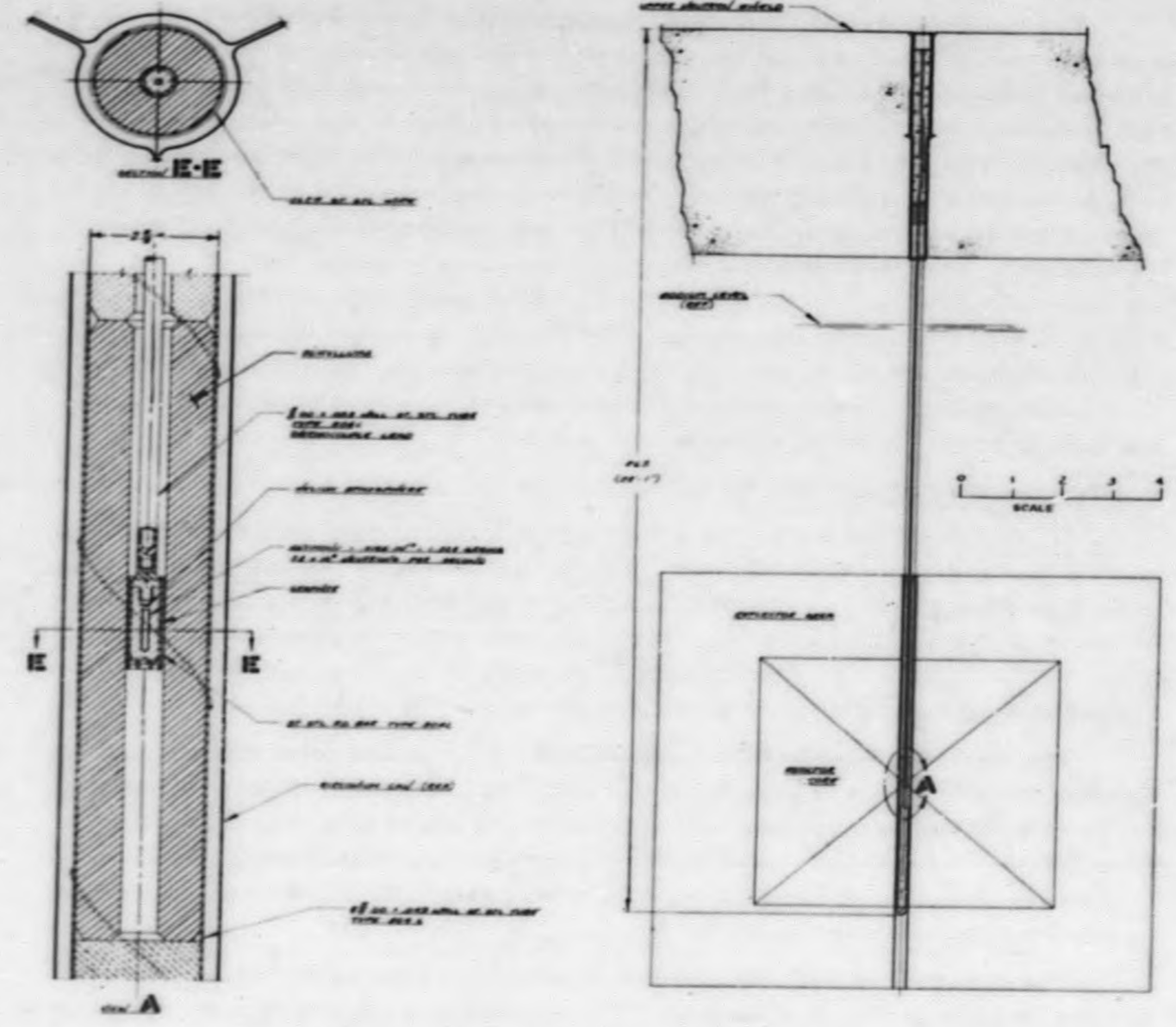Fig. 39. Reactor Instrument Layout

7464-SR1049

Fig. 40. Source Assembly Layout

DECLASSIFIED

X. SHIELDING

A. Side Biological Shield

The arrangement of the side biological shield which surrounds the core tank is shown in Figs. 23 and 24. It consists of approximately 5 feet of re-inforced concrete. In order to prevent damage to the concrete because of high temperature, toluene cooling pipes are imbedded at the inner surface of the shield. The pipes are fastened to the outer surface of the core cavity liner (a 1/4-inch steel plate) and are connected to a ring manifold at the top of the tank. Approximately 30 kw of heat will be removed from the shield through these pipes. This will keep the concrete temperature below 150° F. The toluene inlet temperature will be 95°, and the outlet temperature 125° F. Iron ore aggregate will be used in the concrete for various sections of the reactor shield-ing. In order to calculate the cooling requirements the thermal conductivity of such concrete must be determined. Experimental equipment is now being as-sembled in order to obtain the required data.

B. Top Rotating Shield (C. J. Thompson, M. P. Heisler)

1. Arrangement - The top shielding assembly designed for the SRE con-sists of two major subassemblies; the Ring Shield and the Rotating Shield (Fig. 41). The Ring Shield is an integral portion of the reactor room floor. It will be keyed to the building structure to prevent any rotation after installation. All joints will be sealed by a low melting point alloy to prevent gas leakage. The alloy will be poured into place after installation of the Ring Shield.

The Rotating Shield will be mounted on ball bearings and will rotate in-side the Ring Shield. The top race is attached to the Rotating Shield, and the lower race of the ball bearing will be attached to the inside diameter of the Ring Shield. A locking device will prevent rotation of the Rotating Shield when it is not in operation. The locking device will also lock the Rotating Shield at various index points as required.

The Rotating Shield contains two removable plugs 40 inches in diameter and one plug 16 inches in diameter. These plugs are arranged in such a pattern that with a rotation of the shield all the moderator cells in the reactor will be accessible for removal. Also located in the Rotating Shield are 85 tubes through
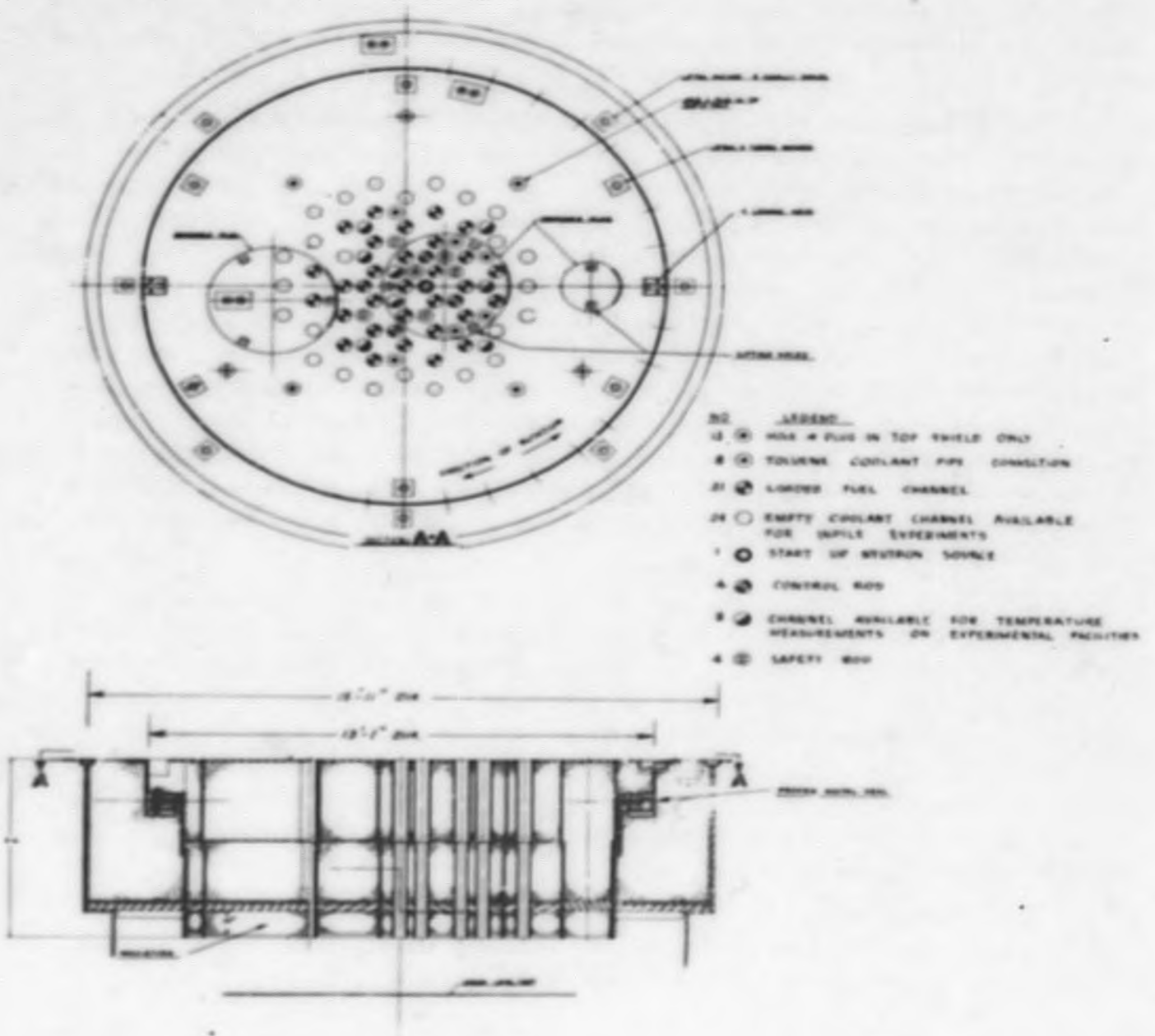
Fig. 41. Top Shield Assembly

which the fuel elements, control rod thimbles, and safety device thimbles must pass. Stepped plugs will fit in the holes, and rubber O-rings will serve as gas seals.

The Rotating Shield is made of a sheet steel form filled with concrete. All concrete will be entirely enclosed and only stainless steel will be exposed to the sodium vapor and helium atmosphere. The steel will be machined to permit a close fit to provide seats for the gas seals. There is no drive mechanism on the Rotating Shield as all fuel elements, control rod thimbles, safety device thimbles and other equipment which goes into the core must be removed before the shield is rotated. The elimination of a power driven rotating mechanism will eliminate the possibility of an accidental rotation of the shield. This would shear off the above mentioned elements. The shield will be rotated by the use of turning anchors, a sheave, and a cable attached to the bridge crane hook. The Rotating Shield uses a low melting point metal for a gas seal. When it is desired to rotate the shield, the metal seal will be melted by tubular heaters which are imbedded in the seal. This will melt the seal liquid and allow the shield to rotate freely.

Preliminary calculations indicate a top shield thickness (magnetite or concrete) of 5 feet-2 inches is required to reduce the radiation to 10 per cent of the AEC tolerance. As indicated in Fig. 41, a layer of lead, a layer of steel plate, and a layer of thermal insulating material are located at the bottom of the shield. The present design specifies steel wool contained in stainless steel cans for the thermal insulation. Based upon a temperature of 1200° F in the sodium pool the heat loss is calculated to be approximately 450 Btu/hr per insulating can. This corresponds to an average heat flux of 620 Btu/hr per square foot of reactor cross section.

The heat generated in the thermal and biological shields is estimated to be approximately 270 Btu/square foot of reactor cross section. This heat is divided among the various gamma sources as follows:

Na decay gammas	28%
Na capture gammas	23%
Core and reflector gammas	3%
Thermal and biological shield capture gammas	46%

2. Coolant System - The total heat flux through the thermal shield amounts to approximately 890 Btu/hr per square foot of reactor area. This corresponds to a total heat loss of 85,000 Btu/hr (25 kw). This heat will be removed by 1-inch diameter toluene cooling pipes imbedded in the lead gamma shield and located approximately 9-1/2 inches apart. Based upon an average temperature of 135° F on the outside of the cooling pipes, the temperature at the bottom of the thermal shield will be approximately 212° F and 188° at the top. As mentioned above, the toluene cooling system must be designed to re- move 85,000 Btu/hr. Including a 20 per cent safety factor, the toluene flow rate for a 20° F temperature rise will be 12,000 pounds/hr, or 28 gpm. This corresponds to a velocity of 11.5 feet per second with a pressure drop of 18.5 psi per hundred feet of pipe. The power required for pumping the toluene under these conditions is approximately 0.3 hp per hundred feet of pipe.

C. Cooling System Components (R. L. Ashley)

A detailed calculation of the specific activity of the sodium in the primary coolant loops indicates it will be 0.10 curie per cc. Approximately 41 per cent of the neutron captures in the sodium will occur in the coolant spaces between the hexagonal moderator cells, while 23 per cent occur in the coolant tubes. The remaining neutron captures occur in the annular space between the reflector cans and the reactor tank and in the sodium pools located above and below the core.

The shielding requirements for all piping and other vessels containing the primary sodium were calculated based upon the use of magnetite ore concrete. The shield thicknesses required to reduce the dosage rate at the shield surface to 10 per cent of AEC tolerance are as follows:

	Shield Thickness (feet)
Piping in main coolant circuit (2)	4.04
Piping in auxiliary coolant circuit (2)	3.55
Main heat exchanger compartment	4.23
Auxiliary heat exchanger compartment	4.00
Fill and drain tank	4.57

XI. REACTOR SERVICES

A. Irradiated Fuel Handling System (F. W. Dodge)

Upon removal of fuel elements from the reactor, they will be cleaned to remove sodium and then stored in a water-filled pond. The arrangement of the fuel handling facilities is shown in Fig. 42. The fuel element will be removed from the reactor by means of a handling coffin and will then be lowered into a portable cleaning cell, which is shown in Fig. 43. The cell will be supported in a water-filled canal by means of a small dolly or carriage which is mounted on wheels. The cell will then be moved to wall-mounted brackets which will position it over a drain connection in the storage pond. Water and helium lines will be connected to the top of the cleaning cell (Fig. 43), and the sodium will be washed off the element by water-spraying. Following this operation the cleaning cell containing the element will be moved to the fuel removal station shown in Fig. 42. While the fuel element is supported by an overhead crane, the cleaning cell will be lowered into a deep well. The fuel element will then be moved to the spent fuel storage area of the pond. From this area the element will be loaded into a shipping coffin.

Design drawings have been prepared for all auxiliary equipment, such as storage racks, grappling devices, and the shipping coffin. In order to take advantage of the water shielding, the shipping coffin is designed so that it may be loaded under water. Detailed drawings of the cleaning cell are being prepared so that a prototype may be fabricated and tested.

B. Fuel Element Handling Coffin (R. Crosgrove, R. Ashley)

A scope drawing has been completed which shows the arrangement of the fuel handling coffin (Fig. 44). This coffin will be used for replacing fuel elements, control rods, and ball safety device components in the reactor. The coffin is designed so that the operations may be performed without contaminating the helium atmosphere in the core tank. Detailed design studies are being made of the mechanical features of the coffin based upon experimental data obtained from the prototype coffin being tested at Santa Susana.

The coffin will be lead shielded for the protection of operating personnel. In order to determine the required thickness of lead, it was necessary to determine the total energy $P_{h\gamma}$ associated with the hard fission product gamma

FUEL CLEANING
STATION No 2

CELL CARRIAGE

CLEANING CELL
IN PLACE

VIEW A·A

SHIPPING COFFIN
LOADING STATION

CONCRETE WALL

SPENT FUEL STORAGE RACKS
/ SHIELDS - STATION No 4

WATER

CLEANING CELL SUPPORT

CELL DRAIN CONNECTION

FUEL REMOVAL - STATION No 3

FUEL CLEANING - STATION No 2

CLEANING CELL CARRIAGE

CLEANING CELL STORAGE

COFFIN UNLOADING - STATION No 1

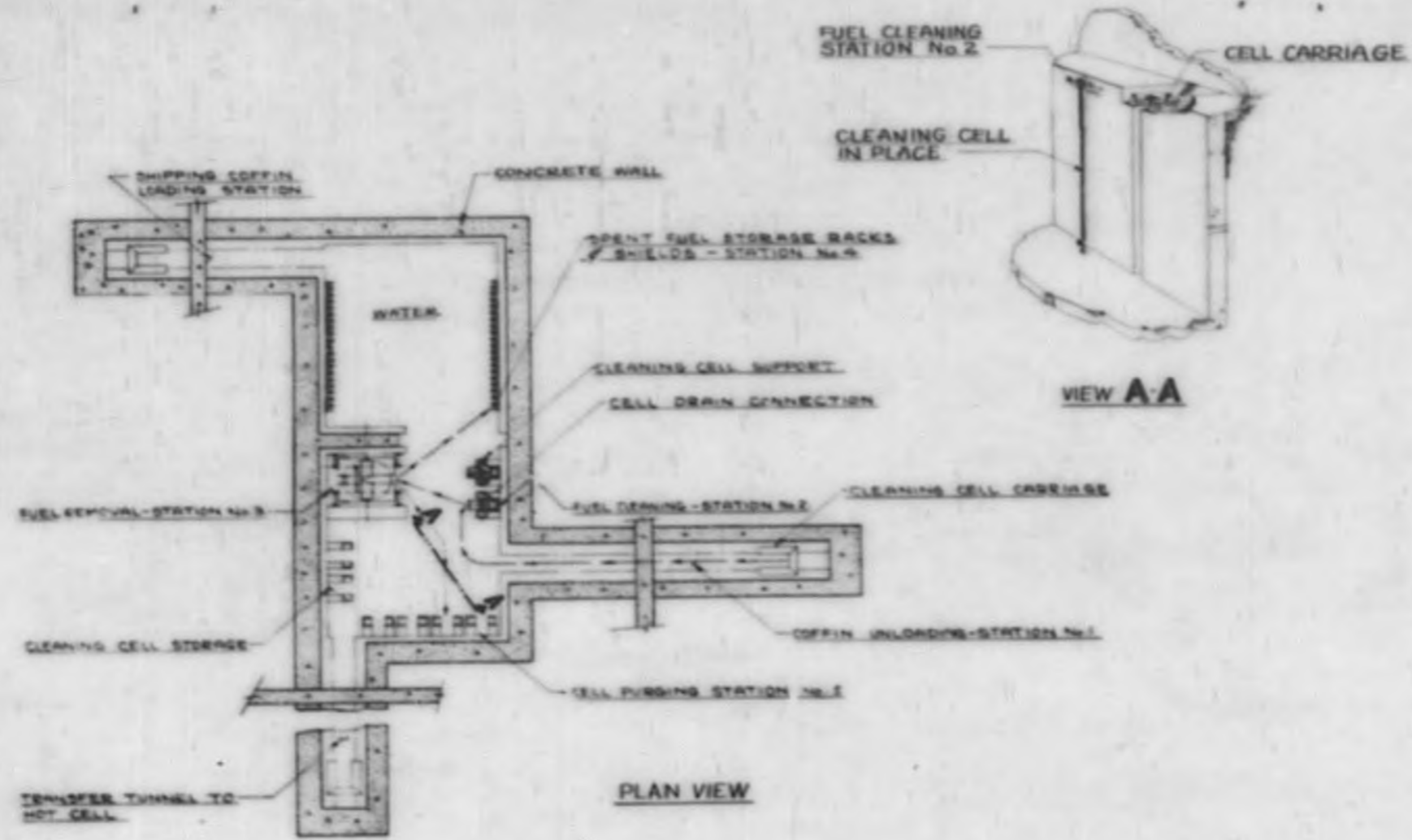CELL PURGING STATION No 2

TRANSFER TUNNEL TO
HOT CELL

PLAN VIEW

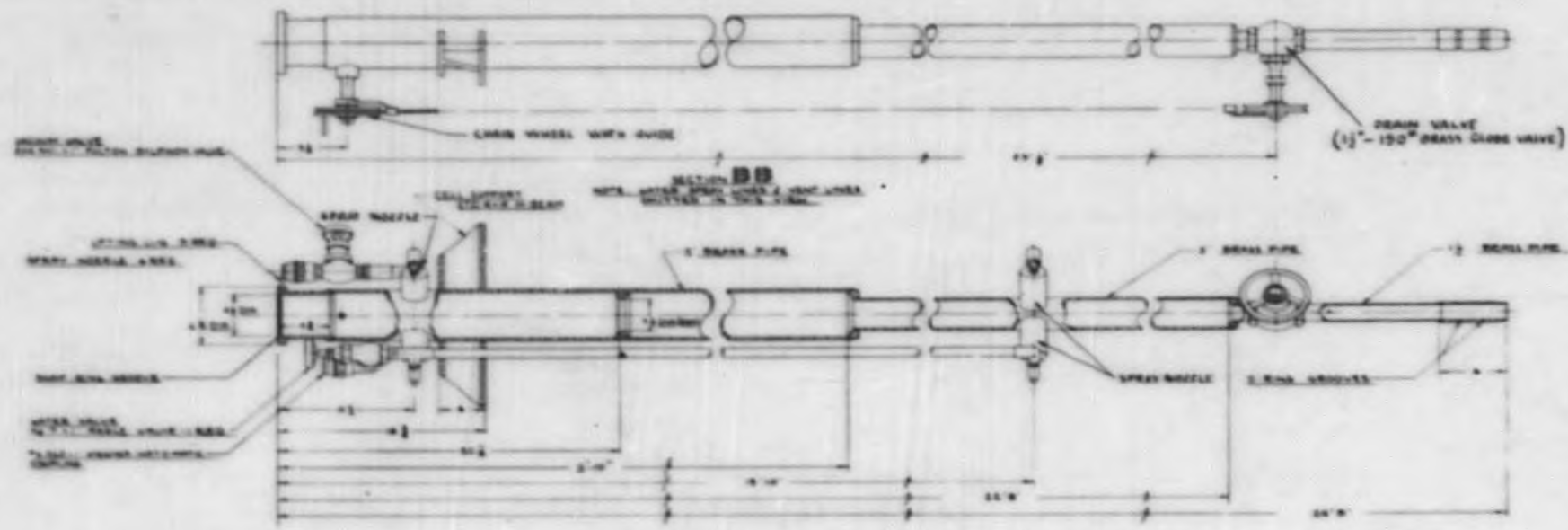Fig. 42.   Irradiated Fuel Handling Equipment Arrangement

Fig. 43. Irradiated Fuel Element Cleaning Cell
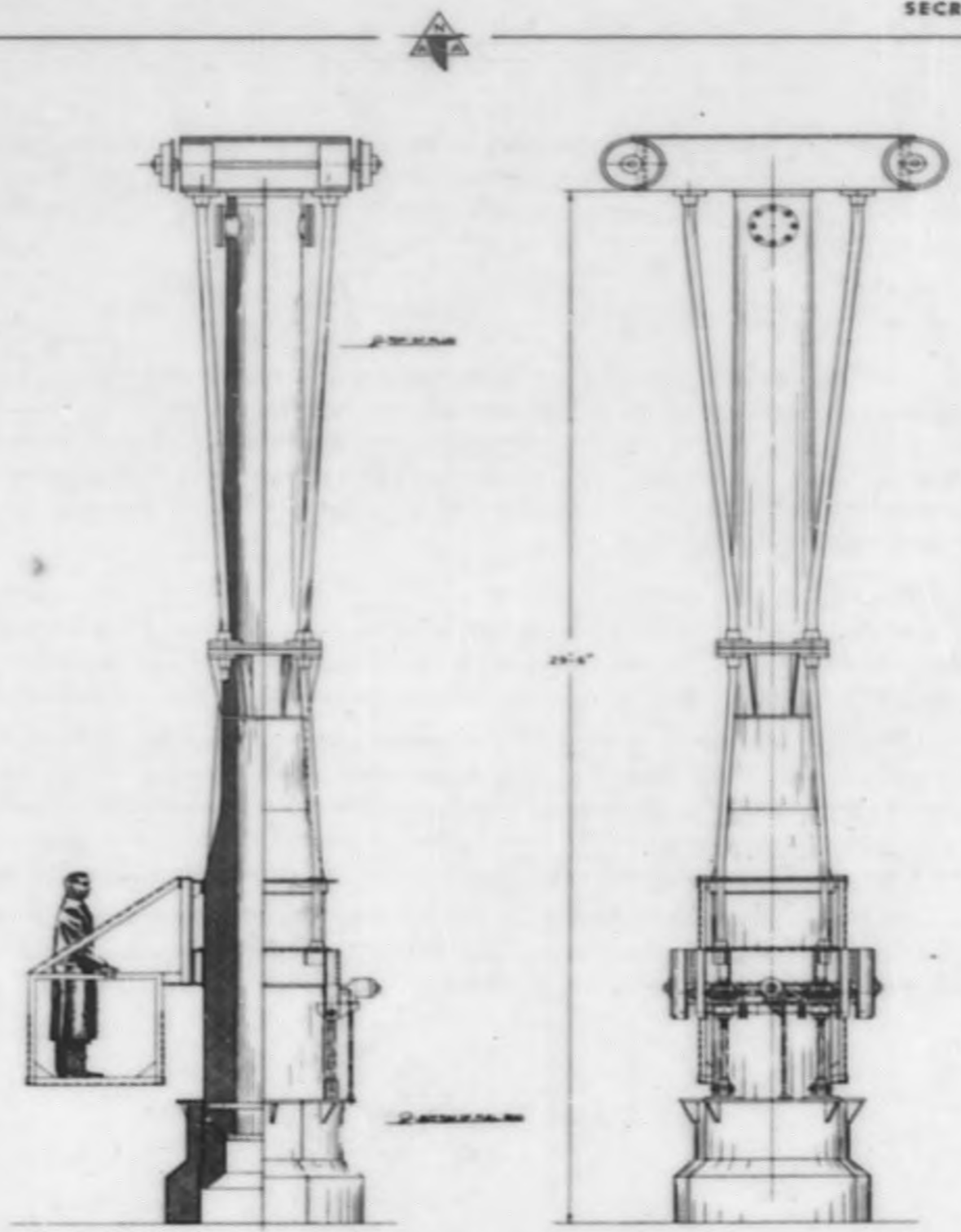
7464-SR1049

Fig. 44. Fuel Element Handling Coffin

emitters ($E_\gamma > 1.6$ Mev) as a function of time after shutdown. Having determined the hard portion of fission product gamma ray spectrum, the effective gamma ray energy, E_{eff}, which should be used for the shield calculations was then calculated.

$$\mu_o(E_{eff}) = \bar{\mu}_o, \text{ such that } e^{-\bar{\mu}_o t} \int S(E) dE = \int S(E) e^{-\mu_o(E)t} dE.$$

The results of the analysis are shown in Figs. 45 and 46. The hard gamma ray emitting fission product isotopes which were used for the calculations are listed in Table III. The calculations indicate a shield thickness of 9 inches of lead is necessary. Three hours after shutdown the radiation level at the surface of a fuel coffin containing a discharged center fuel element (P_o = 725 kw) would be 470 mr/hr.

C. Hot Cell

A preliminary layout drawing has been made for the primary hot cell. This cell will be used for disassembling fuel elements and components which have been removed from the reactor. Detailed drawings have not been made.

The calculations to determine the shield requirements for the cell have been completed. They were based upon the most intense source (a center fuel element) which could be removed from the reactor. A thickness of approximately 3.5 feet of magnetite ore concrete (231 lbs/ft^3) will be required to reduce the radiation rate at the shield surface to 10 per cent of AEC tolerance.

The shielding requirements for the hot cell viewing window are 30 inches of zinc bromide solution (density = 2.52 gm/cc) and nonbrowning glass plus 12 inches of lead glass (density = 6.2 gm/cc).
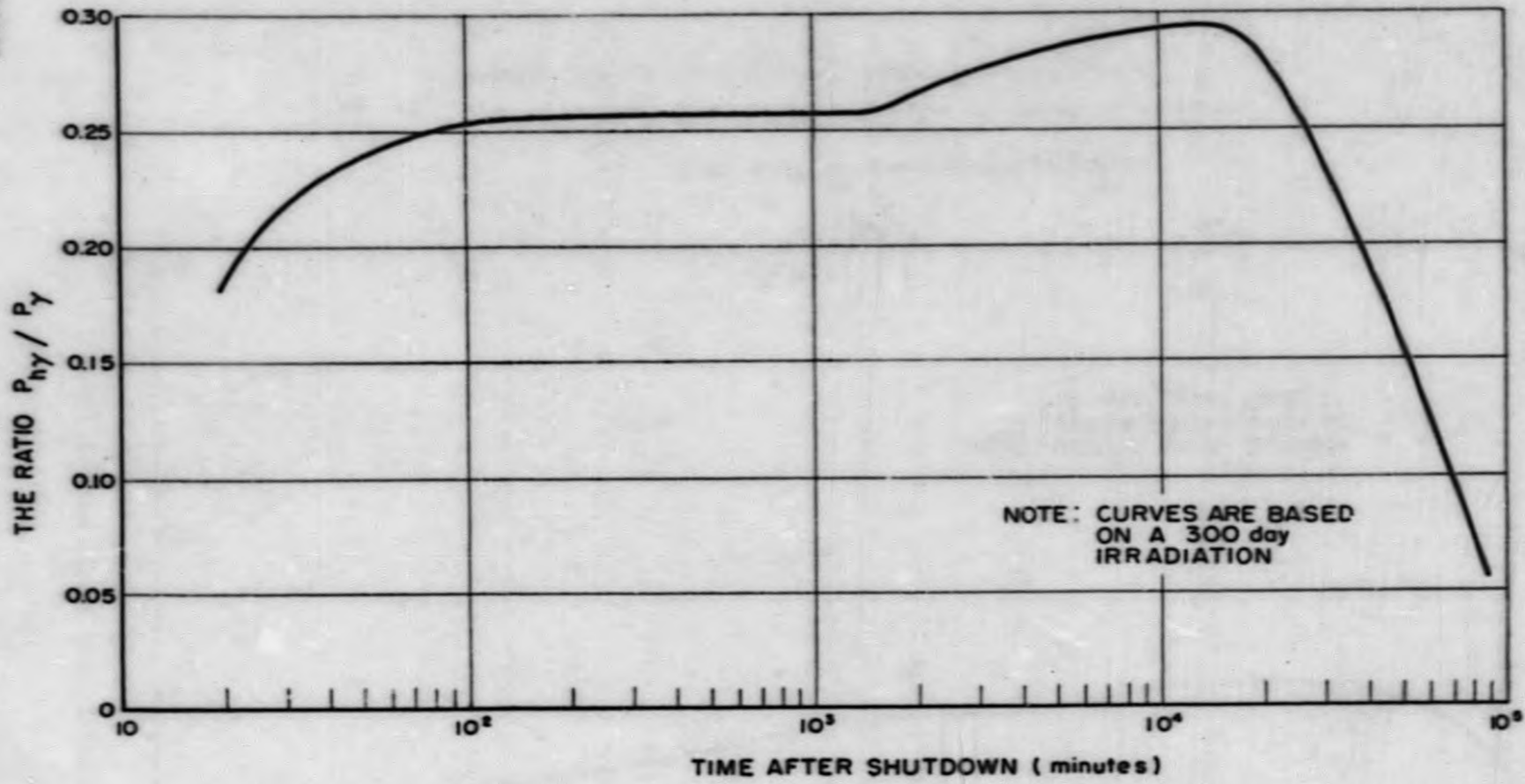
Fig. 45. The Ratio of the Hard Gamma Power to the Delayed Gamma Power as a Function of Time after Shutdown
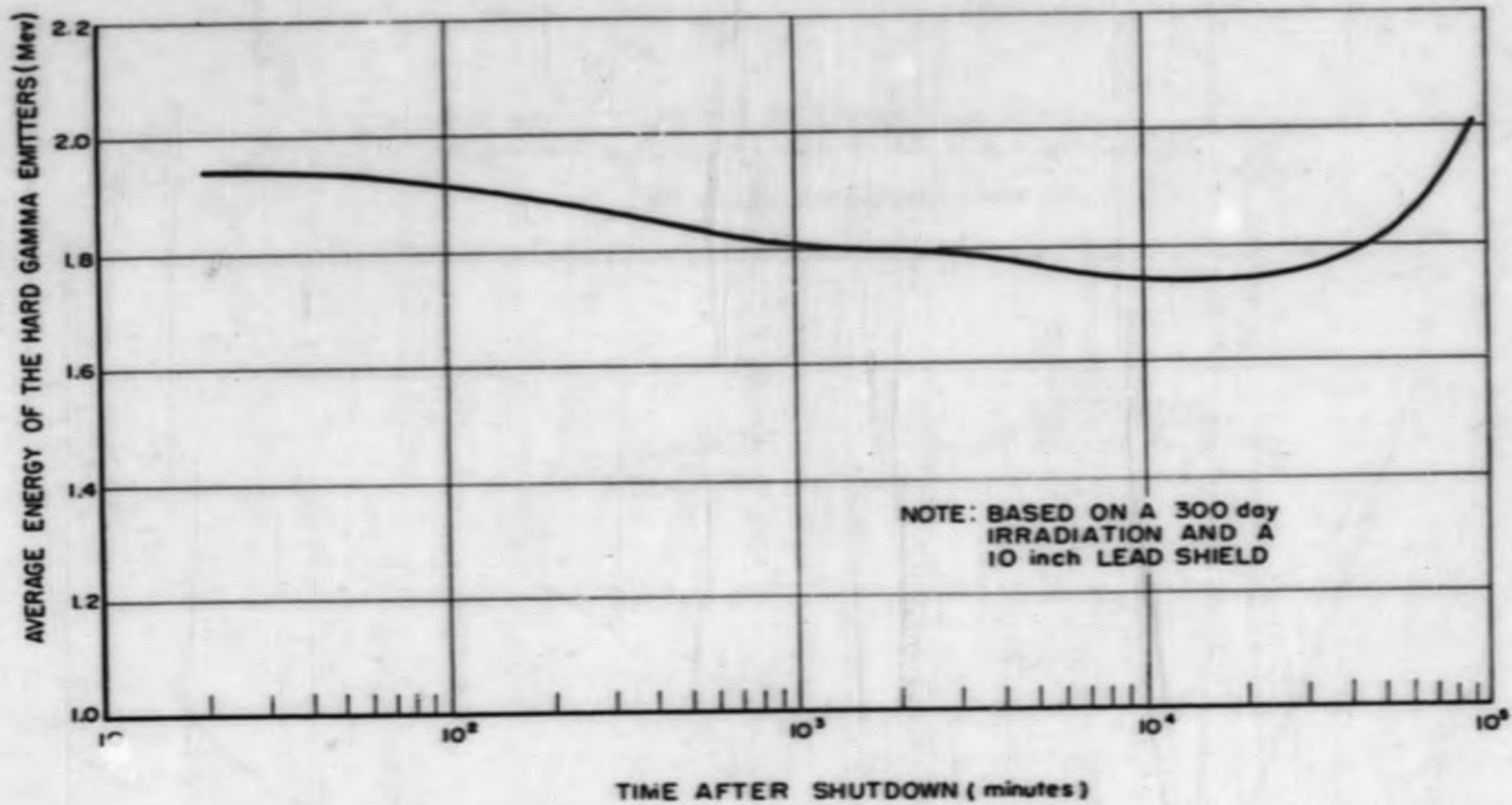
Fig. 46.   The Effective Gamma Ray Energy of the Hard Gamma
Emitters as a Function of Time After Shutdown

TABLE III

HARD GAMMA RAY EMITTING FISSION PRODUCT ISOTOPES

Gamma Emitting Isotope	Gamma Energy (Mev) and Percentage of Gammas Emitted per Disintegration		Portion of Decay Chain Determining Time Dependence after Shutdown	Fission Yield (Per Cent)
Ge^{77}	1.75	(1.0)	Ge^{77} (12 h)	0.007
Kr^{87}	1.9	(12.9)	$Br^{87}(56s) \rightarrow Kr^{87}(78$ m)	2.3
	2.3	(12.5)		
Rb^{88}	1.86	(19)	$Kr^{88}(2.77$ h$) \rightarrow Rb^{88}(17.8$ m)	4.0
	2.8	(15)		
Rh^{106}	2.9	(2.0)	$Ru^{106}(1$ y$) \rightarrow Rh^{106}(30s)$	0.33
Pd^{111*}	1.77	(25)	$Pd^{111*}(5.5$ h)	0.014
Sn^{125}	1.90	(5.0)	$Sn^{125}(9.4$ d)	0.022
Te^{131}	2.4	(22)	$Te^{131*}(30$ h$) \rightarrow Te^{131}(24.8$ m)	3.0
I^{132}	2.0	(2.7)	$Te^{132}(77$ h$) \rightarrow I^{132}(2.4$ h)	3.4
I^{134}	2.3	(1.0)	$Te^{134}(44$ m$) \rightarrow I^{134}(52.5$ m)	5.7
I^{135}	1.8	(73.9)	$Te^{135}(<2$ m$) \rightarrow I^{135}(6.68$ h)	6.0
	2.4	(2.0)		
La^{140}	1.6	(96)	$Ba^{140}(12.8$ d$) \rightarrow La^{140}(40$ h)	6.1
	2.5	(4.0)		
	2.9	(0.1)		
Pr^{144}	2.6	(2.0)	$Ce^{144}(274$ d$) \rightarrow Pr^{144}(17.5$ m)	5.0
Eu^{156}	2.0	(60)	$Sm^{156}(\sim 10$ h$) \rightarrow Eu^{156}(15.4$ d)	0.016

D. Radioactive Liquid Waste Disposal System (H. Richter)

A preliminary study has been made of the requirements for the disposal of radioactive liquid waste. The specifications are based upon the requirements of the Health Physics aspects. A schematic diagram showing the arrangement of a minimum facility for this operation is shown in Fig. 47.

XII. REACTOR SYSTEM ANALYSIS

An analysis of the SRE system is being initiated. The first phase constitutes a study of the steady state and transient control of the reactor and the associated cooling system. Special attention is being directed to the study of transients in the system under scram conditions. The object of this study is to develop thermal shock criteria for the design of the reactor and heat exchange equipment.
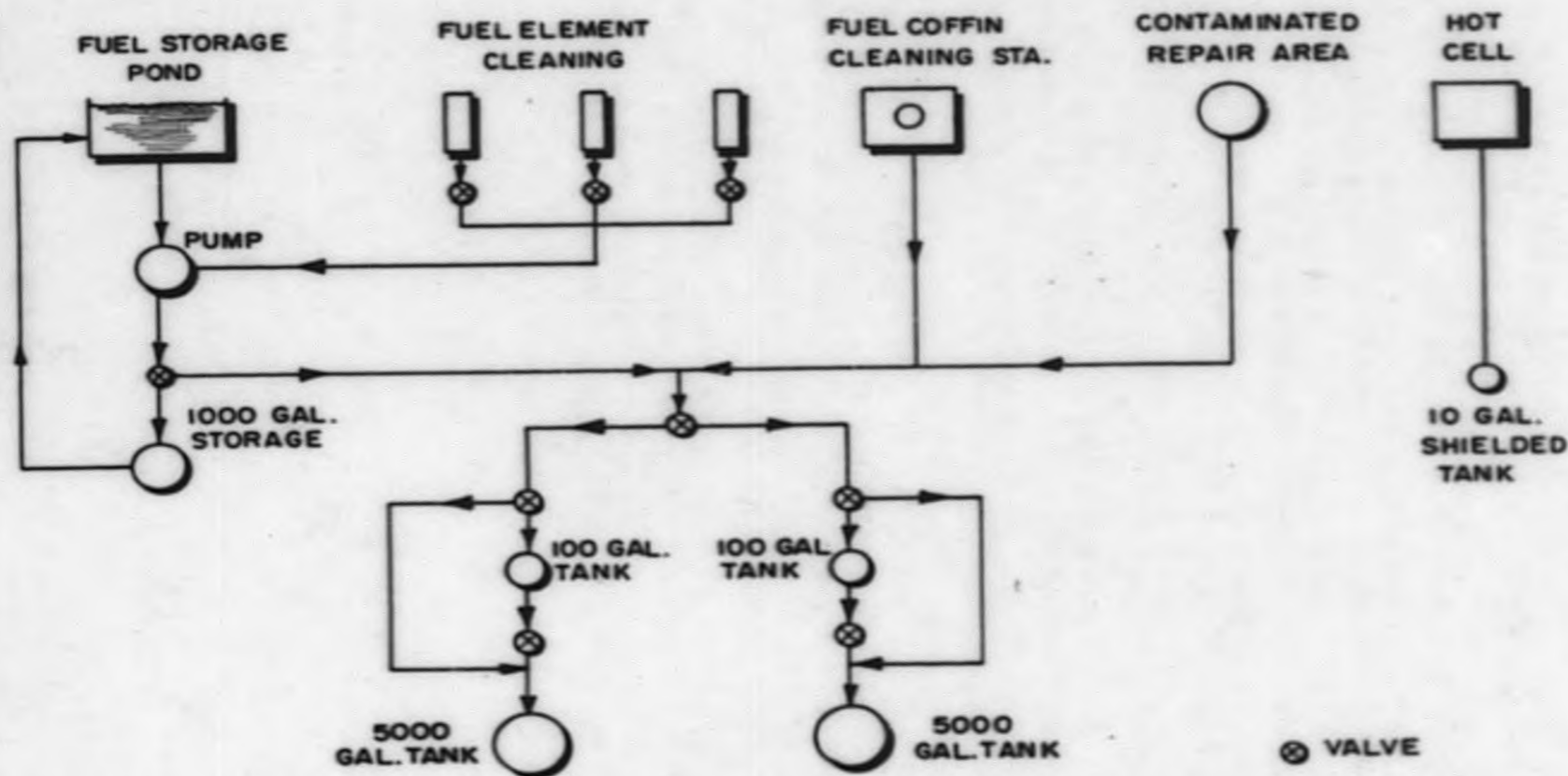
Fig. 47. Schematic of Radioactive Liquid Waste Disposal System

REFERENCES

1. L. R. Hafstad, "The AEC Program for Developing Nuclear Power Plant Technology," TID-2013, p 83, June, 1954.

2. G. M. Inman (ed.) "Sodium Graphite Reactor Quarterly Progress Report, September-November, 1952," NAA-SR-227, May 29, 1953.

3. _____, "Sodium Graphite Reactor Quarterly Progress Report, December, 1952-February, 1953," NAA-SR-260, November 15, 1953.

4. _____, "Sodium Graphite Reactor Quarterly Progress Report, March-May, 1953," NAA-SR-274, March 1, 1954.

5. _____, "Sodium Graphite Reactor Quarterly Progress Report, June-August, 1953," NAA-SR-878, May 15, 1954.

6. _____, "Sodium Graphite Reactor Quarterly Progress Report, September-November, 1953," NAA-SR-956, July 1, 1954.

7. _____, "Sodium Graphite Reactor Quarterly Progress Report, December, 1953-February, 1954," NAA-SR-1027, to be published.

8. R. J. Beeley, et al., "Reactor Evaluation Quarterly Progress Report for August-October, 1953," NAA-SR-845, March 1, 1954.

9. A. Mitchell, et al., "Effect of Temperature on the Resonance Absorption of Neutrons by Uranium," CP-597, April 22, 1943.

10. J. R. Risser, et al., "Surface to Mass Dependence of Effective Resonance Integrals for Uranium-238 Cylinders," ORNL-958, March 20, 1951.

11. A. T. Biehl and D. Woods, "Intra-Cell Neutron Densities, Part I," NAA-SR-138, September 25, 1951.

12. J. L. Hyde and J. Pellarin, "Thermal Neutron Flux Distribution in One-Inch Fuel Rods and Quatrefoils," ANL-4800, August, 1952.

13. C. L. Hogan and R. B. Sawyer, "The Thermal Conductivity of Metals at High Temperature," J. Appl. Phys. 23, 600 (1952).

END